



City Research Online

City St George's, University of London

Citation: Tomic, Ivana (2016). Distributed LQR control of multi-agent systems. (Unpublished Doctoral thesis, City, University of London)

This is the accepted version of the paper.

This version of the publication may differ from the final published version. To cite this item please consult the publisher's version.

Permanent repository link: <https://openaccess.city.ac.uk/id/eprint/15883/>

Copyright and Reuse: Copyright and Moral Rights remain with the author(s) and/or copyright holders. Copies of full items can be used for personal research or study, educational, or not-for-profit purposes without prior permission or charge, unless otherwise indicated, provided that the authors, title and full bibliographic details are credited, a hyperlink and/or URL is given for the original metadata page and the content is not changed in any way. For full details of reuse please refer to [City Research Online policy](#).

City, University of London
School of Mathematics, Computer Science and
Engineering

Distributed LQR Control of Multi-Agent Systems

Ivana Tomić

A dissertation submitted for the degree of
Doctor of Philosophy in Control Theory
October 2016

Abstract

The thesis develops optimal control methods for designing distributed cooperative control schemes in multi-agent networks. First, the model of a completely connected multi-agent network is presented, consisting of identical dynamically decoupled agents controlled by a centralized LQR (Linear Quadratic Regulator) based controller. The structure of the solution, as well as controller's spectral and robustness properties are presented. A special case of centralized control where the optimal solution for the whole network can be constructed from the solution of single agent LQR system is given. The problem is extended to distributed control where the special structure is imposed onto the information flow between agents and only local interaction is considered.

A systematic method is given for computing the performance loss of various distributed control configurations relative to the performance of the optimal centralized controller. Necessary and sufficient conditions are derived for which a distributed control configuration pattern arising from the optimal centralized solution does not entail loss of performance if the initial state vector lies in a certain subspace of state-space which is identified. It is shown that these conditions are always satisfied for systems with communication/control networks corresponding to complete graphs with a single link removed. The procedure is extended for the purposes of analysing the performance loss of an arbitrary distributed configuration. Cost increase due to decentralisation is quantified by introducing three cost measures corresponding to the worst-case, best-case and average directions in which the initial state of the system lies.

Finally, a cooperative scheme is presented for controlling arbitrary formations of low speed experimental UAVs (Unmanned Aerial Vehicles) based on a distributed LQR design methodology. Each UAV acts as an independent agent in the formation and its dynamics are described by a 6-DOF (six degrees-of-freedom) nonlinear model. This is linearised for control design purposes around an operating point corresponding to straight flight conditions and simulated for longitudinal motion. It is shown that the proposed controller stabilises the overall formation and can control effectively the nonlinear multi-agent system. Also, it is illustrated via numerous simulations that the system provides reference tracking and that is robust to environmental disturbances such as nonuniform wind gusts acting on a formation of UAVs and to the loss of communication between two neighbouring UAVs.

Acknowledgements

Though only my name appears on the cover of this dissertation, many other people have contributed to its production and I own my gratitude to all of them.

First and foremost, I could never overstate my gratitude towards Professor George Halikias, for his support, ideas, guidance and encouragement. I have been fortunate to have a supervisor who gave me the freedom to explore on my own, and at the same time thought me how to do research and helped me focus my ideas. In my eyes, you are a person I will always look up to, in all aspects of life. I also appreciate the academic help and support along the way from my second supervisor Professor Nicos Karcianas.

I am greatly indebted to Dr Efstathios Milonidis, whom I have worked with in a very close collaboration on some topics related to this thesis. His kindness, encouragement and sense of humor made him to become more of a mentor and friend to me.

On a more private level, I would like to thank all the amazing people and my fellow students - far too numerous to name them all - that I have meet over the years at City. A special thank you goes to Jovana, Milan, Mio and my other City colleagues who made it too easy to maintain a healthy balance between "fun" and "work".

I am forever indebted to my mum Mirjana to whom this thesis is dedicated to. She gave me the unconditional love and was a source of my strength and courage all these years. Thank you for being the most amazing mother and for giving me more than I could ask for.

Last but not least, I would like to express a heart-felt gratitude to my family with a special mention to my grandmother Milica, my brothers Radomir and Vladimir, and my best friend Gorana. I am lucky to have you all by my side.

Declaration

I grant powers of discretion to the University Librarian to allow the thesis to be copied in whole or in part without further reference to the author. This permission covers only single copies made for study purposes, subject to normal conditions of acknowledgement.

Contents

Abstract	i
Acknowledgements	ii
Declaration	iii
List of Tables	viii
List of Figures	ix
List of Symbols	xiv
Abbreviations	xviii
1 Introduction	1
1.1 Motivation	1
1.2 Thesis Objectives	4
1.3 Thesis Outline	5
1.4 Statement of Contributions	7
1.5 Publications	9
1.6 Summary	9

2	Literature Review	10
2.1	Cooperative Control in Multi-Agent Networks	10
2.2	Distributed Control of Multi-Agent Systems	13
2.2.1	Formation Control	15
2.2.2	Optimal Control	16
2.3	Summary	18
3	Linear Quadratic Regulator	19
3.1	Mathematical Preliminaries	20
3.1.1	Notation	20
3.1.2	Definitions	21
3.2	LQR Problem Description	23
3.3	Gain and Phase Margins of the LQR	27
3.3.1	Return Difference Equality and Inequality	27
3.3.2	Single-Input Systems	30
3.3.3	Multi-Input Systems	32
3.4	Summary	35
4	Centralized Optimal Control Problem	36
4.1	Graph Theory Preliminaries	37
4.2	Centralized LQR Problem Definition	39
4.2.1	Spectral and Robustness Properties of the Centralized LQR Solution	42
4.2.2	Numerical Example: Centralized LQR Multi-Agent Sys- tem	44
4.3	Special Case of the Centralized LQR Problem	47

4.3.1	Problem Definition and Structural Properties of its Solution	47
4.3.2	Numerical Example: Special Case of the Centralized LQR Multi-Agent System	52
4.4	Summary	54
5	Distributed Optimal Control Problem	55
5.1	Distributed LQR Design Method	56
5.1.1	Distributed LQR Multi-Agent System - Numerical Example	59
5.2	Optimal and Near-Optimal Distributed Control Schemes	62
5.2.1	Comparison of Centralized Controller and Distributed Controller	62
5.2.2	Measures of Performance Loss for Distributed Configurations	69
5.2.3	Numerical Example: Performance Loss Analysis for Different Distributed Configurations	71
5.3	Summary	74
6	Application Example: LQR Control of X-RAE1 UAV	75
6.1	Motions of an Aircraft	76
6.2	Coordinate Systems and Axes Transformations	77
6.3	Aircraft Equations of Motion	80
6.3.1	The Force Equations - Translational Dynamics	80
6.3.2	The Moment Equations - Rotational Dynamics	82
6.3.3	External Forces and Moments	83
6.3.4	Complete Set of the Equations of Motion of X-RAE1	87
6.4	Linear Model of X-RAE1	90

6.4.1	Longitudinal and Lateral Equations of Motion	90
6.4.2	Perturbed Equations of Motion	91
6.4.3	Linearised Model for the Straight Flight	92
6.5	LQR Control Design	97
6.6	Summary	102
7	Application Example: Distributed LQR Control of Multi-Agent Network	103
7.1	Distributed LQR Design for Formation Control	104
7.2	Simulation Results	107
7.2.1	Altitude Control and Disturbance Rejection	108
7.2.2	Loss of Communication Between Agents	112
7.3	Summary	116
8	Conclusion	117
8.1	Summary of the Thesis	117
8.2	Directions for Future Work	120

List of Tables

4.1	Eigenvalue distribution in the centralized LQR system for a different choice of weighting matrices	46
5.1	Cost measures for optimal (centralized) LQR design	72
5.2	Cost measures for suboptimal distributed LQR configurations	72
6.1	Trim conditions for a nominal velocity of 30m/s	93

List of Figures

2.1	Different types of controllers (The information flow is represented by arrows.) [MV08]	14
3.1	Closed-loop LQR system	24
3.2	Open-loop LQR system	28
3.3	Classical representation of state feedback LQR system	28
3.4	Unity feedback representation of state feedback LQR system	28
3.5	State feedback open-loop gain	29
3.6	Nyquist plots of $L(j\omega)$. (a) Stable open-loop transfer function. (b) Open-loop transfer function with two unstable poles [Pre02]	30
3.7	Illustration of LQR phase tolerance [Che14]	31
3.8	Nyquist diagram of $\frac{2s+3}{(s+1)^2}$	34
4.1	Fully connected (low-scale) multi-agent network	44
5.1	Large-scale distributed multi-agent network of $N = 100$ agents	59
5.2	Snapshots of formation recovery simulation in the network of $N = 100$ agents where each agent is described by double integrator dynamics	61
5.3	Graph \mathcal{G}_1 and its permuted graph \mathcal{G}_{1_p}	67
5.4	Complete graph with $N_d = 4$ agents perturbed by (1, 2) edge elimination	68

5.5	Fully connected (complete) multi-agent network of $N = 6$ agents	71
5.6	Different distributed configurations for the multi-agent network consisting of $N = 6$ agents	73
5.7	Probability distribution of the performance cost deviation from optimality	74
6.1	The three translational movements and the three rotational movements [Elg13]	76
6.2	Coordinate systems: a) Earth-fixed coordinate system b) Body-fixed coordinate system [Phi10]	77
6.3	True views of the three Euler angles shown following the standard conventions of engineering graphics and descriptive geometry [Phi10]	79
6.4	Graphical representation of the velocity vector \mathbf{V}_T , the angle of attack α and the sideslip angle β [Elg13]	84
6.5	Graphical representation of the thrust \mathbf{T} [Elg13]	86
6.6	Longitudinal aerodynamic forces and moments and thrust representation for X-RAE1	87
6.7	X-RAE1 layout [Mil87]	89
6.8	Forward and downward velocity responses of the open-loop linear X-RAE1 system when a pulse is applied to elevator (solid line) and in the presence of an impulse disturbance in w (dashed line)	95
6.9	Pitch rate and pitch angle responses of the open-loop linear X-RAE1 system when a pulse is applied to elevator (solid line) and in the presence of an impulse disturbance in w (dashed line)	95
6.10	Height response of the open-loop linear X-RAE1 system when a pulse is applied to elevator (solid line) and in the presence of an impulse disturbance in w (dashed line)	96
6.11	Simulink [®] model for LQR control of linear X-RAE1 model . . .	98

6.12	Forward and downward velocity responses of linear and nonlinear X-RAE1 model controlled by LQR in the presence of impulse disturbance and step tracking demand	99
6.13	Pitch rate and pitch angle responses of linear and nonlinear X-RAE1 model controlled by LQR in the presence of impulse disturbance and step tracking demand	99
6.14	Elevator rate and elevator responses of linear and nonlinear X-RAE1 model controlled by LQR in the presence of impulse disturbance and step tracking demand	100
6.15	Height response of linear and nonlinear X-RAE1 model controlled by LQR in the presence of impulse disturbance and step tracking demand	100
6.16	Control inputs of linear and nonlinear X-RAE1 model controlled by LQR in the presence of impulse disturbance and step tracking demand	101
6.17	Simulink [®] model of LQR control of nonlinear X-RAE1 model .	101
7.1	The interconnection structure within the multi-agent network .	104
7.2	Simulink [®] model for LQR-based control of formation consisting of four X-RAE1s	107
7.3	Height responses of the linear LQR multi-agent system controlled by the distributed controller in the presence of impulse disturbance and step tracking demand	108
7.4	Velocity responses of the linear LQR multi-agent system controlled by the distributed controller in the presence of impulse disturbance and step tracking demand	109
7.5	Height responses of the nonlinear LQR multi-agent system controlled by the distributed controller in the presence of impulse disturbance and step tracking demand	110
7.6	Velocity responses of the nonlinear LQR multi-agent system controlled by the distributed controller in the presence of impulse disturbance and step tracking demand	110

7.7	Forward and downward velocity responses of linear and nonlinear agent 1 model controlled by distributed LQR in the presence of impulse disturbance and step tracking demand to each agent in the formation	111
7.8	Pitch rate and pitch angle responses of linear and nonlinear agent 1 model controlled by distributed LQR in the presence of impulse disturbance and step tracking demand to each agent in the formation	111
7.9	Elevator rate and elevator responses of linear and nonlinear agent 1 model controlled by distributed LQR in the presence of impulse disturbance and step tracking demand to each agent in the formation	111
7.10	Height responses of the linear LQR system controlled by the distributed controller in the presence of link failure between agent 1 and agent 2 followed by an impulse disturbance to agent 1 . .	112
7.11	Velocity responses of the linear LQR system controlled by the distributed controller in the presence of link failure between agent 1 and agent 2 followed by an impulse disturbance to agent 1	113
7.12	Height responses of the nonlinear LQR system controlled by the distributed controller in the presence of link failure between agent 1 and agent 2 followed by an impulsive disturbance to agent 1	113
7.13	Velocity responses of the nonlinear LQR system controlled by the distributed controller in the presence of link failure between agent 1 and agent 2 followed by an impulsive disturbance to agent 1	114
7.14	Forward and downward velocity responses of linear and nonlinear agent 1 model controlled by distributed LQR in the presence of link failure between agent 1 and agent 2 followed by an impulse disturbance to agent 1	114

7.15	Pitch rate and pitch angle responses of linear and nonlinear agent 1 model controlled by distributed LQR in the presence of link failure between agent 1 and agent 2 followed by an impulse disturbance to agent 1	115
7.16	Elevator rate and elevator responses of linear and nonlinear agent 1 model controlled by distributed LQR in the presence of link failure between agent 1 and agent 2 followed by an impulse disturbance to agent 1	115

List of Symbols

\mathbf{A}	adjacency matrix
A_{cl}	closed-loop matrix of a single agent LQR system
A_{cl_a}	closed-loop matrix of centralized LQR system
\tilde{A}_{cl}	closed-loop matrix of distributed LQR system
α	angle of attack
β	sideslip angle
\mathbb{C}	field of complex numbers
\mathbb{C}_-	open left-half plane
C_D	drag coefficient
C_l	rolling moment coefficient
C_L	lift coefficient
C_m	pitching moment coefficient
C_n	yawing moment coefficient
C_y	side force coefficient
D	drag
d_i	degree of node i
$d_{max}(\mathcal{G})$	maximum node degree of the graph \mathcal{G}
$\Delta(\mathcal{G})$	degree matrix

δ_T	throttle setting
e_T	eccentricity
ε_T	angular displacement
\mathcal{E}	set of edges
\mathbf{F}	force vector
$F(s)$	return difference transfer matrix
$G(s)$	transfer function of the plant
\mathcal{G}	graph
\mathbf{H}	angular momentum vector
I_x, I_y, I_z	moments of inertia
I_{xy}, I_{yz}, I_{xz}	products of inertia
J	optimal cost
K	LQR gain matrix of a single agent system
\tilde{K}	LQR gain matrix of distributed system
K_a	LQR gain matrix of centralized system
L	lift, rolling moment
$L(\mathcal{G})$	Laplacian matrix of the graph \mathcal{G}
$L(s)$	open-loop transfer matrix from the process' input \mathbf{u} to the controller's output $\hat{\mathbf{u}}$
$\lambda_i(M)$	i th eigenvalue of matrix M
m	mass
M	pitching moment
\mathbf{M}_s	moment vector

N	number of agents (subsystems), yawing moment
η	elevator deflection
Ω_B	angular velocity vector
P	Algebraic Riccati Equation solution of a single agent system, roll rate
\tilde{P}	Algebraic Riccati Equation solution of distributed system
P_a	Algebraic Riccati Equation solution of centralized system
Φ	bank or roll angle
Ψ	azimuth or yaw angle
\bar{q}	dynamic pressure
\tilde{Q}	states weighting matrix of distributed system
Q	states weighting matrix of a single agent system, pitch rate
Q_a	states weighting matrix of centralized system
\mathbf{r}	external reference signal
R	inputs weighting matrix of a single agent system, , yaw rate
\tilde{R}	inputs weighting matrix of distributed system
\mathbb{R}	field of real numbers
R_a	inputs weighting matrix of centralized system
$\Re[s]$	right half plane
R_B^F	rotation matrix used to transform vectors from body to Earth-fixed coordinate system
R_F^B	rotation matrix used to transform vectors from Earth-fixed to body coordinate system
$\mathcal{S}(M)$	spectrum of matrix M
$S(s)$	sensitivity function

T	transformation matrix
\mathbf{T}	thrust vector
$T(s)$	complementary sensitivity function
$T_c(s)$	closed loop transfer matrix
$T_o(s)$	open loop transfer matrix
Θ	elevation or pitch angle
\mathbf{u}	system input vector
U	forward velocity
$U(s)$	Laplace transform of the control input \mathbf{u}
V	side velocity
\mathbf{V}_T	velocity vector
\mathcal{V}	set of nodes (vertices)
W	downward velocity
ω	frequency
ω_n	natural frequency
\mathbf{x}	system state vector
\mathbf{x}_0	initial state vector
\mathbf{y}	system output vector
Y	side force
$Y(s)$	Laplace transform of the control output \mathbf{y}
ζ	damping ratio

Abbreviations

ARE	Algebraic Riccati Equation
DMPC	Distributed Model Predictive Control
DOF	Degree of Freedom
LMI	Linear Matrix Inequality
LQR	Linear Quadratic Regulator
LTR	Loop Transfer Recovery
MILP	Mixed Integer Linear Programming
NMPC	Nonlinear Model Predictive Control
RPV	Remotely Piloted Vehicle
UAV	Unmanned Aerial Vehicle
UGV	Unmanned Ground Vehicle
UUV	Unmanned Underwater Vehicle

Chapter 1

Introduction

In this first chapter we briefly establish the context for the work developed in this thesis. We also provide an overview of thesis objectives followed by the thesis outline and the statement of contributions. Finally, we give the list of publications which were prepared in the course of this work.

1.1 Motivation

Nowadays, many fields of human lives are being dominated by use of large, complex systems which are made of identical or near-identical subsystems. Cooperation between them plays a crucial role, so it is desired to develop an understanding of the behaviour of such interconnected systems. Such systems can be found in:

- Nature - motion of clusters of fish, insects, etc. moving together;
- Man-made systems - such as transportation systems, systems for surveillance, etc.;
- Human body - such as intestinal system [KD05].

Cooperative control has emerged as a topic of significant interest to the controls community as a way to control these complex systems. It can be related to the areas where some type of repetition between the interconnected subsystems occurs. The main area of interest in cooperative control is how to manipulate these subsystems called *agents* and information exchange between

them in order to provide coordinated behaviour [Jin07]. An agent can represent a cellular phone, an internet router, an airplane, or even a smart sensor with microprocessor. It is desired to understand the behaviour of such a system when the number of agents is very large, but also when control of such an interconnected system is decentralized or distributed. Furthermore, interconnection topology between the agents can have fixed structure or time-varying structure depending on the type of system. Fixed interconnection structure can be observed in flight formations, human body, etc., while some examples of time-varying structure can be flock of birds, schools of fish, etc. [KD05].

Cooperative control poses many significant theoretical and practical issues. The difficulties arising in analysing or designing complex systems are often reduced when such systems are viewed as an interconnection of subsystems. In this case, the problem of information exchange is constantly present due to the limitations and failures in communication that can occur between agents (e.g. bandwidth limitations, loss of connectivity, decision when and to whom to communicate, etc.). Furthermore, instead of having a centralized coordination scheme that does not scale well with the number of agents, distributed algorithms are often deployed. Then, only neighbour-to-neighbour interaction is assumed to ensure convergence of all agents to a common goal. However, while centralized control guarantees the optimal solution, in distributed control the information exchange is limited which usually results in the solution that deviates from optimality.

Recently control of multi-agent systems has received considerable attention due to its broad spectrum of applications, such as formation control ([JLM02], [CW05]), satellite clustering [BLH01], flocking ([OS06], [TJP07]), distributed sensor networks [CMKB04], air traffic control [TPS98], congestion control in communication networks [PDL01], etc. Due to the very broad scope of issues that can be identified in the area, cooperative control problems can be provisionally divided into four groups [Sha07]:

1. *Distributed control and computations* is perhaps one of the most important aspects of cooperative control. Distributed control relying on distributed computations, as well as on computations among the network's interacting components, is needed in order to achieve satisfactory distribution of information between agents. This principle is widely used in multivehicle motion planning in order to create the trajectories to guide a number of vehicles to desired destination without colliding

with obstacles and between themselves. Also, by using the consensus algorithm approach ([JLM02], [BHOT05], [OSFM07]), large collections of vehicles can be synchronised with the use of local information provided by neighbouring agents, even in the case of time-varying network topologies. Some other interesting areas where distributed control and computations are widely applied include: nonlinear model predictive control (NMPC) [BM99], task assignment approaches in multivehicle motion planning ([Mur00], [AMS07]), etc.

2. *Adversarial interactions problems* emphasise the fact that systems should be able to plan their trajectory strategically even if agents operate in hostile environments [ED02]. This can be formulated as a general optimisation problem for computing defender trajectories to intercept hostile positions. Mixed integer linear programming (MILP) is a specific form of problems here which can be extended to problem of forecasting adversaries under the lack of knowledge in opponents strategies [MSA07].
3. *Uncertain evolution problems* model agents operating in uncertain environments via estimation and adaptation methods. Therefore, cooperative control is widely used in situations where some model parameters have to be estimated and hybrid modes have to be created [MD07]. For example, process of construction of an evasion trajectory would benefit from knowledge of the target assignments of vehicles. Since there is no explicit communication between vehicles' and targets, a vehicles assignment must be estimated based on the assumed model. Another goal of cooperative control is to enable the communication between agents during the exploration of unknown environments, as well as reporting this information back to humans ([CT04], [LCT⁺04]).
4. *Complexity management* methods attempt to reduce computational complexity by introducing effective approximations (see e.g. [CGW91], [AC03]). For example, by introducing a lattice structure, the set of all possible states for linear systems with bounded disturbances and measurement noise can be easily constructed [DVM04].

In this context, the main theme of the work is analysis of distributed control methods, formulated as general optimal control problems, and their application in systems consisting of a large number of mobile agents. Rather than focusing on general dynamical systems, we consider the specific application area of *distributed formation control of UAVs*.

1.2 Thesis Objectives

The main objectives of this thesis are:

- To introduce the theoretical framework on which this thesis has been developed. This includes the LQR-based control design and the representation of LQR's guaranteed robustness properties.
- To extend the framework in the form of centralized and distributed LQR control to networks consisting of a large number of subsystems (agents) known as multi-agent networks.
- To analyse the structure of centralized and distributed LQR solutions, their spectral properties, as well as the robust properties of the centralized and distributed controllers.
- To present a method for comparing with respect to performance cost the family of distributed LQR-suboptimal controllers with the optimal centralized controller.
- To quantify the cost increase due to decentralization by introducing different cost measures.
- To apply the proposed control designs to the effective altitude control of arbitrary formations of UAVs described by high-order dynamical systems which are approximated by their linearised models.
- To show via numerical simulations that the proposed controllers are able to stabilise the system and are robust to environmental disturbances and to loss of communication between agents.
- To show that the proposed control designs can be used to successfully stabilise the nonlinear model for a standard set of initial conditions.
- To summarise the results presented and outline future extensions and possible research directions.

In the next section an outline of the thesis will be presented.

1.3 Thesis Outline

This section gives chapter-by-chapter outline of the thesis:

- *Chapter 1* - The first section of the chapter gives some background and motivation to the topic. Then, the objectives of the thesis are summarised which is followed by a statement of contributions. Finally, the list of publications which were prepared in the course of this thesis is given.
- *Chapter 2* - In this chapter an overview of related work reported in the literature is presented to set the stage for the main results derived in subsequent chapters. In particular, we discuss up-to-date research in the areas of cooperative and distributed control, and their application to large-scale UAV networks.
- *Chapter 3* - In this chapter some of the methods and techniques of what is known as "optimal control" are presented. The branch of optimal control called linear optimal control is introduced for the control of a linear system where all states are measured and available for feedback. Hence full-state feedback design is applied, which gives a number of attractive properties, such as good gain and phase margins, good tolerance to nonlinearities, etc. Further, stability and robustness properties of the optimal LQR are presented for the case of single-input systems, which are then extended to the case of multi-input systems.
- *Chapter 4* - In this chapter LQR theory is applied to multi-agent networks consisting of identical dynamically decoupled systems (agents). Bidirectional communication is assumed to exist between each pair of agents, and this type of problem is known as centralized optimal control problem. The structure of centralized LQR solution is presented, which is followed by spectral and robustness properties of the centralized LQR controller. In the last section of this chapter a special case of centralized LQR control is analysed where a different structure is imposed on the augmented state weighting matrix. It is shown that in this case the solution of (large-scale) centralized LQR system can be constructed from the solution of a single agent LQR system which is then illustrated through an example.
- *Chapter 5* - In this chapter the method for designing the distributed

controller for dynamically decoupled multi-agent systems is presented: a stabilising distributed controller can be found by solving a single LQR problem whose size depends on the maximum vertex degree of the graph. The effectiveness of this approach is illustrated through an example of large-scale multi-agent network where individual agents are described by double integrator dynamics. Next, the method for comparing the family of distributed LQR-suboptimal controllers with the optimal centralized controller has been presented. A procedure is extended for analysing the performance loss of an arbitrary distributed configuration which is illustrated via an example.

- *Chapter 6* - In this chapter we present 6-DOF dynamical model of an experimental RPV (Remotely Piloted Vehicle), namely X-RAE1. The equations of motion of an aircraft are derived by using force and moment equations. Also, the external forces and moments are taken into account which leads to a nonlinear model described by six equations of motion. This model is then linearised and decomposed into two motions for a specific set of flight conditions. In the last section we propose the LQR control design for altitude control and disturbance rejection for the linearised X-RAE1 model. Also, it is shown that the proposed LQR controller can be used successfully to stabilise the nonlinear X-RAE1 model for a standard set of initial conditions.
- *Chapter 7* - This chapter provides an extension to Chapter 5 where the LQR control design for X-RAE1 model is given. Distributed cooperative scheme for controlling arbitrary formations of low speed experimental UAVs is presented. Through the numerous simulations we investigate whether the proposed controller is robust to environmental disturbances such as nonuniform wind gusts acting on a formation and to the loss of communication between a pair of agents. Also, the altitude control problem was studied where each agent is given an external step command to track.
- *Chapter 8* - In the final chapter, the results presented in this thesis are summarised and connections to other related areas are highlighted. In addition, we provide future extensions and possible research directions arising from this work.

Next, we give the statement of contributions.

1.4 Statement of Contributions

In Chapter 3 we introduce the theoretical framework on which this thesis has been developed. This includes the revision of relevant ideas from optimal control, mainly LQR-based control and LQR's robustness properties, and also from graph theory. The presented results are relevant for the exposition in the subsequent chapters, which represent the contributions of this thesis. A brief statement of main thesis contributions is given in the following paragraphs:

1. We review the structure and spectral properties of the solution of the (large-scale) centralized LQR system. We propose a special case of centralized LQR control where by imposing a specific structure on the weighting matrices, the solution can be constructed by solving a single agent ARE (Algebraic Riccati Equation).
2. We review the structure and spectral properties of the solution of the (large-scale) distributed LQR system. We show that the proposed distributed controller preserves the gain and phase margin properties which are guaranteed in classical LQR control. We illustrate the effectiveness of distributed LQR approach through an example of a multi-agent network consisting of agents described by double integrator dynamics.
3. We develop the method for comparing with respect to the performance cost the family of distributed LQR-suboptimal controllers with the optimal centralized controller. We quantify the cost increase due to decentralization by looking into worst-case, best-case and average deviation from optimality. Additionally, necessary and sufficient conditions have been derived for which a distributed control configuration pattern arising from the optimal centralized solution does not entail loss of performance if the initial state vector lies in a certain subspace of state-space which is identified. We extend the procedure for analysing the performance loss of an arbitrary distributed configuration which is illustrated via an example.

Additionally, in Chapter 6 we review the derivation of 6-DOF nonlinear model of an experimental RPV, X-RAE1, and its linearisation for a specific set of flight conditions. We augment the existing model by actuator dynamical model and by an additional state in order to show that the proposed design provides altitude control. We propose LQR-based control design to stabilise the X-

RAE1. Then, we extend the problem to distributed cooperative scheme for controlling arbitrary formations of UAVs. Through the numerous simulations we show that the proposed schemes are robust to environmental disturbances such as nonuniform wind gusts acting on a formation and to the communication loss between a pair of agents. In this context, we verify that the proposed distributed LQR framework can be used to efficiently control a multi-agent network comprising high order nonlinear dynamics for a specific set of initial conditions.

1.5 Publications

The following conference publications were prepared in the course of this thesis.

- I. Tomić and G. D. Halikias, Robustness properties of distributed configurations in multi-agent systems, *6th IFAC Symposium on System Structure and Control*, IFAC-PapersOnLine, 49(9):86–91, 2016.
- I. Tomić and G. D. Halikias, Performance analysis of distributed control configurations in LQR multi-agent system design, *11th UKACC International Conference on Control*, September 2016. In press.
- I. Tomić, E. Milonidis, and G. D. Halikias, LQR distributed cooperative control of a formation of low-speed experimental UAVs, *11th UKACC International Conference on Control*, September 2016. In press.

1.6 Summary

In this chapter the motivation for the work carried out in this thesis was presented to set the stage for the results derived in subsequent chapters. Additionally, the thesis objectives were given, as well as the thesis outline and the statement of contributions. The chapter was concluded by the list of publications.

Next, the literature review of the related work reported in the literature will be given. In particular, up-to-date research in the areas of cooperative and distributed control, and their application to large-scale UAV networks will be discussed.

Chapter 2

Literature Review

The work presented in this thesis falls in the general field of cooperative control in multi-agent networks. The purpose of this chapter is to give a description of the related work reported in the literature to set the stage for the main results derived in subsequent chapters.

First, we give an introduction to the area of cooperative control in multi-agent networks which is currently progressing in multiple fields. Then, a detailed discussion on recent advances in distributed control techniques for multi-agent systems is given. The discussion is focused mainly in the area of formation control, as it is particularly relevant for the core simulation work of the thesis.

2.1 Cooperative Control in Multi-Agent Networks

As mentioned earlier, cooperation between agents is typically defined as a process of working together towards the same end. Lack of cooperation between the elements in a networked setting would certainly not lead to achieving the goals that were set. Thus, there is a growing interest in defining the framework that will enable large systems to exhibit such cooperative behaviour and reach a certain level of agreement (consensus) that depends on the state of all agents. For a detailed introduction into the area of cooperation and consensus and their many, diverse applications see for instance the surveys by [RBA05], [OSFM07] and [Mur07].

Control of dynamical agents coupled to each other through an information flow network has emerged as a topic of significant interest in recent years. One of the possible realisations for such a system is to use consensus protocols. The first formal study of consensus problems goes back to DeGroot in 1960s ([DeG74]) and was related to development of the basic ideas of statistical consensus theory in management science and statistics. Almost two decades later the view proposed in [DeG74] was developed in different contexts, such as fusion of sensor data ([LK89], [XBL05], [OSS05]), medicine ([WM97]), oscillators synchronisation ([JMB04], [SPL05], [PJ05]), or simulation of flocking behaviour ([Rey87], [VCBJ+95]).

The initial work on consensus and cooperation in networked dynamical systems was based on bi-directional information exchange between neighbouring agents, where the network topology is represented by using undirected communication graph. Examples can be found in [Tsi84], [TBA86], [Rey87], and [VCBJ+95]. Later, this work has been extended to accommodate directed communication graphs for instance in [OSM04] and [RBA05]. Additionally, [OSM04] introduced a protocol that allows nodes to perform asynchronous update (not all of them at the same time).

Further generalisation of the problem allowed the inclusion of switching topologies and agent dynamics, as shown in [TJP03a], [TJP03b], and [JLM02]. Most of these papers are related to unconstrained problems where external conditions are not considered. Usually, constrained consensus problems are addressed by one of the following three approaches: leader-following approach ([Wan91], [FM04], [JME06]), virtual structure-based approach ([TL96], [BLH00]), and behaviour-based approach ([BA98], [VSH99], [LBY03]). All three approaches are systematically reviewed in [Kno11].

In addition to the study of the consensus and cooperative control for systems with simple dynamics, for example single-integrator dynamics and double-integrator dynamics, ([LDCH10], [Tun08]) consensus problem for nonlinear systems was also considered by a number of authors. The main nonlinear systems dynamics studied in the consensus problem include nonholonomic mobile robots ([DK07]), rigid bodies ([NL08], [Ren07]), complex networks ([ZLL06]), etc.

The theoretical framework for solving problems in dynamical systems by using consensus technology was proposed in [OSM03] and [OSM04]. Authors devel-

oped protocols for reaching consensus in fixed, but also in switching network topologies. In addition, presence of communication time-delays was taken into account, along with the nature of the information flow (directed or undirected).

The beforementioned framework was of fundamental importance in design of distributed algorithms for motion coordinated tasks such as rendezvous in [CMB06], flocking in [OS06], and formation control in [Fax02], [OSM02], [FM04]; as well as information processing tasks in sensor networks (see e.g. [OSS05], [OS05], [SOSM05]).

A detailed discussion on recent advances in distributed control techniques for multi-agent systems is given next. The overview is focused mainly in the area of formation control, as the core simulation work of this thesis is related to this particular topic.

2.2 Distributed Control of Multi-Agent Systems

In [Sha07], the author highlights the fact that in a broad spectrum of applications, ranging from robotics and formation flight to civil engineering, distributed controllers with limited information of the system are increasingly replacing centralized controllers which rely on the complete knowledge of the system. Often the information exchange is captured as a graph, and many researchers have obtained novel results by combining graph theory and control approaches, see e.g. [BPD02], [LFM07].

Multi-agent systems are formed from a large number of dynamical subsystems, such as unmanned aerial vehicles (UAVs), unmanned ground vehicles (UGVs), unmanned underwater vehicles (UUVs), satellites, or mobile robots. In this thesis we are interested in UAVs that can be defined as autonomous flying vehicles equipped with sensing devices that have many potential military and civil applications, but are also of great scientific significance in academic research; however, results presented in this thesis can be applied to any other type of multi-agent network.

In general, there are three possible control methods for multi-agent systems, centralized, decentralized and distributed control. Comparison of all these methods has been undertaken in [MV09] and conclusions tend to favour distributed control. The authors also provided an example of satellite formation control in [MV08] where they showed that centralized solution provides optimal performance, but it becomes infeasible as the number of satellites and the distance between them increases. A completely decentralized solution where each satellite has its own controller is more beneficial; however this approach is usually not able to guarantee the required level of performance as positioning criteria between satellites have to be considered. Distributed control architecture is proposed as an alternative solution where additional communication between neighbouring satellites is employed. All three control configurations are depicted in Figure 2.1.

Distributed control approaches can be grouped into different categories depending on the assumptions made on:

- The type of system that should be controlled (linear, nonlinear, continuous-

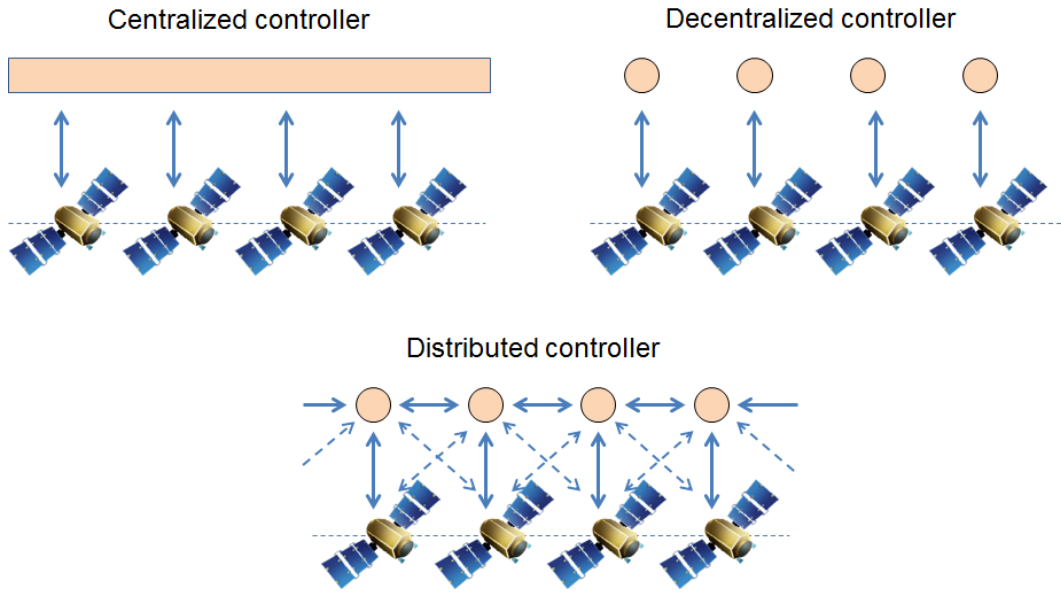


Figure 2.1: Different types of controllers (The information flow is represented by arrows.) [MV08]

time, discrete-time, etc.),

- The type of interaction between subsystems (dynamics, constraints),
- The model of information exchange, and
- The control design technique used.

Dynamically coupled systems are the most studied, see for example [WD73], [CJKT02], [LCD04]. In this thesis we focus on *decoupled systems* as our lives are affected by the enormous use of networks of independently actuated systems on a daily basis. Some examples are networks of vehicles in formation, network of cameras used for surveillance, production units in power plants, etc. In a descriptive way, dynamically decoupled multi-agent systems can be defined as a collection of subsystems that can be independently actuated, but share a common objective which forces them to interact with each other. Coupling between subsystems is described by a communication graph, at each node of which the models of the neighbouring nodes are used to predict its behaviour.

Distributed control techniques are widely used in different areas of multi-agent networks. Therefore, we narrowed our further overview to the topics of formation control and optimal control which is given next.

2.2.1 Formation Control

The problem of coordinating a predefined multivehicle formation while moving in space, known as *formation control*, is a topic of considerable interest to the controls community. This is mainly due to its advantages over conventional systems, such as a reduction of system cost, an increase in the efficiency and robustness of the system, etc., see e.g. [SB00]. In general, we can identify two different approaches in formation control depending on whether a group reference exists or not. These two methods are known as *formation tracking* and *formation producing*, respectively. For us it is more meaningful to study formation control in the presence of a group reference that is assumed as the objective for the whole group.

The analysis of a formation of interacting and cooperating identical subsystems, where the communication topology of the network was modelled using graph theory, was first proposed in [FM04]. Further, necessary and sufficient stability conditions for a given communication topology were derived. This framework was used in [PW09] to establish robust controller properties for an arbitrary communication topology and any number of subsystems, whereas previous solutions were adequate only for undirected communication networks.

The overview of existing literature in formation tracking is usually based on the approaches used in stability analysis and these can be divided into four different categories [RC11]:

1. Matrix theory approach - It is mainly based on the properties of the augmentation of reducible or irreducible nonnegative matrices [QWH08]. More examples where this approach has been used can be found in [CRL09], [RA08], [XWL09], etc.
2. Potential function approach - A controller is designed based on the gradient of the chosen potential function which can be defined as an extension to flocking phenomenon. For more details see [OS06], [SWL09], [Do08].
3. Lyapunov-based approach - Where system stability is provided by finding a proper Lyapunov function. Some examples found in the literature are: [DF08], [GAP⁺09] and [PLS08].
4. Other approaches - Such as partial differential equations approach in [FTBG06], neural networks approach in [DJ09], etc.

2.2.2 Optimal Control

In contrast to classical control where the primary aim was to stabilise the plant, optimal control provides analytical designs that are not supposed merely to be stable, but to be the *best* possible (i.e. optimal) in some sense.

In distributed multi-agent networks optimal control is usually studied in the context of convergence speed (i.e. how fast consensus is achieved) or cost function optimisation. For more details on convergence speed analysis the reader is referred to [OSM04], [OT09] and [AB09]. Alternatively, a cost function can be defined at the level of an agent or at the level of the whole network. In this thesis, we are interested in global cost functions where the performance of the whole group is considered.

Most of the research in the area of distributed multi-agent optimal control is based on the concept of distributed model predictive control (DMPC) presented in [Kev05], [KBB05] and [KBB06]. This framework was simplified to the case of identical unconstrained linear time-invariant systems and the application of LQR-based theory to distributed control was introduced. This allowed the emergence of a simple control approach that can be applied to a class of systems for which existing methods are either not efficient or would not be directly applicable. Next, we give examples from different areas where LQR distributed control was successfully applied due to its guaranteed robustness properties (see [SA76]).

In [CR10] an LQR-based method was proposed for optimal control of multi-vehicle systems with single-integrator dynamics in a continuous-time setting. In [LG09], the authors analysed the influence of the topology of the interconnection graph on the closed-loop performance achieved by subsystems in a distributed LQR framework. In [DMEP11], the authors proposed a Linear Matrix Inequality (LMI) based distributed LQR design with guaranteed LQR cost for identical dynamically coupled systems. In this case, the solution depends on the total number of agents, while in [BK08] (for a similar LQR cost function) this was derived as a function of the maximum vertex degree. In addition, an estimate of the bound on the maximum time delay that can be accommodated was also obtained. In [WYGL13], it was shown that the distributed LQR control law guarantees not only optimal performance at the network level but also a convergence rate for the group of subsystems. However, in many applications full state information is not always available for controller design. Therefore,

a procedure for designing distributed observer-based controllers has been developed in [GS14]. The problem of introducing delayed relative information with respect to neighbouring agents to the classical local optimal control law was considered in [SME13]. Authors demonstrated that for some cases the introduction of delays leads to the better performance (in terms of the LQR cost) than when a traditional decentralised approach is used.

An alternative approach to structured distributed controllers that has appeared in the literature is given in [LFJ11] and [LFJ12]. By employing the augmented Lagrangian method the structured optimal feedback gains can be designed without the knowledge of a stabilising structured gain to initiate the algorithm. Also, in [FZLW14] the authors used inverse optimal approach to design distributed cooperative control protocols for identical linear systems that guarantee consensus and global optimality with respect to a positive definite quadric performance index.

The distributed H_2 and H_∞ control problems for multi-agent systems were analysed in [LDC11]. The authors showed that the H_∞ performance limit of the network controlled by a distributed controller is equal to the minimal H_∞ norm of an individual agent, while in the H_2 case the performance limit scales with the size of the network.

The present work is inspired by [BK08] where the authors proposed an approach which leads to an elegant and powerful result: the synthesis of stabilising distributed control laws can be obtained by using a simple local LQR problem whose size depends on the maximum vertex degree of the graph.

2.3 Summary

In this chapter up-to-date research in the areas of cooperative and distributed control, and their application to large-scale UAV networks were discussed. The main approaches in formation tracking were introduced, as well as the application of distributed control techniques to the area of optimal control.

In the next chapter the fundamental and necessary methods and techniques of optimal control will be introduced. The overview will be focused on linear quadratic regulator problems and their stability and robustness properties. These will be crucial in the application of optimal and suboptimal LQR-based controllers to multi-agent network control in Chapter 4 and Chapter 5 which represent the main contributions of this thesis.

Chapter 3

Linear Quadratic Regulator

In this chapter some of the methods and techniques of what is known as "optimal control" are presented. In contrast to classical control where the primary aim was to stabilise the plant, optimal control provides analytical designs that are not supposed merely to be stable, but to be the *best* possible (i.e. optimal) systems in some sense. For more details see [AM89].

We are assuming that the plant controlled is linear, as well as the controller used. This branch of optimal control is known as *linear optimal control* and the methods considered here are termed *Linear Quadratic (LQ) methods*. Further, we are assuming that all states are measured and available for feedback. Hence full-state feedback design is applied, which gives a number of attractive properties, such as good gain and phase margins, good tolerance to nonlinearities, etc.

In the next few sections the necessary mathematical preliminaries are given first. Then, linear quadratic regulator problem is introduced for the case of a single linear system. Stability and robustness properties of the optimal LQR are presented for the case of single-input systems, which are then extended to the case of multi-input systems. The stability margins of the LQR controller will be used in a future chapter to guarantee asymptotic stability of a distributed LQR-based control scheme.

3.1 Mathematical Preliminaries

In this section we summarise the mathematical notation and definitions used throughout the thesis.

3.1.1 Notation

Notation 1. I_n denotes the identity matrix of dimension n , $I_n \in \mathbb{R}^{n \times n}$.

Notation 2. $\mathbf{a} \in \mathbb{R}^{n \times 1}$ denotes the column vector, such that $\mathbf{a} = [a_1, \dots, a_n]^T$.

Notation 3. M^T and \mathbf{a}^T denote the transpose of the matrix M and the vector $\mathbf{a} = [a_1, \dots, a_n]^T$, respectively.

Notation 4. $M^H = \bar{M}^T$ denotes the conjugate transpose of the matrix M .

Notation 5. $A \otimes B$ denotes the Kronecker product of A and B . Let $A \in \mathbb{R}^{m \times n}$ and $B \in \mathbb{R}^{p \times q}$, then:

$$A \otimes B = \begin{pmatrix} a_{11}B & a_{12}B & \dots & a_{1n}B \\ a_{21}B & a_{22}B & \dots & a_{2n}B \\ \vdots & \vdots & \ddots & \vdots \\ a_{m1}B & a_{m2}B & \dots & a_{mn}B \end{pmatrix} \in \mathbb{R}^{mp \times nq}.$$

Notation 6. Let $M \in \mathbb{R}^{n \times n}$. Then, $M[1 : i, 1 : j]$ denotes the block in M consisting of first i rows of M and first j columns of M where $i, j = 1, \dots, n$.

Notation 7. Let $M \in \mathbb{R}^{n \times n}$. The spectrum of M is denoted as $\mathcal{S}(M) = \{\lambda_1(M), \lambda_2(M), \dots, \lambda_n(M)\}$. If the spectrum is real, $\lambda_i(M)$ denotes the i th eigenvalue of M indexed in decreasing order.

3.1.2 Definitions

Definition 3.1.1. A matrix $M \in \mathbb{R}^{n \times n}$ is called *stable* or *Hurwitz matrix* if all its eigenvalues have negative real part, i.e. $\mathcal{S}(M) \subseteq \mathbb{C}_-$.

Definition 3.1.2. A matrix $M \in \mathbb{C}^{n \times n}$ is called *Hermitian* if $M = M^H$, where M^H is its conjugate transpose.

Definition 3.1.3. Let $A \in \mathbb{R}^{n \times n}$ and $B \in \mathbb{R}^{n \times n}$. The matrix A will be *similar* to B if there is an invertible matrix $P \in \mathbb{R}^{n \times n}$, such that $A = P^{-1}BP$. In this case, A and B have the same characteristic equation, and hence, the same eigenvalues and corresponding algebraic multiplicities. This can be easily proved as follows:

$$\begin{aligned} \det(A - \lambda I) &= \det(P^{-1}BP - \lambda I) = \det(P^{-1}BP - \lambda P^{-1}IP) = \\ &= \det(P^{-1}(B - \lambda I)P) = \det(P^{-1}) \det(B - \lambda I) \det(P) = \\ &= \det(P^{-1}P) \det(B - \lambda I) = \det(B - \lambda I). \end{aligned}$$

Definition 3.1.4. [ZDG96] A finite dimensional linear time-invariant dynamical system can be described by the following set of equations:

$$\begin{aligned} \dot{\mathbf{x}} &= A\mathbf{x} + B\mathbf{u}, \quad \mathbf{x}(0) = \mathbf{x}_0 \\ \mathbf{y} &= C\mathbf{x} + D\mathbf{u} \end{aligned} \tag{3.1}$$

where $\mathbf{x} \in \mathbb{R}^{n \times 1}$, $\mathbf{u} \in \mathbb{R}^{m \times 1}$, and $\mathbf{y} \in \mathbb{R}^{p \times 1}$ are the system state vector, system input vector, and system output vector, respectively. Further, $\mathbf{x}(0)$ is the initial state vector, while A , B , C and D are appropriately dimensioned real constant matrices.

Definition 3.1.5. [ZDG96] The dynamical system $\dot{\mathbf{x}}(t) = A\mathbf{x} + B\mathbf{u}$, $\mathbf{x}(0) = \mathbf{x}_0$, where $A \in \mathbb{R}^{n \times n}$ and $B \in \mathbb{R}^{n \times m}$, is said to be *controllable* if for any initial state \mathbf{x}_0 , $t_1 > 0$ and final state \mathbf{x}_1 , there exist an input $\mathbf{u}(\cdot)$ such that the solution of the system satisfies $\mathbf{x}(t_1) = \mathbf{x}_1$.

Definition 3.1.6. [ZDG96] The dynamical system $\dot{\mathbf{x}}(t) = A\mathbf{x} + B\mathbf{u}$, $\mathbf{y} = C\mathbf{x} + D\mathbf{u}$, where $A \in \mathbb{R}^{n \times n}$, $B \in \mathbb{R}^{n \times m}$, $C \in \mathbb{R}^{p \times n}$ and $D \in \mathbb{R}^{p \times m}$, is said to be *observable* if for any $t_1 > 0$, initial state \mathbf{x}_0 can be determined uniquely from the time history of the input $\mathbf{u}(t)$ and the output $\mathbf{y}(t)$ in the interval $[0, t_1]$.

Definition 3.1.7. *The pair (A, B) is stabilisable if (A, B) is controllable or if the uncontrollable eigenvalues of A , if any, have negative real parts, i.e. $\mathcal{S}(A) \subseteq \mathbb{C}_-$.*

Definition 3.1.8. *The pair (A, C) is detectable if (A, C) is observable or if the unobservable eigenvalues of A , if any, have negative real parts, i.e. $\mathcal{S}(A) \subseteq \mathbb{C}_-$.*

Definition 3.1.9. [BK08] *The class of matrices denoted as $\mathcal{K}_{n,m}^N(\mathcal{G})$ for a graph \mathcal{G} can be defined as follows:*

$$\begin{aligned} \mathcal{K}_{n,m}^N(\mathcal{G}) = & \{M \in \mathbb{R}^{nN \times mN} \mid M_{ij} = 0 \text{ if } (i, j) \notin \mathbf{A}, \\ & (M_{ij} = M[(i-1)n+1 : in, (j-1)m+1 : jm] \text{ if } (i, j) \in \mathbf{A} \\ & \text{where } i, j = 1, 2, \dots, N_d\} \end{aligned}$$

where \mathbf{A} is the adjacency matrix defined in Section 4.1 and N is the number of agents.

3.2 LQR Problem Description

Consider a collection of N dynamical agents with identical dynamics. The i th agent is described by the continuous-time dynamical system:

$$\dot{\mathbf{x}}_i(t) = A\mathbf{x}_i + B\mathbf{u}_i, \quad \mathbf{x}_i(0) = \mathbf{x}_{i0} \quad (3.2)$$

where $A \in \mathbb{R}^{n \times n}$, $B \in \mathbb{R}^{n \times m}$ and $\mathbf{x}_i(t) \in \mathbb{R}^n$, $\mathbf{u}_i(t) \in \mathbb{R}^m$ are the state and input vectors at time t , respectively.

The standard infinite time horizon LQR control problem for system (3.2) is to find the control input that minimizes a quadratic cost function:

$$J(\mathbf{u}_i(t), \mathbf{x}_{i0}) = \int_0^\infty (\mathbf{x}_i(t)^T Q \mathbf{x}_i(t) + \mathbf{u}_i(t)^T R \mathbf{u}_i(t)) dt \quad (3.3)$$

with weighting matrices $Q = Q^T \geq 0$ and $R = R^T > 0$. The matrix Q can be also expressed as $Q = C^T C$ where C is a $p \times n$ matrix, with $p \leq n$. The fact that R is strictly positive definite implies that there always exists a non-zero cost associated with the control law, unless $\mathbf{u} \equiv \mathbf{0} \forall t \in [0, \infty]$. The positive semi definiteness of Q implies the potential irrelevance of some linear states combination for the problem at hand [Pre02].

Given an initial condition \mathbf{x}_{i0} vector, it can be shown (e.g. see [KS72]) that the optimal control input is given by

$$\mathbf{u}_i = -K \mathbf{x}_i \quad (3.4)$$

where K is the LQR gain matrix given by

$$K = R^{-1} B^T P \quad (3.5)$$

and P is the unique symmetric positive definite solution of the following ARE:

$$A^T P + P A - P B R^{-1} B^T P + Q = 0. \quad (3.6)$$

Equation (3.6) is nonlinear in P . The existence and uniqueness of a positive definite stabilising solution (i.e. $\mathcal{S}(A - B R^{-1} B^T P) \subseteq \mathbb{C}_-$) is guaranteed by the controllability of (A, B) pair and observability of (A, C) pair (see Definition 3.1.5 and Definition 3.1.6). Necessary and sufficient controllability and observability conditions are well known and given in the theorems that follow.

Theorem 3.2.1. [ZDG96] *The following statements are equivalent:*

1. (A, B) is controllable.
2. The controllability matrix $C_o = \begin{bmatrix} B & AB & A^2B & \dots & A^{n-1}B \end{bmatrix}$ has full rank.
3. The matrix $[A - \lambda I, B]$ has full rank for all $\lambda \in \mathbb{C}$.
4. There exist no eigenvector ξ of A ($\xi \neq \mathbf{0}$) such that $\xi^T B = \mathbf{0}$.
5. The controllability Gramian $W_c(t) = \int_0^t e^{A\tau} B B^T e^{A^T \tau} d\tau$ is positive definite for any $t > 0$.

Theorem 3.2.2. [ZDG96] *The following statements are equivalent:*

1. (A, C) is observable.
2. The observability matrix $O_b = \begin{bmatrix} C^T & (CA)^T & (CA^2)^T & \dots & (CA^{n-1})^T \end{bmatrix}^T$ has full rank.
3. The matrix $\begin{bmatrix} A - \lambda I \\ C \end{bmatrix}$ has full rank for all $\lambda \in \mathbb{C}$.
4. There exist no eigenvector ξ of A ($\xi \neq \mathbf{0}$) such that $C\xi = \mathbf{0}$.
5. The observability Gramian $W_o(t) = \int_0^t e^{A^T \tau} C^T C e^{A\tau} d\tau$ is positive definite for any $t > 0$.

If these conditions are satisfied, then the i th closed-loop system:

$$\dot{\mathbf{x}}_i(t) = (A - BK)\mathbf{x}_i \tag{3.7}$$

is asymptotically stable. The closed-loop block diagram of the optimal LQR controller for system (3.2) is shown in Fig. 3.1.

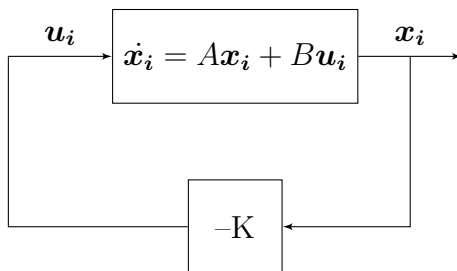


Figure 3.1: Closed-loop LQR system

In addition, when $\mathbf{u}_i = -K\mathbf{x}_i$ the cost function (3.3) will attain its minimum for

$$J(\mathbf{u}_i(t), \mathbf{x}_{i0}) = \int_0^\infty (\mathbf{x}_i(t)^T (Q + K^T R K) \mathbf{x}_i(t)) dt. \quad (3.8)$$

In order to compute the optimal cost J , consider the positive quadratic function $V(t)$, such that $V(t) = \mathbf{x}_i^T \tilde{P} \mathbf{x}_i$, where \tilde{P} is the solution of the Lyapunov equation of the closed-loop system given by

$$\tilde{P}(A - BK) + (A - BK)^T \tilde{P} + Q + K^T R K = 0. \quad (3.9)$$

Then, the decay rate of $V(t)$ is

$$-\dot{V}(t) = -\frac{d}{dt}(\mathbf{x}_i^T \tilde{P} \mathbf{x}_i) = -\mathbf{x}_i^T \tilde{P} \dot{\mathbf{x}}_i - \dot{\mathbf{x}}_i^T \tilde{P} \mathbf{x}_i. \quad (3.10)$$

By substituting (3.7) into (3.10) and using (3.9), one gets

$$\begin{aligned} -\frac{d}{dt}(\mathbf{x}_i^T \tilde{P} \mathbf{x}_i) &= -\mathbf{x}_i^T [(A - BK)^T \tilde{P} + \tilde{P}(A - BK)] \mathbf{x}_i \\ &= \mathbf{x}_i^T (Q + K^T R K) \mathbf{x}_i. \end{aligned} \quad (3.11)$$

Comparison of the two sides results in (3.9) which is true for any \mathbf{x}_i . Therefore, the minimum value of the cost can be evaluated as

$$\begin{aligned} J(\mathbf{u}_i(t), \mathbf{x}_{i0}) &= \int_0^\infty (\mathbf{x}_i(t)^T (Q + K^T R K) \mathbf{x}_i(t)) dt = -\mathbf{x}_i^T \tilde{P} \mathbf{x}_i \Big|_0^\infty \\ &= -\mathbf{x}_i(\infty)^T \tilde{P} \mathbf{x}_i(\infty) + \mathbf{x}_i(0)^T \tilde{P} \mathbf{x}_i(0). \end{aligned} \quad (3.12)$$

Since $A - BK$ is Hurwitz, then $\mathbf{x}_i(t) \rightarrow 0$ for any $\mathbf{x}_{i0} \in \mathbb{R}^n$ and the minimum cost will be attained for

$$J = \mathbf{x}_i(0)^T \tilde{P} \mathbf{x}_i(0) = \mathbf{x}_{i0}^T \tilde{P} \mathbf{x}_{i0}. \quad (3.13)$$

Furthermore, by substituting $K = R^{-1} B^T P$ and after some algebra (3.9) becomes:

$$\tilde{P}A - \tilde{P}B R^{-1} B^T P + A^T \tilde{P} - P B R^{-1} B^T \tilde{P} + Q + P B R^{-1} B^T P = 0 \quad (3.14)$$

which, when compared with (3.6), is identically satisfied by $\tilde{P} = P$. Thus, the

optimal cost related to the solution of LQR problem will be

$$J = \min \int_0^{\infty} (\mathbf{x}_i(t)^T Q \mathbf{x}_i(t) + \mathbf{u}_i(t)^T R \mathbf{u}_i(t)) dt = \mathbf{x}_{i0}^T P \mathbf{x}_{i0} \quad (3.15)$$

where $\mathbf{x}_{i0} = \mathbf{x}_i(0)$.

The closed-loop system poles are directly dependent on the matrices Q and R . In the case when controlled variables are not clearly identified, Q is chosen in such way that term $\mathbf{x}_i(t)^T Q \mathbf{x}_i(t)$ represents the total energy in the system i , while positive definite matrix R is multiplied by an adjustable parameter ρ in order to achieve reasonable fast closed-loop poles without excessive values of the control effort [Pre02]. A simple and reasonable choice for the matrices Q and R in (3.15) is given by *Bryson's rule* [FPEN01]. According to this rule both Q and R have a diagonal structure where individual diagonal elements are given by

$$Q_{ii} = \frac{1}{\text{maximum acceptable value of } \mathbf{x}_i^2}, \quad i = 1, \dots, n$$

$$R_{ii} = \frac{1}{\text{maximum acceptable value of } \mathbf{u}_i^2}, \quad i = 1, \dots, m.$$

Although Brysons rule usually gives good results, often it is just the starting point for a trial-and-error iterative design procedure which aims to obtaining desirable properties for the closed-loop LQR system.

Next, we discuss the assumptions made about the controllability of (A, B) pair and observability of (A, C) pair. These can be relaxed to the notion of stabilisability and detectability (see Definition 3.1.7 and Definition 3.1.8) which is summarised in the theorem that follows.

Theorem 3.2.3. [ZDG96] *Consider the time invariant system in (3.2) where (A, B) pair is stabilisable. If the cost function is defined as (3.3) with $Q = C^T C \geq 0$ and $R > 0$, the solution P to the ARE:*

$$A^T P + P A - P B R^{-1} B^T P + Q = 0 \quad (3.16)$$

will exist and the optimal control is given by $\mathbf{u}_i = -R^{-1} B^T P \mathbf{x}_i$. Furthermore, if (A, C) is detectable, then the closed-loop system is stable and P is positive semi definite solution, i.e. $P \geq 0$.

Proof. See [ZDG96]. □

3.3 Gain and Phase Margins of the LQR

In this section the gain and phase margins for the single-input LQR systems will be reviewed. These two concepts will be generalised to the case of multi-input systems.

The *gain margin* of an internally stable feedback system is the largest amount by which the loop gain can be changed while preserving the stability of the system. By convention, a closed-loop system which is always stable, no matter how large the gain becomes, has an infinite gain margin. On the other side, the *phase margin* can be described as the minimum amount of negative phase shift needed to make the part of the Nyquist plot, corresponding to $\omega \geq 0$, to pass through $-1 + i0$ point [AM89]. Nyquist plot is used to access the stability criterion proposed by Nyquist, based on the theory of functions of one complex variable due to Cauchy. Cauchy's theorem is concerned with mapping contours in a complex s -plane which is described in more details later [DB00].

First, we will present some background results pertaining to the open-loop and closed-loop transfer functions of LQR systems. Also, we will introduce the concept of return difference transfer matrix and extend it further to the concept of return difference equality/inequality.

3.3.1 Return Difference Equality and Inequality

In order to establish the gain and phase margins for single-input LQR systems defined in Definition 3.1.4, we have to consider the open-loop system depicted in Figure 3.2. The transfer function of the plant is given by

$$G(s) = \frac{Y(s)}{U(s)} = (sI - A)^{-1}B \quad (3.17)$$

where $U(s)$ and $Y(s)$ are the Laplace transforms of the control input $\mathbf{u}(t)$ and the output $\mathbf{y}(t)$. Then, the open loop transfer matrix is

$$T_o(s) = K(sI - A)^{-1}B. \quad (3.18)$$

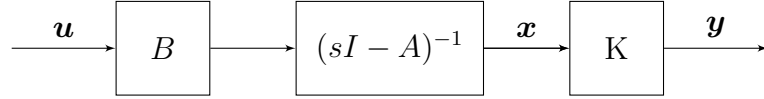


Figure 3.2: Open-loop LQR system

The plant with the optimal LQR gain K is given in Figure 3.3.

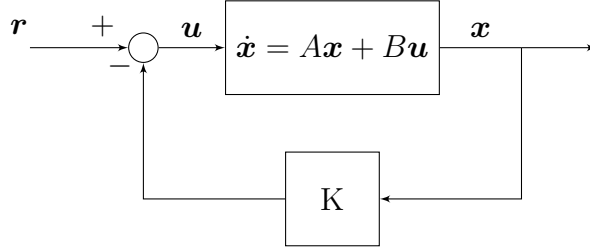


Figure 3.3: Classical representation of state feedback LQR system

In order to establish the gain margin property of LQR, the classical representation of the state feedback in Figure 3.3 is not suitable. Therefore, the scheme can be redrawn as the unity feedback representation which is depicted in Figure 3.4.

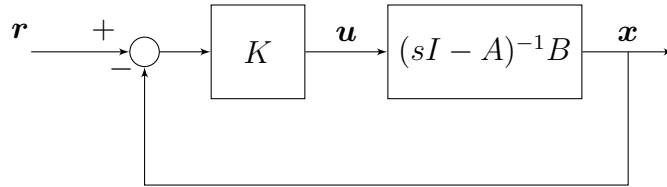


Figure 3.4: Unity feedback representation of state feedback LQR system

Then, introducing an external reference signal \mathbf{r} the closed loop transfer matrix is given by

$$T_c(s) = K(sI - A + BK)^{-1}B. \quad (3.19)$$

In order to derive the return difference transfer matrix we consider a breaking point at the input side of the closed-loop LQR system in Figure 3.4. The new scheme is depicted in Figure 3.5 and the open-loop transfer matrix from the process' input \mathbf{u} to the controller's output $\hat{\mathbf{u}}$ is given by

$$L(s) = K(sI - A)^{-1}B. \quad (3.20)$$

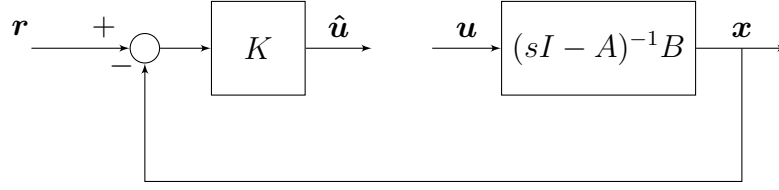


Figure 3.5: State feedback open-loop gain

The return difference transfer matrix for the same system is defined as a difference of the signal before and after feedback loop and is given by

$$F(s) = I + K(sI - A)^{-1}B = I + L(s). \quad (3.21)$$

The discussion below is based on the optimal return difference relation which is known as *Kalman's equality* which is summarised in the proposition that follows (for more details see [Lew86], [KS72], [GJ86]).

Proposition 3.3.1. *For the LQR criterion in (3.3) the following equality holds*

$$(I + L(-s)^T)R(I + L(s)) = R + F(-s)^T Q F(s) \quad (3.22)$$

where $F(s)$ and $L(s)$ are as described in (3.20) and (3.21), respectively. By setting s in (3.22) to equal to $j\omega$ and using the fact that for real-rational transfer functions

$$F(-j\omega)^T = F(j\omega)^H, \quad L(-j\omega)^T = L(j\omega)^H, \quad F(j\omega)^H F(j\omega) \geq 0$$

the *Kalman's inequality* can be derived which is one of many important consequences of (3.22) and is given by

$$(I + L(j\omega))^H R (I + L(j\omega)) \geq R, \quad \forall \omega \in \mathbb{R}. \quad (3.23)$$

Proof. See [Hes05]. □

Proposition 3.3.1 will be used in next sections to derive gain and phase margin properties for the single-input systems which is then extended to the multi-input case.

3.3.2 Single-Input Systems

For the single-input process $L(j\omega)$ is a scalar transfer function. Therefore, if we divide both sides of Kalman's inequality (3.23) by the scalar R we get:

$$|1 + L(j\omega)| \geq 1, \quad \forall \omega \in \mathbb{R}. \quad (3.24)$$

This implies that the Nyquist diagram of $L(j\omega)$ will always remain outside a circle of unit radius centred at $-1 + i0$. Also, the asymptotic stability of the closed-loop system limits the number of counterclockwise encirclements of the point $-1 + i0$ to the number of poles of the transfer function $L(j\omega)$ lying in $\Re[s] \geq 0$. Further, two significant implications can be noted which are given next:

- *Positive gain margin* - If gain is multiplied by a constant factor $\beta > 1$ the Nyquist plot expands radially and the stability is preserved as the the number of counterclockwise encirclements of $-1 + i0$ stays equal to the number of poles of the transfer function $L(j\omega)$ lying in $\Re[s] \geq 0$.
- *Negative gain margin* - If gain is multiplied by a constant factor $1 > \beta > 0.5$ the Nyquist plot contracts radially; however, the number of encirclement still does not change and this corresponds to the negative gain margin of $20 \log_{10}(0.5) = -6\text{dB}$.

Therefore, the infinite gain margin property for the LQR is established, but with the downside margin of $\frac{1}{2}$. Two possible Nyquist plots of $L(j\omega)$ are given in Figure 3.6. Note that, in Figure 3.6 (b) point A could cross -1 if gains

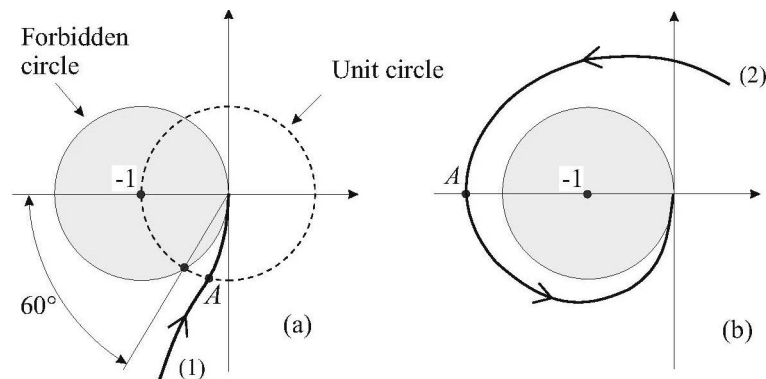


Figure 3.6: Nyquist plots of $L(j\omega)$. (a) Stable open-loop transfer function. (b) Open-loop transfer function with two unstable poles [Pre02]

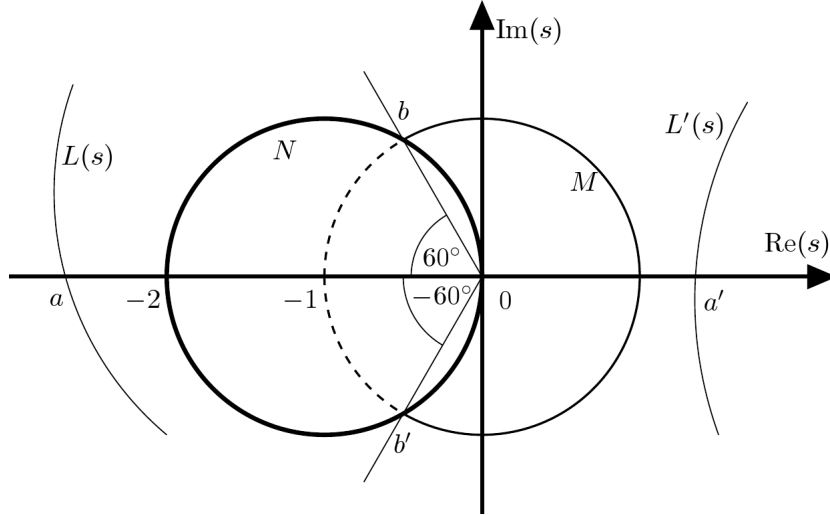


Figure 3.7: Illustration of LQR phase tolerance [Che14]

were reduced. However, this will not happen as long as multiplying factor β is larger than $\frac{1}{2}$.

The phase margin is determined from the points on the $\omega \geq 0$ part of the Nyquist diagram, that are at unit distance from the origin. The maximum phase tolerance corresponds to the phase angles of the intersection points b and b' between unit circle M centred $(0, 0)$ and unit circle N centred at $(-1, 0)$ which is depicted in Figure 3.7. The smallest angle that will allow points on the unit circle that are outside the prohibited area to reach $(-1, 0)$ by moving in clockwise direction, is 60° . Therefore, the phase margin is bounded from below by 60° .

Additionally, for the single-input case we can define the sensitivity function $S(s)$ and the complementary sensitivity function $T(s)$ by

$$S(s) = \frac{1}{1 + L(s)}, \quad T(s) = \frac{L(s)}{1 + L(s)}, \quad (3.25)$$

respectively. The Kalman's inequality in (3.23) guarantees following:

$$|S(j\omega)| \leq 1, \quad \forall \omega \in \mathbb{R} \quad (3.26)$$

$$|T(j\omega) - 1| \leq 1, \quad |T(j\omega)| \leq 2, \quad \Re[T(j\omega)] \geq 0, \quad \forall \omega \in \mathbb{R}. \quad (3.27)$$

In order to provide a good disturbance rejection the sensitivity function should be small. Also, for a good reference tracking and good noise rejection the complementary sensitivity function should be close to one [Hes05].

The gain and phase margins are not the only robustness indicators. As an additional measure of how much the system is robust *module margin* can be used, which defines the minimal distance between the Nyquist curve and the critical point $(-1, 0)$. Module margin corresponds to the inverse of the infinity norm of the sensitivity function and it quantifies how sensitive is the closed-loop system to variations of the considered plant. Additionally, good module margin implies good gain and phase margins and sometimes it can be seen as a better robustness indicator [GKL03].

Next, the gain and margin analysis is extended to multi-input systems.

3.3.3 Multi-Input Systems

Results obtained for single-input case can be extended to multi-input systems, such that for each control channel the theory will guarantee good performance for gain margins between $\frac{1}{2}$ and ∞ and for the phase margin greater than 60° .

The starting point is still the return difference or Kalman's inequality in (3.23) from which we have:

$$F(j\omega)^H R F(j\omega) \geq R, \quad \forall \omega \in \mathbb{R}. \quad (3.28)$$

where $F(j\omega) = I + K(j\omega I - A)^{-1}B$ is the return difference transfer matrix.

If $R = \rho I$, where ρ is an adjustable positive parameter, it can be proved (see [SA76]) that

$$F(j\omega)^H F(j\omega) \geq I. \quad (3.29)$$

Then, (3.29) implies that there is at least 60° of phase margin in each input channel, while the gain in each channel can be increased indefinitely without losing stability with a margin of at least 6dB against gain reductions. For more details we refer the reader to [SA76].

For more general R the complete analysis of gain and phase margins in multi-input systems is given in [AM89]. These results are omitted here as we assume the diagonal structure of R throughout the thesis, which corresponds to the results in [SA76] which are presented here.

Additionally, let $\sigma(F)$ be any singular value of F . Then, it can be easily shown

that [AM89]:

$$\sigma[F(j\omega)] \geq 1 \quad (3.30)$$

which implies that the minimum singular value of $F(j\omega)$, $\underline{\sigma}[F(j\omega)]$, is bounded from below by 1 for all $\omega \in \mathbb{R}$. This property is not easily revealed for the case of general matrix R . For more details we refer the reader to [AM89]. Next, we give an example on multivariable feedback system robustness properties.

Numerical Example - Multivariable Feedback System Robustness Properties

Consider the linear system specified by

$$\begin{aligned} \begin{pmatrix} \dot{x}_1 \\ \dot{x}_2 \end{pmatrix} &= \begin{pmatrix} -1 & 0 \\ 0 & -1 \end{pmatrix} \begin{pmatrix} x_1 \\ x_2 \end{pmatrix} + \begin{pmatrix} 1 & b_{12} \\ 0 & 1 \end{pmatrix} \begin{pmatrix} u_1 \\ u_2 \end{pmatrix} \\ \begin{pmatrix} y_1 \\ y_2 \end{pmatrix} &= \begin{pmatrix} x_1 \\ x_2 \end{pmatrix}. \end{aligned} \quad (3.31)$$

If the following feedback compensation is used:

$$\begin{aligned} u_1 &= -x_1 + u_{c1} \\ u_2 &= -x_2 + u_{c2} \end{aligned} \quad (3.32)$$

the closed-loop system becomes:

$$\begin{pmatrix} \dot{x}_1 \\ \dot{x}_2 \end{pmatrix} = \begin{pmatrix} -2 & -b_{12} \\ 0 & -2 \end{pmatrix} \begin{pmatrix} x_1 \\ x_2 \end{pmatrix} + \begin{pmatrix} 1 & b_{12} \\ 0 & 1 \end{pmatrix} \begin{pmatrix} u_{c1} \\ u_{c2} \end{pmatrix}. \quad (3.33)$$

The return difference matrix, $F(s) = I + G(s)$, is given by

$$F(s) = \begin{pmatrix} \frac{s+2}{s+1} & \frac{b_{12}}{s+1} \\ 0 & \frac{s+2}{s+1} \end{pmatrix} \quad (3.34)$$

and thus

$$|I + G(s)| - 1 = \frac{2s + 3}{(s + 1)^2}. \quad (3.35)$$

The Nyquist diagram of $\frac{2s+3}{(s+1)^2}$ is depicted in Figure 3.8. In terms of SISO robustness properties, the system has an infinite upward gain margin, a negative gain margin of $-\frac{1}{3}$ and a phase margin of $\pm 106^\circ$. However, the analysis

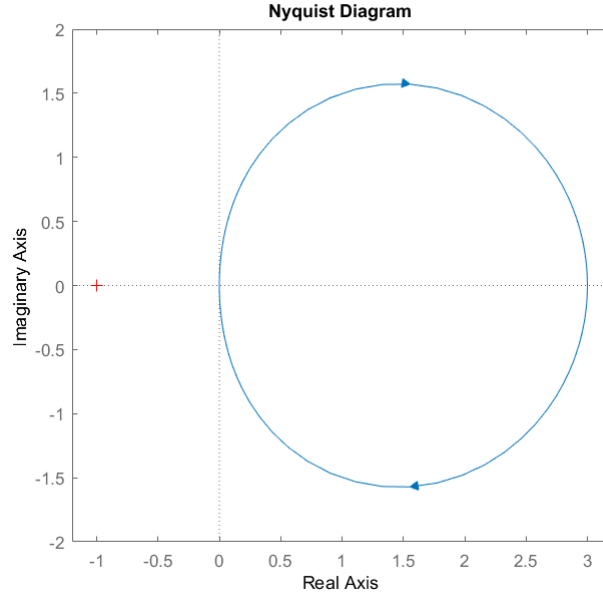


Figure 3.8: Nyquist diagram of $\frac{2s+3}{(s+1)^2}$

does not take into account the effect of b_{12} , which when too large leads the closed-loop system to instability. Hence, the minimum singular value of return difference matrix has to be examined.

Let assume that $b_{12} = 50$ in (3.33), and LQR weights are defined as $R = 1$ and $Q = 3 \begin{pmatrix} 2601 & -50 \\ -50 & 1 \end{pmatrix}$. Then, the closed-loop matrix becomes

$$A_{cl} = A - BR^{-1}B^TK = -2I.$$

The return difference matrix is given by

$$I + G(s) = \begin{pmatrix} \frac{s+2}{s+1} & 0 \\ 0 & \frac{s+2}{s+1} \end{pmatrix} \quad (3.36)$$

and the minimum singular value of return difference matrix is

$$\underline{\sigma}[I + G(j\omega)] = \left(\frac{\omega^2 + 4}{\omega^2 + 1} \right)^{\frac{1}{2}} > 1 \quad (3.37)$$

which satisfies (3.30). For more details on intermediate calculations the reader is referred to [LSA81].

3.4 Summary

This chapter provided an overview of fundamental results in the field of optimal control, particularly in the area of linear quadratic regulator problems. The presented results will be relevant for the exposition in the following chapters, which represent the contributions of this thesis.

The results presented here will be extended to the LQR multi-agent control in the next chapter. By assuming that the network consists of identical dynamically decoupled systems, an optimal LQR controller will be defined to control the system. This problem is known as centralized optimal control problem and the properties of its solution will be analysed. Also, necessary preliminaries from the area of graph theory will be given.

Chapter 4

Centralized Optimal Control Problem

In this chapter the LQR theory is applied to the network of identical dynamically decoupled systems (agents) defined in Section 3.2. The communication between agents is represented by using graph theory tools. Therefore, some preliminaries in the area of graph theory are given first. Bidirectional communication is assumed to exist between each pair of agents, and this type of problem is known as *centralized optimal control problem* for undirected networks.

Next, the structure of centralized LQR solution is presented, which is followed by spectral and robustness properties of the centralized LQR system. These are illustrated through an example of (low-scale) multi-agent system that is stabilised by using a centralized LQR controller.

In the last section of this chapter a special case of centralized LQR control is presented where a different structure is imposed on the augmented state weighting matrix. It is shown that in this case the solution of (large-scale) centralized LQR problem can be constructed from the solution of a single agent LQR system as long as the stability of the plant is preserved. Alternatively, in the case of an unstable plant, the stabilising solution can be found by solving two low-dimensional ARE's. Both cases are illustrated via an example.

4.1 Graph Theory Preliminaries

The set of N identical dynamical subsystems in (3.1) forms a communication network of subsystems, called *agents*. The underlying network is represented as a *graph*, described by the pair

$$\mathcal{G} = (\mathcal{V}, \mathcal{E}) \quad (4.1)$$

where \mathcal{V} is the set of nodes (or vertices), $\mathcal{V} = \{1, 2, \dots, N\}$, and $\mathcal{E} \subseteq \mathcal{V} \times \mathcal{V}$ is the set of edges, $\mathcal{E} \subseteq \{(i, j) : i, j \in \mathcal{V}, j \neq i\}$. If $i, j \in \mathcal{V}$ and $(i, j) \in \mathcal{E}$, then i and j are said to be adjacent (or neighbours) which is denoted as $i \sim j$. A graph \mathcal{G} is called *connected* if there exists a path between any two nodes of the graph. We assume that there is no edge from a node to itself (i.e. no self loops) and that the edge between nodes i and j is *undirected*. For an undirected graph $(i, j) \in \mathcal{E}$ implies that $(j, i) \in \mathcal{E}$, i.e. the communication between two nodes (or agents) is bidirectional.

The number of neighbours of each node, d_i for $i = 1, 2, \dots, N$, is called its *degree* or *valency*. Therefore, the *degree matrix* $\Delta(\mathcal{G})$ of a graph \mathcal{G} is a diagonal matrix, which (i, i) entry is the degree of node i . Let $d_{max}(\mathcal{G})$ denote the maximum node degree of the graph \mathcal{G} . An undirected graph is said to be *complete* if every pair of distinct nodes is connected by a unique edge. In this case, all nodes will have the same degree, $d_i = N - 1$, where N is the number of nodes (agents) and $i = 1, \dots, N$.

Any undirected graph can be represented by its *adjacency matrix*, $\mathbf{A}(\mathcal{G})$, which is a matrix with 0 – 1 elements. Let $\mathbf{A}_{i,j} \in \mathbb{R}$ be the (i, j) element of $\mathbf{A}(\mathcal{G})$, then the following is true:

$$\begin{aligned} \mathbf{A}_{i,i} &= 0, \quad \forall i = 1, 2, \dots, N, \\ \mathbf{A}_{i,j} &= 0 \text{ if } (i, j) \notin \mathcal{E} \quad \forall i, j = 1, 2, \dots, N, \quad i \neq j, \\ \mathbf{A}_{i,j} &= 1 \text{ if } (i, j) \in \mathcal{E} \quad \forall i, j = 1, 2, \dots, N, \quad i \neq j. \end{aligned} \quad (4.2)$$

Note that for undirected graphs, the adjacency matrix is symmetric ($\mathbf{A}^T(\mathcal{G}) = \mathbf{A}(\mathcal{G})$).

Another way of describing a graph is through its *Laplacian matrix*, $L(\mathcal{G})$. The

graph Laplacian matrix is defined as follows:

$$L(\mathcal{G}) = \Delta(\mathcal{G}) - \mathbf{A}(\mathcal{G}). \quad (4.3)$$

The following properties of Laplacian matrices of graphs and their spectra were established by several authors (see for example [Kel67], [AM85], [Moh91]):

1. For undirected graphs, $L(\mathcal{G})$ is positive semi definite and symmetric matrix. Therefore, $L(\mathcal{G})$ has only real eigenvalues.
2. The spectrum of $L(\mathcal{G})$ is denoted as: $\mathcal{S}(L(\mathcal{G})) = \{\lambda_1(L(\mathcal{G})), \dots, \lambda_N(L(\mathcal{G}))\}$, where the eigenvalues are arranged in decreasing order, i.e. $\lambda_1(L(\mathcal{G})) \geq \lambda_2(L(\mathcal{G})) \geq \dots \geq \lambda_{N-1}(L(\mathcal{G})) \geq \lambda_N(L(\mathcal{G}))$.
3. Every Laplacian matrix is singular and its smallest eigenvalue $\lambda_N(L(\mathcal{G})) = 0$ and a corresponding eigenvector is $(1, 1, \dots, 1)^T$. The algebraic multiplicity of its zero eigenvalue implies the number of connected components in the graph. So, $\lambda_N(L(\mathcal{G})) = 0$ and $\lambda_{N-1}(L(\mathcal{G})) > 0$ if and only if \mathcal{G} is connected.
4. The second smallest eigenvalue, $\lambda_{N-1}(L(\mathcal{G}))$, plays the special role in graph theory. It is known as the *algebraic connectivity* of the graph, that is closely related to the classical connectivity parameters of graphs (the vertex connectivity and the edge connectivity).

4.2 Centralized LQR Problem Definition

In this section the concept of LQR control will be extended to the existence of (large-scale) augmented system which consists of N subsystems with identical dynamics. Then, the dynamics of these N subsystems, indexed as $1, 2, \dots, N$, considered in total, are described by

$$\dot{\mathbf{x}}(t) = A_a \mathbf{x} + B_a \mathbf{u}, \quad \mathbf{x}(0) = \mathbf{x}_0 \quad (4.4)$$

where the column vectors $\mathbf{x}(t) = [x_1(t)^T, x_2(t)^T, \dots, x_N(t)^T]^T$ and $\mathbf{u}(t) = [u_1(t)^T, u_2(t)^T, \dots, u_N(t)^T]^T$ collect the states and inputs of the N systems, while $A_a = I_N \otimes A$ and $B_a = I_N \otimes B$, with A and B defined as in (3.2).

The LQR problem for the system (4.4) is described through the cost function which contains terms for weighting the difference between i th and j th system states, as well as the i th system state and input:

$$J(\mathbf{u}(t), \mathbf{x}_0) = \int_0^\infty \left(\sum_{i=1}^N (\mathbf{x}_i(t)^T Q_{ii} \mathbf{x}_i(t) + \mathbf{u}_i(t)^T R_{ii} \mathbf{u}_i(t)) + \sum_{i=1}^N \sum_{j=1}^N \left((\mathbf{x}_i(t) - \mathbf{x}_j(t))^T Q_{ij} (\mathbf{x}_i(t) - \mathbf{x}_j(t)) \right) \right) dt. \quad (4.5)$$

Equation (4.5) can be rewritten using the more compact notation as

$$J(\mathbf{u}(t), \mathbf{x}_0) = \int_0^\infty (\mathbf{x}(t)^T Q_a \mathbf{x}(t) + \mathbf{u}(t)^T R_a \mathbf{u}(t)) dt \quad (4.6)$$

where the matrices Q_a and R_a have the following structure:

$$Q_a = \begin{pmatrix} Q_{a11} & Q_{a12} & \cdots & Q_{a1N} \\ Q_{a21} & Q_{a22} & \cdots & Q_{a2N} \\ \vdots & \vdots & \ddots & \vdots \\ Q_{aN1} & Q_{aN2} & \cdots & Q_{aN N} \end{pmatrix} \quad (4.7)$$

and

$$R_a = I_N \otimes R \quad (4.8)$$

with

$$\begin{aligned}
Q_{a_{ii}} &= \sum_{k=1}^N Q_{ik}, \text{ for } i = 1, \dots, N, \\
Q_{a_{ij}} &= -Q_{ij}, \text{ for } i, j = 1, \dots, N, \ i \neq j, \\
Q_{ii} &= Q_{ii}^T \geq 0 \text{ and } R_{ii} = R_{ii}^T > 0 \text{ for } \forall i, \\
Q_{ij} &= Q_{ij}^T = Q_{ji} \geq 0 \text{ for } \forall i \neq j.
\end{aligned} \tag{4.9}$$

The following assumptions apply throughout this section for $Q = Q^T \geq 0$ and Q_a as in (4.7).

Assumption 4.2.1. (Local stabilisability and observability) *The pair (A, B) is stabilisable and the pair (A, C) is observable, where C is any matrix such that $C^T C = Q$.*

Assumption 4.2.2. (Global stabilisability and observability) *The pair (A_a, B_a) is stabilisable and the pair (A_a, C_a) is observable, where C_a is any matrix such that $C_a^T C_a = Q_a$.*

Remark 4.2.1. *Note that the local stabilisability of (A, B) implies the global stabilisability of (A_a, B_a) , due to the block diagonal structure of A_a and B_a , which is not necessarily true for the case of local and global observability.*

Correspondingly, given the initial conditions, \mathbf{x}_0 , the control input:

$$\mathbf{u} = -R_a^{-1} B_a^T P_a \mathbf{x} \tag{4.10}$$

minimises the cost function (4.6) subject to $\dot{\mathbf{x}}(t) = A_a \mathbf{x} + B_a \mathbf{u}$, $\mathbf{x}(0) = \mathbf{x}_0$, where P_a is the symmetric positive definite stabilising solution of the following large-scale ARE:

$$A_a^T P_a + P_a A_a - P_a B_a R_a^{-1} B_a^T P_a + Q_a = 0. \tag{4.11}$$

Positive-definiteness of P_a is the consequence of global observability. The properties of the solution and its structure are summarised in the theorem that follows.

Theorem 4.2.1. [BK08] *Assume the weighting matrices (4.9) of the (large-*

scale) LQR problem (4.4)-(4.5) are chosen as

$$\begin{aligned} Q_{a_{ii}} &= Q_1 \text{ for } i = 1, \dots, N \text{ and} \\ Q_{a_{ij}} &= Q_2 \text{ for } j = 1, \dots, N, \quad i \neq j. \end{aligned} \quad (4.12)$$

Let $P_a \in \mathbb{R}^{nN \times nN}$ be the stabilising solution of (4.11) whose individual blocks are denoted as $P_{a_{ij}} = P_a[(i-1)n+1 : in, (j-1)n+1 : jn]$ with $i, j = 1, \dots, N$. Then, the following are true:

1. $\sum_{j=1}^N P_{a_{ij}} = P$ for all $i = 1, \dots, N$, where $P \in \mathbb{R}^{n \times n}$ is the symmetric positive definite solution of the ARE associated with a single system LQR problem:

$$A^T P + PA - PBR^{-1}B^T P + Q_1 = 0. \quad (4.13)$$

2. $\sum_{j=1}^N K_{a_{ij}} = K$ for all $i = 1, \dots, N$, where $K = R^{-1}B^T P$ is the gain matrix of a single system LQR problem.
3. All off-diagonal blocks of P_a , namely $P_{a_{ij}}$ for $i \neq j$, are equal symmetric negative semi-definite matrices, denoted as $P_{a_{12}} \leq 0$. Furthermore, the matrix $P_{a_{12}}$ is the negative semi-definite solution of ARE:

$$A_{cl}^T P_{a_{12}} + P_{a_{12}} A_{cl} + N P_{a_{12}} X P_{a_{12}} - Q_2 = 0 \quad (4.14)$$

where $A_{cl} = A - BR^{-1}B^T P$ and $X = BR^{-1}B^T$. Note that (4.14) is the ARE corresponding to an LQR problem for the stable system (A_{cl}, B) with weighting matrices Q_2 and NR .

4. The (large-scale) LQR gain matrix K_a is of the form:

$$K_a = \begin{pmatrix} K_{a_{11}} & K_{a_{12}} & \dots & K_{a_{12}} \\ K_{a_{12}} & K_{a_{11}} & \dots & K_{a_{12}} \\ \vdots & \vdots & \ddots & \vdots \\ K_{a_{12}} & K_{a_{12}} & \dots & K_{a_{11}} \end{pmatrix} \quad (4.15)$$

where $K_{a_{11}}$ and $K_{a_{12}}$ depend on N, A, B, Q_1, Q_2 and R .

5. The unique symmetric positive definite solution to (4.11) has the struc-

ture:

$$P_a = \begin{pmatrix} P_{a_{11}} & P_{a_{12}} & \cdots & P_{a_{12}} \\ P_{a_{12}} & P_{a_{11}} & \cdots & P_{a_{12}} \\ \vdots & \vdots & \ddots & \vdots \\ P_{a_{12}} & P_{a_{12}} & \cdots & P_{a_{11}} \end{pmatrix} \quad (4.16)$$

in which the diagonal blocks can be expressed as: $P_{a_{11}} = P - (N - 1)P_{a_{12}}$.

Properties of the presented centralized solution, together with gain margins of centralized LQR system are given next.

4.2.1 Spectral and Robustness Properties of the Centralized LQR Solution

The next corollary of Theorem 4.2.1 follows from the gain margin properties of the LQR, which are described in Section 3.3.

Corollary 4.2.1.1. *The system $(A - BR^{-1}B^T P, B)$ in (4.14) will remain stable if the gain matrix is multiplied by any constant factor β , such that $\beta > \frac{1}{2}$. Therefore, $A - BR^{-1}B^T P + \beta NBR^{-1}B^T P_{a_{12}}$ will be Hurwitz or stable matrix for any $\beta > \frac{1}{2}$.*

Remark 4.2.2. *The constant factor β in Corollary 4.2.1.1 can be considered to be equal to 0 and the system will remain stable, as $A - BR^{-1}B^T P$ is stable by itself using (3.7).*

Remark 4.2.3. *There exists a class of systems for which β can be any positive real number, i.e. $\beta \geq 0$, but stability has to be tested for the interval $(0, \frac{1}{2}]$. This follows from the fact that the stability of $A - BR^{-1}B^T P$ does not necessarily guarantees the stability of $A - BR^{-1}B^T P + \beta NBR^{-1}B^T P_{a_{12}}$. For more information see [BK08].*

These properties of the (large-scale) centralized LQR system will be used in Chapter 5 to analyse the stability and the robustness properties of the proposed distributed LQR design. The preliminary result which characterises the spectrum of the closed-loop matrix for the (large-scale) centralized LQR system is given next:

Theorem 4.2.2. Let $A_{cl} = A - BR^{-1}B^T P$ be the closed-loop matrix of the (single system) LQR problem in (3.2)-(3.3) with state and control weighting matrices Q and R , respectively. Let P be the symmetric positive definite solution of (3.6). Also, let $A_{cl_a} = A_a - B_a R_a^{-1} B_a^T P_a$ be the closed-loop matrix of the (large-scale) centralized LQR problem in (4.4)-(4.6) with state and control weighting matrices Q_a and R_a , respectively, and P_a is the symmetric positive definite solution of (4.11) that can be decomposed into N^2 blocks of dimension $n \times n$ as

$$P_a = \begin{pmatrix} P_{a_{11}} & P_{a_{12}} & \cdots & P_{a_{12}} \\ P_{a_{12}} & P_{a_{11}} & \cdots & P_{a_{12}} \\ \vdots & \vdots & \ddots & \vdots \\ P_{a_{12}} & P_{a_{12}} & \cdots & P_{a_{11}} \end{pmatrix}. \quad (4.17)$$

Then, the spectrum of A_{cl_a} , i.e. $\mathcal{S}(A_{cl_a})$, is given by

$$\mathcal{S}(A_{cl_a}) = \mathcal{S}(A_{cl}) \cup \underbrace{\mathcal{S}(A_{cl_{1-2}}) \cup \cdots \cup \mathcal{S}(A_{cl_{1-2}})}_{(N-1) \text{ times}} \quad (4.18)$$

where $A_{cl_{1-2}} = A - BR^{-1}B^T(P_{a_{11}} - P_{a_{12}})$, in which $P_{a_{11}}$ and $P_{a_{12}}$ are $n \times n$ blocks of P_a defined in (4.17).

Proof. By substituting (4.17) into $A_{cl_a} = A_a - B_a R_a^{-1} B_a^T P_a$, the closed-loop matrix of the (large-scale) centralized LQR system becomes:

$$A_{cl_a} = \begin{pmatrix} A - X P_{a_{11}} & -X P_{a_{12}} & \cdots & -X P_{a_{12}} \\ -X P_{a_{12}} & A - X P_{a_{11}} & \cdots & -X P_{a_{12}} \\ \vdots & \vdots & \ddots & \vdots \\ -X P_{a_{12}} & -X P_{a_{12}} & \cdots & A - X P_{a_{11}} \end{pmatrix} \quad (4.19)$$

where $X = BR^{-1}B^T$. Matrix in (4.19) can be transformed into block lower-triangular form through the similarity transformation $A_{cl_t} = T A_{cl_a} T^{-1}$, where the transformation matrix T is given by

$$T = \begin{pmatrix} I & -I & 0 & \cdots & 0 \\ 0 & I & -I & \cdots & 0 \\ \vdots & \vdots & \ddots & \ddots & \vdots \\ 0 & 0 & \cdots & \ddots & -I \\ 0 & 0 & \cdots & \cdots & I \end{pmatrix}. \quad (4.20)$$

It can be shown that after a number of straightforward algebraic calculations the transformed closed-loop matrix, denoted as A_{cl_t} , becomes

$$A_{cl_t} = \begin{pmatrix} A - XP_{a_{1-2}} & 0 & 0 & \dots & 0 \\ 0 & A - XP_{a_{1-2}} & 0 & \dots & 0 \\ \vdots & \vdots & \ddots & \ddots & \vdots \\ 0 & 0 & \dots & A - XP_{a_{1-2}} & 0 \\ -XP_{a_{12}} & -2XP_{a_{12}} & \dots & -(N-1)XP_{a_{12}} & A - XP \end{pmatrix}$$

where $P_{a_{1-2}} = P_{a_{11}} - P_{a_{12}}$ and $P = P_{a_{11}} + (N-1)P_{a_{12}}$ is the symmetric positive definite solution to a (single system) LQR problem. Since eigenvalues of a matrix are preserved under similarity transformations (see Definition 3.1.3) equation (4.18) follows. \square

Results presented in Section 4.2 are illustrated through an example of multi-agent LQR system which is given next.

4.2.2 Numerical Example: Centralized LQR Multi-Agent System

Consider a network of $N = 4$ agents whose interconnection structure is represented by the complete graph depicted in Figure 4.1.

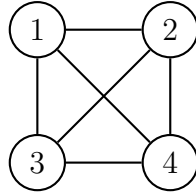


Figure 4.1: Fully connected (low-scale) multi-agent network

The agents' collective dynamics are given by

$$\dot{\mathbf{x}} = A_{a_1} \mathbf{x} + B_{a_1} \mathbf{u}, \quad \mathbf{x}(0) = \mathbf{x}_0 \quad (4.21)$$

where $A_{a_1} = I_4 \otimes A_1$ and $B_{a_1} = I_4 \otimes B_1$ with A_1 and B_1 defined as

$$A_1 = \begin{pmatrix} -1 & 0 & 2 \\ -2 & -3 & -4 \\ 1 & 0 & -1 \end{pmatrix}, \quad B_1 = \begin{pmatrix} 1 & 1 \\ 0 & 2 \\ -1 & 3 \end{pmatrix}. \quad (4.22)$$

The stabilising solution of the above (large-scale) centralized LQR problem is denoted as P_{a_1} whose structure is given in (4.16). The state matrix of the closed-loop large-scale system is $A_{cl_{a_1}} = A_{a_1} - B_{a_1}R_a^{-1}B_{a_1}^T P_{a_1}$, while P_1 and $A_{cl_1} = A_1 - B_1R_1^{-1}B_1^T P_1$ are the stabilising solution and the closed-loop matrix of the corresponding single-agent LQR problem, respectively.

The cost function defined in (4.6) initially uses the following weights for the state information: $Q_{a_{ii}} = Q_1 = I_3$, $Q_{a_{ij}} = Q_2 = I_3$, while the weight on the control effort is set as $R_1 = I_2$, $R_a = I_2 \otimes R_1$. For more details on the structure of state and control weighting matrices see (4.7)-(4.9). By solving the optimal LQR problems the following stabilising solutions are obtained:

$$P_1 = \begin{pmatrix} 0.513 & -0.103 & -0.020 \\ -0.103 & 0.166 & -0.099 \\ -0.020 & -0.099 & 0.392 \end{pmatrix} \quad \text{and} \quad P_{a_1} = \begin{pmatrix} P_{a_{11}} & P_{a_{12}} & P_{a_{12}} \\ P_{a_{12}} & P_{a_{11}} & P_{a_{12}} \\ P_{a_{12}} & P_{a_{12}} & P_{a_{11}} \end{pmatrix}$$

in which

$$P_{a_{11}} = \begin{pmatrix} 1.411 & -0.382 & -0.030 \\ -0.382 & 0.661 & -0.373 \\ -0.030 & -0.373 & 0.897 \end{pmatrix},$$

$$P_{a_{12}} = \begin{pmatrix} -0.299 & -0.093 & -0.017 \\ -0.093 & -0.165 & 0.091 \\ -0.017 & 0.091 & -0.169 \end{pmatrix}.$$

Results are reproduced for four additional sets of weighting matrices. In particular, in the second simulation the difference in the system's states is more heavily weighted relative to the individual agent's states, while in the third simulation this is reversed. Then, the weight on control effort is changed in the same manner. The eigenvalue distribution for each simulation is shown in Table 4.1 in which $A_{cl_{1-2}} = A_1 - B_1R_1^{-1}B_1^T(P_{a_{11}} - P_{a_{12}})$.

The example shows that the stabilising effect of the centralized LQR design is independent of the LQR weighting matrices selection. Thus this can be selected freely in order to achieve the global performance objective. Further, the example supports theoretical results on the spectrum of closed-loop system presented in Theorem 4.2.2, as well as the properties of diagonal and off-

Table 4.1: Eigenvalue distribution in the centralized LQR system for a different choice of weighting matrices

Weighting matrices	$\mathcal{S}(A_{cl_1})$	$\mathcal{S}(A_{cl_{1-2}})$	$\mathcal{S}(A_{cl_{a_1}})$
$Q_1 = I_3$	-2.127	-2.843	-2.127
$Q_2 = I_3$	$-3.402 + i1.528$	-4.724	-2.843 (3 times)
$R_1 = I_2$	$-3.402 - i1.528$	-7.523	$-3.402 \pm i1.528$ -4.724 (3 times) -7.523 (3 times)
$Q_1 = 0.1I_3$	$-1.427 + i1.392$	-2.705	$-1.427 \pm i1.392$
$Q_2 = I_3$	$-1.427 - i1.392$	-4.899	-2.705 (3times)
$R_1 = I_2$	-2.899	-6.424	-2.898 -4.899 (3times) -6.424 (3times)
$Q_1 = 10I_3$	-3.273	-3.396	-3.273
$Q_2 = I_3$	-5.052	-5.562	-3.396 (3times)
$R_1 = I_2$	-11.436	-13.731	-5.052 -5.562 (3times) -11.436 -13.731 (3times)
$Q_1 = I_3$	-3.273	-3.548	-3.273
$Q_2 = I_3$	-5.052	-9.460	-3.548 (3times)
$R_1 = 0.1I_2$	-11.436	-26.550	-5.052 -9.460 (3times) -11.436 -26.550 (3times)
$Q_1 = I_3$	$-1.427 + i1.392$	-2.282	$-1.427 \pm i1.392$
$Q_2 = I_3$	$-1.427 - i1.392$	$-2.645 + i1.393$	-2.282 (3times)
$R_1 = 10I_2$	-2.899	$-2.645 - i1.393$	-2.899 -2.645 + i1.393 (3times) -2.645 - i1.393 (3times)

diagonal block structure of P_{a_1} described in Theorem 4.2.1.

4.3 Special Case of the Centralized LQR Problem

In this section a special case of centralized LQR controller is considered by imposing a different weighting structure on the states of the system. Main results are illustrated through an example of multi-agent network consisting of identical dynamically decoupled agents.

4.3.1 Problem Definition and Structural Properties of its Solution

Consider the network of N agents whose dynamics are described as in (4.4). The LQR problem for the system (4.4) and weighting matrices Q_{aa} and R_a is described by the cost function

$$J(\mathbf{u}(t), \mathbf{x}_0) = \int_0^\infty (\mathbf{x}(t)^T Q_{aa} \mathbf{x}(t) + \mathbf{u}(t)^T R_a \mathbf{u}(t)) dt. \quad (4.23)$$

Please note that when compared to the cost function in (4.6), a different structure is imposed relative to the structure defined by weighting matrix Q_a . This new weight matrix is denoted as Q_{aa} and is given by

$$Q_{aa} = \begin{pmatrix} Q_{aa11} & Q_{aa12} & \cdots & Q_{aa1N} \\ Q_{aa21} & Q_{aa22} & \cdots & Q_{aa2N} \\ \vdots & \vdots & \ddots & \vdots \\ Q_{aaN1} & Q_{aaN2} & \cdots & Q_{aaNN} \end{pmatrix} \quad (4.24)$$

with

$$\begin{aligned} Q_{aa_{ii}} &= \sum_{j=1, j \neq i}^N Q_{ij}, \text{ for } i = 1, \dots, N, \\ Q_{aa_{ij}} &= -Q_{ij}, \text{ for } i, j = 1, \dots, N, \quad i \neq j, \\ Q_{ij} &= Q_{ij}^T = Q_{ji} \geq 0 \text{ for } \forall i \neq j. \end{aligned} \quad (4.25)$$

Assumptions made on local and global stabilisability and observability apply throughout this section as well (see Assumption 4.2.1 and Assumption 4.2.2). Therefore, the new (large-scale) centralized system can be described by the

following ARE:

$$A_a^T P_{aa} + P_{aa} A_a - P_{aa} B_a R_a^{-1} B_a^T P_{aa} + Q_{aa} = 0 \quad (4.26)$$

in which P_{aa} is the symmetric positive definite stabilising solution. Properties of the solution and its structure are summarised in Theorem 4.3.1, which is followed by result which characterises the spectrum of the (large-scale) closed-loop centralized LQR system in (4.23)-(4.26).

Theorem 4.3.1. *Assume that the weighting matrix Q_{aa} in (4.24) of the (large-scale) LQR problem is constructed as*

$$Q_{ij} = Q \text{ for } i, j = 1, \dots, N, \quad i \neq j. \quad (4.27)$$

Let $P_{aa} \in \mathbb{R}^{nN \times nN}$ be the unique symmetric positive definite solution to (4.26) whose individual blocks are denoted as $P_{aa_{ij}} = P_{aa}[(i-1)n+1 : in, (j-1)n+1 : jn]$ with $i, j = 1, \dots, N$. Then, P_{aa} is of the form:

$$P_{aa} = \begin{pmatrix} P_1 + E & -\frac{P_1}{N-1} + E & \dots & -\frac{P_1}{N-1} + E \\ -\frac{P_1}{N-1} + E & P_1 + E & \dots & -\frac{P_1}{N-1} + E \\ \vdots & \vdots & \ddots & \vdots \\ -\frac{P_1}{N-1} + E & \dots & \dots & P_1 + E \end{pmatrix} \quad (4.28)$$

in which P_1 is the symmetric positive definite solution of the ARE associated with a single-agent LQR problem:

$$A^T P_1 + P_1 A - \frac{N}{N-1} P_1 B R^{-1} B^T P_1 + (N-1)Q = 0 \quad (4.29)$$

and E is the stabilising solution of the low-dimensional ARE:

$$A^T E + E A - N E B R^{-1} B^T E = 0. \quad (4.30)$$

Therefore, the solution of (large-scale) centralized LQR problem reduces to the solution of two low-dimensional AREs.

Proof. The assumptions made in (4.27) and (4.28), and block-diagonal structure of A_a and B_a in (4.26) imply that the set of AREs in (4.26) reduces to a single ARE equation. In order to reduce complexity of the proof, we assume

that $N = 3$. Therefore, (4.26) can be expanded as:

$$\begin{aligned} & \begin{pmatrix} A^T \tilde{P}_1 + A\tilde{P}_1 & -A^T \tilde{P}_2 - A\tilde{P}_2 & -A^T \tilde{P}_2 - A\tilde{P}_2 \\ -A^T \tilde{P}_2 - A\tilde{P}_2 & A^T \tilde{P}_1 + A\tilde{P}_1 & -A^T \tilde{P}_2 - A\tilde{P}_2 \\ -A^T \tilde{P}_2 - A\tilde{P}_2 & -A^T \tilde{P}_2 - A\tilde{P}_2 & A^T \tilde{P}_1 + A\tilde{P}_1 \end{pmatrix} + \begin{pmatrix} 2Q & -Q & -Q \\ -Q & 2Q & -Q \\ -Q & -Q & 2Q \end{pmatrix} - \\ & - \begin{pmatrix} \tilde{P}_1 & -\tilde{P}_2 & -\tilde{P}_2 \\ -\tilde{P}_2 & \tilde{P}_1 & -\tilde{P}_2 \\ -\tilde{P}_2 & -\tilde{P}_2 & \tilde{P}_1 \end{pmatrix} \begin{pmatrix} X & 0 & 0 \\ 0 & X & 0 \\ 0 & 0 & X \end{pmatrix} \begin{pmatrix} \tilde{P}_1 & -\tilde{P}_2 & -\tilde{P}_2 \\ -\tilde{P}_2 & \tilde{P}_1 & -\tilde{P}_2 \\ -\tilde{P}_2 & -\tilde{P}_2 & \tilde{P}_1 \end{pmatrix} = \begin{pmatrix} 0 & 0 & 0 \\ 0 & 0 & 0 \\ 0 & 0 & 0 \end{pmatrix} \end{aligned} \quad (4.31)$$

in which $\tilde{P}_1 = P_1 + E$, $\tilde{P}_2 = \frac{P_1}{2} - E$ and $X = BR^{-1}B^T$. After some algebra, problem in (4.31) reduces to two low dimensional AREs:

$$A^T P_1 + P_1 A - \frac{3}{2} P_1 B R^{-1} B^T P_1 + 2Q = 0 \quad (4.32)$$

and

$$A^T E + EA - 3EBR^{-1}B^T E = 0. \quad (4.33)$$

The fact that the pair (A, B) is stabilisable implies the stabilisability of $(A, \sqrt{3/2}B)$ and $(A, \sqrt{3}B)$. Similarly, the detectability of (A, Q) implies the detectability of $(A, 2Q)$ and $(A, 0)$ for a Hurwitz matrix A . Therefore, P_1 and E are the stabilising solutions of (4.32) and (4.33), respectively, and the solution of (large-scale) LQR problem can be constructed as:

$$P_c = \begin{pmatrix} P_1 + E & -\frac{P_1}{2} + E & -\frac{P_1}{2} + E \\ -\frac{P_1}{2} + E & P_1 + E & -\frac{P_1}{2} + E \\ -\frac{P_1}{2} + E & -\frac{P_1}{2} + E & P_1 + E \end{pmatrix}.$$

The proof can be easily generalised to networks of arbitrary size. Thus, for the network of N agents it is necessary to solve two low-dimensional AREs in (4.29) and (4.30). Then, the solution of (large-scale) LQR problem can be constructed by using the structure in (4.28). \square

An extension to the Theorem 4.3.1 that takes into account the stability of matrix A is given next.

Remark 4.3.1. *For a stable (Hurwitz) matrix A (i.e. $\mathcal{S}(A) \subseteq \mathbb{C}_-$) E is $n \times n$ zero matrix. This implies that the solution of (large-scale) centralized problem reduces to the solution of single ARE in (4.29) and the solution can*

be constructed as:

$$P_c = \begin{pmatrix} P_1 & -\frac{P_1}{N-1} & \cdots & -\frac{P_1}{N-1} \\ -\frac{P_1}{N-1} & P_1 & \cdots & -\frac{P_1}{N-1} \\ \vdots & \vdots & \ddots & \vdots \\ -\frac{P_1}{N-1} & \cdots & \cdots & P_1 \end{pmatrix}. \quad (4.34)$$

For matrix A that has one or more unstable modes (i.e. $\mathcal{S}(A) \not\subseteq \mathbb{C}_-$) the constructed solution, P_c , in (4.34) is no longer equal to the solution of large-scale system, P_{aa} . Also, P_c is not the stabilising solution based on Theorem 4.3.2. In this case, the difference between P_{aa} and P_c can be cancelled by the 'correction factor', E , that is the stabilising solution of (4.30). Then, for the network of N agents the constructed solution is of the following structure:

$$P_c = \begin{pmatrix} P_1 + E & -\frac{P_1}{N-1} + E & \cdots & -\frac{P_1}{N-1} + E \\ -\frac{P_1}{N-1} + E & P_1 + E & \cdots & -\frac{P_1}{N-1} + E \\ \vdots & \vdots & \ddots & \vdots \\ -\frac{P_1}{N-1} + E & \cdots & \cdots & P_1 + E \end{pmatrix}. \quad (4.35)$$

Therefore, for unstable matrix A the solution of (large-scale) centralized LQR problem reduces to the solution of two low-dimensional ARE's. Furthermore, $\text{rank}(E)$ equals the number of unstable modes (eigenvalues) of A .

Theorem 4.3.2. Let $A_{cl_1} = A - \frac{N}{N-1}BR^{-1}B^T P_1$ be the closed-loop matrix of the low-dimensional LQR problem described by the ARE in (4.29) where $(N-1)Q$ and $\sqrt{\frac{N}{N-1}}R$ are state and control weighting matrices, respectively, and P_1 is the symmetric positive definite solution of (4.29). Similarly, let $A_{cl_{aa}} = A_a - B_a R_a^{-1} B_a^T P_{aa}$ be the closed-loop matrix of the (large-scale) centralized LQR problem in (4.26) with state and control weighting matrices Q_{aa} and R_{aa} , respectively, and let P_{aa} be the symmetric positive definite solution of (4.26). Then, P_{aa} has the following form:

$$P_{aa} = \begin{pmatrix} P_1 & -\frac{P_1}{N-1} & \cdots & -\frac{P_1}{N-1} \\ -\frac{P_1}{N-1} & P_1 & \cdots & -\frac{P_1}{N-1} \\ \vdots & \vdots & \ddots & \vdots \\ -\frac{P_1}{N-1} & \cdots & \cdots & P_1 \end{pmatrix} \quad (4.36)$$

Further, the spectrum of $A_{cl_{aa}}$, i.e. $\mathcal{S}(A_{cl_{aa}})$, is given by

$$\mathcal{S}(A_{cl_{aa}}) = \mathcal{S}(A) \cup \underbrace{\mathcal{S}(A_{cl_1}) \cup \dots \cup \mathcal{S}(A_{cl_1})}_{(N-1) \text{ times}}. \quad (4.37)$$

Proof. In order to prove the theorem we are using the same methodology as in Theorem 4.1. Starting from the (large-scale) closed loop system, $A_{cl_{aa}} = A_a - B_a R_a^{-1} B_a^T P_{aa}$, and using the similarity transformation $A_{cl_{aa_t}} = T A_{cl_a} T^{-1}$, where the transformation matrix T is given by

$$T = \begin{pmatrix} I & -I & 0 & \dots & 0 \\ 0 & I & -I & \dots & 0 \\ \vdots & \vdots & \ddots & \ddots & \vdots \\ 0 & 0 & \dots & \ddots & -I \\ 0 & 0 & \dots & \dots & I \end{pmatrix} \quad (4.38)$$

we get

$$A_{cl_{aa_t}} = \begin{pmatrix} A - X_1 P_1 & 0 & 0 & \dots & 0 \\ 0 & A - X_1 P_1 & 0 & \dots & 0 \\ \vdots & \vdots & \ddots & \ddots & \vdots \\ 0 & 0 & \dots & A - X_1 P_1 & 0 \\ \frac{1}{N-1} X P_1 & \frac{2}{N-1} X P_1 & \dots & \frac{N-1}{N-1} X P_1 & A \end{pmatrix} \quad (4.39)$$

where $X_1 = \frac{N}{N-1} B R^{-1} B^T$ and $X = B R^{-1} B^T$. Since eigenvalues of a matrix are preserved under similarity transformations (see Definition 3.1.3) equation (4.37) follows. \square

4.3.2 Numerical Example: Special Case of the Centralized LQR Multi-Agent System

Consider the multi-agent network whose interconnection structure is depicted in Figure 4.1. The agents' collective dynamics is given by

$$\dot{\mathbf{x}} = A_{a_2}\mathbf{x} + B_{a_2}\mathbf{u}, \quad \mathbf{x}(0) = \mathbf{x}_0 \quad (4.40)$$

where $A_{a_2} = I_4 \otimes A_2$ and $B_{a_2} = I_4 \otimes B_2$ with A_2 and B_2 are defined initially as

$$A_2 = \begin{pmatrix} -1 & 0 & -2 \\ -2 & -3 & -4 \\ 1 & 0 & -1 \end{pmatrix}, \quad B_2 = \begin{pmatrix} 1 & 1 \\ 0 & 2 \\ -1 & 3 \end{pmatrix}. \quad (4.41)$$

The LQR cost function is defined as in (4.6) with

$$Q_{a_2} = \begin{pmatrix} 3Q_2 & -Q_2 & -Q_2 & -Q_2 \\ -Q_2 & 3Q_2 & -Q_2 & -Q_2 \\ -Q_2 & -Q_2 & 3Q_2 & -Q_2 \\ -Q_2 & -Q_2 & -Q_2 & 3Q_2 \end{pmatrix} \quad \text{and} \quad R_{a_2} = I_4 \otimes R_2 \quad (4.42)$$

where $Q_2 = I_3$ and $R_2 = I_2$. A_2 is a stable (Hurwitz) matrix since $\mathcal{S}(A_2) = \{-3, -1 \pm i1.414\}$. Then, the stabilising solution of the (large-scale) LQR system in (4.40) is of the following form

$$P_{aa_2} = \begin{pmatrix} P_2 + E_2 & -\frac{1}{3}P_2 + E_2 & -\frac{1}{3}P_2 + E_2 & -\frac{1}{3}P_2 + E_2 \\ -\frac{1}{3}P_2 + E_2 & P_2 + E_2 & -\frac{1}{3}P_2 + E_2 & -\frac{1}{3}P_2 + E_2 \\ -\frac{1}{3}P_2 + E_2 & -\frac{1}{3}P_2 + E_2 & P_2 + E_2 & -\frac{1}{3}P_2 + E_2 \\ -\frac{1}{3}P_2 + E_2 & -\frac{1}{3}P_2 + E_2 & -\frac{1}{3}P_2 + E_2 & P_2 + E_2 \end{pmatrix} \quad (4.43)$$

in which

$$P_2 = \begin{pmatrix} 1.098 & -0.289 & 0.016 \\ -0.289 & 0.496 & -0.281 \\ 0.016 & -0.281 & 0.696 \end{pmatrix}, \quad E_2 = \begin{pmatrix} 0 & 0 & 0 \\ 0 & 0 & 0 \\ 0 & 0 & 0 \end{pmatrix} \quad (4.44)$$

are the solutions of the following AREs, respectively:

$$\begin{aligned} A^T P_2 + P_2 A - \frac{4}{3} P_2 B R^{-1} B^T P_2 + 3Q_2 &= 0 \\ A^T E_2 + E_2 A - 4E_2 B R^{-1} B^T E_2 &= 0. \end{aligned} \quad (4.45)$$

Therefore, for stable matrix A , stabilising solution of augmented multi-agent system can be constructed by solving a low-dimensional ARE which supports theoretical results presented in Theorem 4.3.1.

Next let consider different matrix A_2 , such that

$$A_2 = \begin{pmatrix} -1 & 0 & -2 \\ -2 & 3 & -4 \\ 1 & 0 & -1 \end{pmatrix}$$

and $\mathcal{S}(A_2) = \{3, -1 \pm i1.414\}$ (i.e. A_2 has one unstable mode). Then, solutions of (4.45) are

$$P_2 = \begin{pmatrix} 20.116 & -32.937 & 18.521 \\ -32.937 & 56.543 & -32.049 \\ 18.521 & -32.049 & 18.702 \end{pmatrix}, E_2 = \begin{pmatrix} 1.500 & -2.250 & 1.500 \\ -2.250 & 3.375 & -2.250 \\ 1.500 & -2.250 & 1.500 \end{pmatrix}$$

and P_{aa_2} is constructed as in (4.43). Moreover, $\text{rank}(E) = 1$ which corresponds to the number of unstable modes of A_2 , as claimed in Remark 4.3.1.

Finally, let us consider anti-stable matrix A_2 such that

$$A_2 = \begin{pmatrix} 1 & 0 & 2 \\ 2 & 3 & 4 \\ -1 & 0 & 1 \end{pmatrix}$$

and $\mathcal{S}(A_2) = \{3, 1 \pm i1.414\}$ (i.e. A_2 has three unstable mode). Similarly, solutions of (4.45) are

$$P_2 = \begin{pmatrix} 1.626 & -0.554 & 0.059 \\ -0.554 & 2.205 & -0.131 \\ 0.059 & -0.131 & 0.566 \end{pmatrix}, E_2 = \begin{pmatrix} 0.086 & -0.016 & 0.019 \\ -0.016 & 0.160 & 0.060 \\ 0.019 & 0.060 & 0.096 \end{pmatrix}$$

and P_{aa_2} is constructed as in (4.43). Again $\text{rank}(E)$ corresponds to the number of unstable modes of A_2 .

4.4 Summary

In this chapter the framework for multi-agent LQR-based control was presented. By assuming bidirectional communication between each pair of agents, an optimal solution was obtained. Spectral and robustness properties of the solution were analysed. Also, a special case of centralized control was presented where the size of the problem that has to be solved reduces to a single agent problem.

In the case of limited communication between agents the proposed centralized framework becomes inadequate and distributed solutions have to be deployed. Hence, the results presented here will be extended for the use in a distributed multi-agent setting which will be given in the next chapter. Additionally, these two different designs will be compared with respect to their performance cost.

Chapter 5

Distributed Optimal Control Problem

In this chapter the method for designing the distributed controller for dynamically decoupled multi-agent systems introduced in [BK08] is presented. The subsystems can be actuated independently, but share a common objective which forces them to interact with each other. Coupling between subsystems is described by a communication graph, at each node of which the models of the neighbouring nodes are used to predict its behaviour. Such an approach leads to an elegant and powerful result: A stabilising distributed controller can be found by solving a single LQR problem whose size depends on the maximum vertex degree of the graph. The effectiveness of this approach is illustrated through an example of large-scale multi-agent network where individual agents are described by double integrator dynamics.

Next, the method for comparing the family of distributed LQR-suboptimal controllers that has been introduced in [BK08] with the optimal centralized controller is presented. It is shown that for any distributed control configuration which differs from a complete graph by a single link, there is no performance loss if the initial state vector lies in a certain subspace of state-space. Additionally, near-optimal schemes are identified. The procedure is extended by analysing the performance loss of an arbitrary distributed configuration which is illustrated through an example. The results presented allow the application of the method described in [BK08] to decentralized control schemes optimised with respect to controller structure.

5.1 Distributed LQR Design Method

The collective dynamics of N_d identical and decoupled dynamical subsystems can be described as

$$\dot{\tilde{\mathbf{x}}}(t) = \tilde{A}\tilde{\mathbf{x}} + \tilde{B}\tilde{\mathbf{u}}, \quad \tilde{\mathbf{x}}(0) = \tilde{\mathbf{x}}_0 \quad (5.1)$$

where $\tilde{\mathbf{x}}(t) = [\tilde{x}_1(t)^T, \tilde{x}_2(t)^T, \dots, \tilde{x}_{N_d}(t)^T]^T$ and $\tilde{\mathbf{u}}(t) = [\tilde{u}_1(t)^T, \tilde{u}_2(t)^T, \dots, \tilde{u}_{N_d}(t)^T]^T$ are the vectors which collect the states and inputs of the N_d systems, while $\tilde{A} = I_{N_d} \otimes A$ and $\tilde{B} = I_{N_d} \otimes B$, where A and B are defined as in (3.2). Systems (4.4) and (5.1) differ only in the number of subsystems (or agents). System (4.4) refers to the augmented centralized optimal problem with N agents, while system (5.1) with tilted notation refers to the distributed optimal problem with N_d agents.

The *distributed optimal control problem* is defined as [BK08]:

$$\begin{aligned} \min_{\tilde{K}} \tilde{J}(\tilde{\mathbf{u}}(t), \tilde{\mathbf{x}}_0) &= \int_0^\infty (\tilde{\mathbf{x}}(t)^T \tilde{Q} \tilde{\mathbf{x}}(t) + \tilde{\mathbf{u}}(t)^T \tilde{R} \tilde{\mathbf{u}}(t)) dt \\ \text{subj. to } \dot{\tilde{\mathbf{x}}}(t) &= \tilde{A}\tilde{\mathbf{x}} + \tilde{B}\tilde{\mathbf{u}}, \quad \tilde{\mathbf{x}}(0) = \tilde{\mathbf{x}}_0 \\ \tilde{K} &\in \mathcal{K}_{n,m}^{N_d}(\mathcal{G}), \\ \tilde{Q} &\in \mathcal{K}_{n,n}^{N_d}(\mathcal{G}), \quad \tilde{R} = I_{N_d} \otimes R \end{aligned} \quad (5.2)$$

where $\tilde{Q} = \tilde{Q}^T \geq 0$ and $\tilde{R} = \tilde{R}^T > 0$ while the class of metrics denoted as $\mathcal{K}_{n,m}^{N_d}(\mathcal{G})$ is defined in Definition 3.1.9.

The problem in (5.2) is considered as non-deterministic polynomial-time problem (or NP-hard problem). Instead of solving (5.2) the procedure for designing a *suboptimal* distributed controller is proposed in Theorem 5.1.1. Before stating the theorem, we need to define the matrix that reflects the interconnection structure in network, as well as the necessary eigenvalue properties, which are given next.

Let $M \in \mathbb{R}^{N_d \times N_d}$ be a symmetric and positive semi-definite matrix such that:

$$\lambda_i(M) > \frac{N_{min}}{2}, \quad \forall \lambda_i(M) \in \mathcal{S}(M) \setminus \{0\}. \quad (5.3)$$

Please note that N_d denotes the number of agents in the distributed system, while N_{min} is the minimum size of the problem (number of agents) that has to be solved in order to construct the stabilising distributed controller. Throughout the whole thesis M will be defined by using the notion of the adjacency

matrix, $\mathbf{A}(\mathcal{G})$, as

$$M = aI_{N_d} - b\mathbf{A}(\mathcal{G}), \quad b \geq 0 \quad (5.4)$$

where a and b are adjustable parameters. In order to guarantee closed-loop stability, the choice of a and b is restricted to

$$a - bd_{max} > \frac{N_{min}}{2} \quad (5.5)$$

or

$$a - bd_{max} \geq 0 \quad (5.6)$$

for the less strict stability case defined in Remark 4.2.3.

Lemma 5.1.1. *Let $A \in \mathbb{R}^{m \times m}$, $B \in \mathbb{R}^{n \times n}$ and $C \in \mathbb{R}^{m \times m}$. Consider two matrices $A_a \in \mathbb{R}^{nm \times nm}$ and $C_a \in \mathbb{R}^{nm \times nm}$, such that $A_a = I_N \otimes A$ and $C_a = B \otimes C$. Then, $\mathcal{S}(A_a + C_a) = \bigcup_{i=1}^n \mathcal{S}(A + \lambda_i(B)C)$, where $\lambda_i(B)$ is the i th eigenvalue of B .*

The procedure for designing the suboptimal distributed controller is given next.

Theorem 5.1.1. [BK08] *Consider the (large-scale) LQR problem in (5.1) with cost function:*

$$J(\tilde{\mathbf{u}}(t), \tilde{\mathbf{x}}_0) = \int_0^\infty (\tilde{\mathbf{x}}(t)^T \tilde{Q} \tilde{\mathbf{x}}(t) + \tilde{\mathbf{u}}(t)^T \tilde{R} \tilde{\mathbf{u}}(t)) dt \quad (5.7)$$

where \tilde{Q} and \tilde{R} are structured as in (4.7)-(4.9) with

$$\begin{aligned} \tilde{Q}_{ii} &= \tilde{Q}_1 \text{ for all } i = 1, \dots, N_d \text{ and} \\ \tilde{Q}_{ij} &= \tilde{Q}_2 \text{ for all } j = 1, \dots, N_d, \quad i \neq j. \end{aligned}$$

Let P_{min} be the symmetric positive definite solution of the ARE associated with the centralized LQR problem (4.11), but of size corresponding to $N_{min} = d_{max}(\mathcal{G}) + 1$ agents. Using Theorem 4.2.1, P_{min} has the following structure:

$$P_{min} = \begin{pmatrix} P_{a11} & P_{a12} & \cdots & P_{a12} \\ P_{a12} & P_{a11} & \cdots & P_{a12} \\ \vdots & \vdots & \ddots & \vdots \\ P_{a12} & \cdots & \cdots & P_{a11} \end{pmatrix}. \quad (5.8)$$

Furthermore, $P_{a11} = P - (N_{min} - 1)P_{a12}$, where P is the symmetric positive definite solution to the (single agent) LQR problem (4.13) with weighting matrices

\tilde{Q}_1 and R .

Then, the distributed controller can be constructed as:

$$\tilde{K} = I_{N_d} \otimes R^{-1} B^T P - M \otimes R^{-1} B^T P_{a_{12}} \quad (5.9)$$

corresponding to the closed loop system:

$$\tilde{A}_{cl} = \tilde{A} - \tilde{B}\tilde{K} = I_{N_d} \otimes A + (I_{N_d} \otimes B)\tilde{K} \quad (5.10)$$

which is asymptotically stable.

Proof. The eigenvalues of the closed-loop system (5.10) are:

$$\mathcal{S}(\tilde{A}_{cl}) = \mathcal{S}(I_{N_d} \otimes (A - XP) + M \otimes (XP_{a_{12}})) \quad (5.11)$$

where $X = BR^{-1}B^T$. Using Lemma 5.1.1, the spectrum becomes

$$\begin{aligned} \mathcal{S}(\tilde{A}_{cl}) &= \mathcal{S}(I_{N_d} \otimes (A - XP) + M \otimes (XP_{a_{12}})) \\ &= \bigcup_{i=1}^N \mathcal{S}(A - XP + \lambda_i(M)XP_{a_{12}}). \end{aligned} \quad (5.12)$$

For $\lambda_i(M) = 0$, $A - XP + \lambda_i(M)XP_{a_{12}}$ is stable using Remark 4.2.2. If $\lambda_i(M) \neq 0$, the spectrum will be stable as long as $\lambda_i(M) > \frac{1}{2}$, using Corollary 4.2.1.1, which applies by (5.3). \square

Remark 5.1.1. *Theorem 5.1.1 constructs one local controller which can be used to control a collection of identical dynamically decoupled systems. Also, it is enough to solve a low-dimensional LQR problem ($N_{min} = d_{max}(\mathcal{G}) + 1$) from where the full-size distributed controller can be constructed.*

Remark 5.1.2. *By selecting matrix M properly, the robustness properties of the large-scale centralized controller (described in Corollary 4.2.1.1) will be preserved in the distributed design. Also, using Remark 4.2.3, for a special class of systems, the restriction on the choice of M can be relaxed as*

$$\lambda_i(M) \geq 0, \quad \forall \lambda_i(M) \in \mathcal{S}(M). \quad (5.13)$$

In order to calculate the performance cost of the proposed distributed controller, the solution to Lyapunov equation associated with the problem has to be found; this is summarised in the next proposition.

Proposition 5.1.1. Consider the distributed controller designed as in Theorem 5.1.1 with the asymptotically stable closed loop system (5.10). The minimum cost is given by

$$J(\tilde{\mathbf{u}}, \tilde{\mathbf{x}}_0) = \tilde{\mathbf{x}}_0^T \tilde{P} \tilde{\mathbf{x}}_0 \quad (5.14)$$

where \tilde{P} is the unique solution of the following Lyapunov equation:

$$\tilde{A}_{cl}^T \tilde{P} + \tilde{P} \tilde{A}_{cl} + \tilde{Q} + \tilde{K}^T \tilde{R} \tilde{K} = 0 \quad (5.15)$$

with $\tilde{A}_{cl} = I_{N_d} \otimes A + (I_{N_d} \otimes B) \tilde{K}$.

Proof. See [BK08]. □

The effectiveness of this approach is illustrated through an example which is given next.

5.1.1 Distributed LQR Multi-Agent System - Numerical Example

Consider a network of $N = 100$ identical, dynamically decoupled agents described by double-integrator dynamics in both spatial dimensions:

$$\ddot{\mathbf{x}}_i = \mathbf{u}_{x,i}, \quad \ddot{\mathbf{y}}_i = \mathbf{u}_{y,i}, \quad i = 1, \dots, 100. \quad (5.16)$$

The interconnection structure is depicted in Figure 5.5.

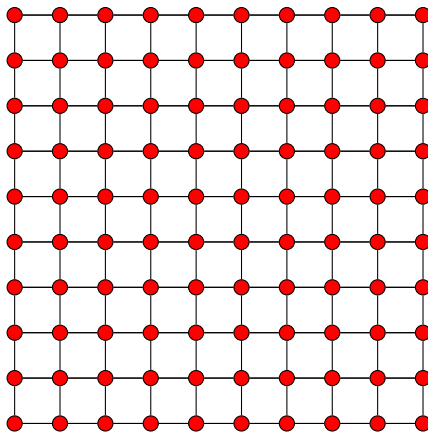


Figure 5.1: Large-scale distributed multi-agent network of $N = 100$ agents

The collective dynamics in a state-space formulation are given by

$$\dot{\tilde{\mathbf{x}}}(t) = \tilde{A}\tilde{\mathbf{x}} + \tilde{B}\tilde{\mathbf{u}}, \quad \tilde{\mathbf{x}}(0) = \tilde{\mathbf{x}}_0 \quad (5.17)$$

where $\tilde{A} = I_{100} \otimes A$ and $\tilde{B} = I_{100} \otimes B$ with A and B defined as

$$A = \begin{pmatrix} 0.1 & 1 & 0 & 0 \\ 0 & -0.1 & 0 & 0 \\ 0 & 0 & 0.1 & 1 \\ 0 & 0 & 0 & -0.1 \end{pmatrix}, \quad B = \begin{pmatrix} 0 & 0 \\ 1 & 0 \\ 0 & 0 \\ 0 & 1 \end{pmatrix}. \quad (5.18)$$

Damping elements are added to the diagonal of matrix A such that local and global stabilisability assumptions in Section 4 are satisfied. Then, the LQR problem for a formation in Figure 5.5 is defined as

$$\min_{\tilde{K}} \tilde{J}(\tilde{\mathbf{u}}(t), \tilde{\mathbf{x}}_0) \quad \text{subj. to } \dot{\tilde{\mathbf{x}}} = \tilde{A}\tilde{\mathbf{x}} + \tilde{B}\tilde{\mathbf{u}}, \quad \tilde{\mathbf{x}}(0) = \tilde{\mathbf{x}}_0$$

where the cost function $\tilde{J}(\tilde{\mathbf{u}}(t), \tilde{\mathbf{x}}_0)$ is defined as in (5.7) with \tilde{Q} (its diagonal and off-diagonal blocks) and \tilde{R} structured as $\tilde{Q}_{ii} = \text{diag}(5, 0, 5, 0)$, $\tilde{Q}_{ij} = \text{diag}(-1, 0, -1, 0)$ and $\tilde{R} = I_{100} \otimes R$ in which $R = I_2$.

The maximum degree within the network is $d_{max} = 4$. Therefore, the minimum size of the problem that has to be solved in order to obtain a distributed stabilising solution is $N_{min} = 5$. By solving an ARE corresponding to the centralized network of 5 agents, a stabilising solution of the following form will be obtained using Theorem 4.2.1:

$$P_{min} = \begin{pmatrix} P_{a_{11}} & P_{a_{12}} & P_{a_{12}} & P_{a_{12}} & P_{a_{12}} \\ P_{a_{12}} & P_{a_{11}} & P_{a_{12}} & P_{a_{12}} & P_{a_{12}} \\ P_{a_{12}} & P_{a_{12}} & P_{a_{11}} & P_{a_{12}} & P_{a_{12}} \\ P_{a_{12}} & P_{a_{12}} & P_{a_{12}} & P_{a_{11}} & P_{a_{12}} \\ P_{a_{12}} & P_{a_{12}} & P_{a_{12}} & P_{a_{12}} & P_{a_{11}} \end{pmatrix}. \quad (5.19)$$

Then, distributed gain matrix is constructed as

$$\tilde{K} = I_{100} \otimes R^{-1}B^T P - M \otimes R^{-1}B^T P_{a_{12}} \quad (5.20)$$

where $P = P_{a_{11}} + 4P_{a_{12}}$ and $M = 4I_{100} - \mathbf{A}$ (\mathbf{A} is the adjacency matrix). Matrix M is chosen to satisfy the less conservative stability conditions given in Theorem 5.1.1.

The simulation results are depicted in Figure 5.2 at different time instances. Agents are initially disturbed by random disturbances and the control aim is to recover the initial formation depicted in Figure 5.1. As the snapshots in Figure 5.2 demonstrate, the formation is successfully recovered in steady state and the controller used is indeed stabilising.

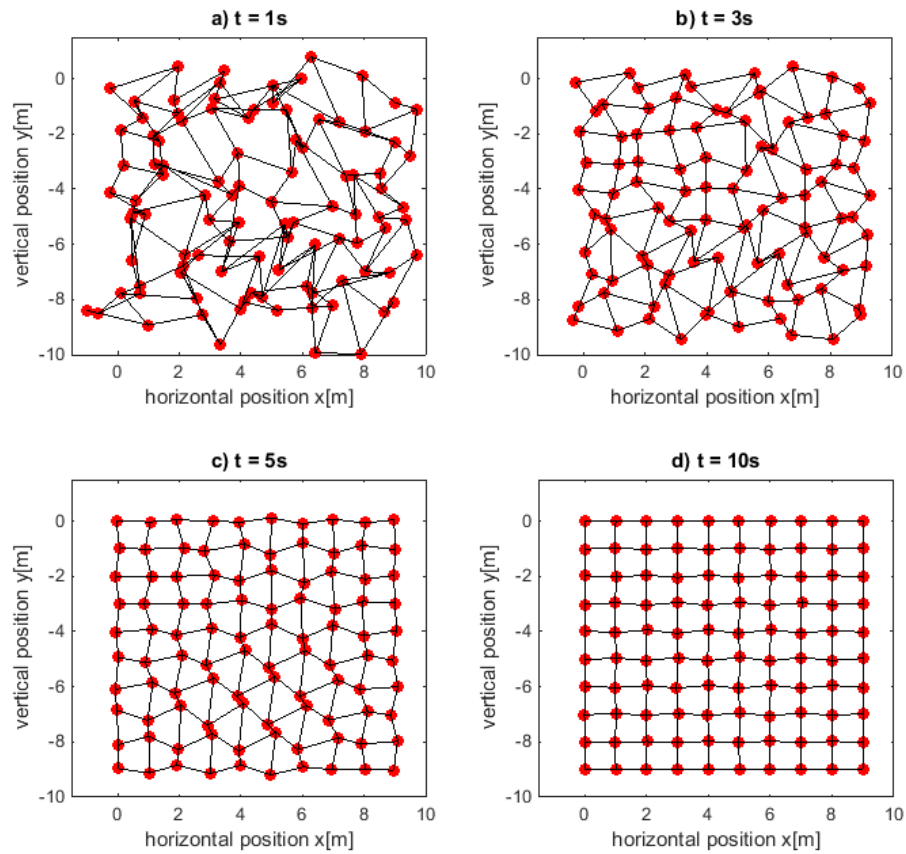


Figure 5.2: Snapshots of formation recovery simulation in the network of $N = 100$ agents where each agent is described by double integrator dynamics

5.2 Optimal and Near-Optimal Distributed Control Schemes

In this section a method for identifying optimal and near-optimal distributed control schemes is proposed. The two control designs presented in Section 4.2 and Section 5.1 are compared with regards to their performance level. Perturbation analysis is used to describe the effect of the edge(s) elimination from the communication network. Please note that the next results are valid for multi-agent systems consisting of at least four agents. Also, only bidirectional communication is considered (i.e. undirected graphs) as in the real life multi-agent networks the agent failure usually implies the loss of communication in both directions.

5.2.1 Comparison of Centralized Controller and Distributed Controller

Consider the distributed suboptimal control problem given in Section 5.1 with gain matrix

$$\tilde{K} = I_{N_d} \otimes R^{-1}B^T P - M \otimes R^{-1}B^T P_{a_{12}} \quad (5.21)$$

where the communication network is described by a complete graph, i.e. $d_{max} = N_d - 1$. Then, \tilde{K} in (5.21) is equivalent to the centralized large-scale gain matrix in (4.15) and optimality is preserved. Through the whole section we consider the analysis of a system with the less strict stability condition. Therefore, matrix M satisfies (5.6) with $b = 1$ and $a = d_{max}$ and gain matrix of a complete graph with $N_d > 4$ is given by

$$K_a = \begin{pmatrix} R^{-1}B^T P_{a_{11}} & -R^{-1}B^T P_{a_{12}} & \dots & -R^{-1}B^T P_{a_{12}} \\ -R^{-1}B^T P_{a_{12}} & R^{-1}B^T P_{a_{11}} & \dots & -R^{-1}B^T P_{a_{12}} \\ \vdots & \vdots & \ddots & \vdots \\ -R^{-1}B^T P_{a_{12}} & \dots & \dots & R^{-1}B^T P_{a_{11}} \end{pmatrix} \quad (5.22)$$

where $P_{a_{11}} = P - (N_d - 1)P_{a_{12}}$. Edge(s) elimination from a fully connected network can be considered as a perturbation on the centralized large-scale problem. This is equivalent to a distributed communication network, where at least one subsystem is not connected to at least one other subsystem. Elimination of the (i, j) th edge results in $\mathbf{A}(i, j) = \mathbf{A}(j, i) = 0$ and also cancels the

corresponding blocks in K_a . The resulting K_a matrix will be called the perturbed gain matrix, \tilde{K} . For example, in the network of N agents elimination of $(1, 2)$ edge (*i.e.* $(1, 2) \notin \mathcal{E}$) is described by

$$\tilde{K} = \begin{pmatrix} R^{-1}B^T P_{a_{11}} & 0 & \dots & -R^{-1}B^T P_{a_{12}} \\ 0 & R^{-1}B^T P_{a_{11}} & \dots & -R^{-1}B^T P_{a_{12}} \\ \vdots & \vdots & \ddots & \vdots \\ -R^{-1}B^T P_{a_{12}} & \dots & \dots & R^{-1}B^T P_{a_{11}} \end{pmatrix}. \quad (5.23)$$

Then, two gain matrices in (5.22) and (5.23) will differ by ΔK , *i.e.* $\Delta K = K_a - \tilde{K}$. In the case of $(1, 2) \notin \mathcal{E}$, ΔK is given by

$$\Delta K = \begin{pmatrix} 0 & -R^{-1}B^T P_{a_{12}} & \dots & 0 \\ -R^{-1}B^T P_{a_{12}} & 0 & \dots & 0 \\ \vdots & \vdots & \ddots & \vdots \\ 0 & 0 & \dots & 0 \end{pmatrix}. \quad (5.24)$$

The following result can now be established:

Theorem 5.2.1. *Suppose that the assumptions of Theorem 5.1.1 hold and let $E = \tilde{P} - P_a$ where P_a is defined in (4.11) and \tilde{P} is the solution of the Lyapunov equation:*

$$(A_a - B_a \tilde{K})^T \tilde{P} + \tilde{P}(A_a - B_a \tilde{K}) + \tilde{K}^T R_a \tilde{K} + Q_a = 0. \quad (5.25)$$

Then, $E = E^T$ is the unique positive semi-definite solution of the following Lyapunov equation:

$$\tilde{A}_{cl}^T E + E \tilde{A}_{cl} + (\Delta K)^T R_a \Delta K = 0 \quad (5.26)$$

in which $\tilde{A}_{cl} = A_a - B_a R_a^{-1} B_a^T P_a + B_a \Delta K$ is Hurwitz. In particular, $E = E^T > 0$ if and only if the pair $(A_a - B_a R_a^{-1} B_a^T P_a, \Delta K)$ is observable.

Proof. The set of Lyapunov equations describing these two problems is

$$(A_a - B_a K_a)^T P_a + P_a (A_a - B_a K_a) + K_a^T R_a K_a + Q_a = 0 \quad (5.27)$$

$$(\tilde{A} - \tilde{B} \tilde{K})^T \tilde{P} + \tilde{P} (\tilde{A} - \tilde{B} \tilde{K}) + \tilde{K}^T \tilde{R} \tilde{K} + \tilde{Q} = 0. \quad (5.28)$$

As the number of subsystems and their dynamics are identical for both prob-

lems, the set can be rewritten as

$$(A_a - B_a K_a)^T P_a + P_a (A_a - B_a K_a) + K_a^T R_a K_a + Q_a = 0 \quad (5.29)$$

$$(A_a - B_a \tilde{K})^T \tilde{P} + \tilde{P} (A_a - B_a \tilde{K}) + \tilde{K}^T R_a \tilde{K} + Q_a = 0. \quad (5.30)$$

First note that since $A_a - B_a K_a$ and $A_a - B_a \tilde{K}$ are Hurwitz $P_a \geq 0$ and $\tilde{P} \geq 0$. The difference between these two solutions, E , is defined as $E = \tilde{P} - P_a$. Substitution of $\tilde{P} = P_a + E$, $K_a = R_a^{-1} B_a^T P_a$ and $\tilde{K} = K_a - \Delta K$ into (5.29) and (5.30) gives

$$\begin{aligned} & A_a^T P_a + P_a A_a - P_a B_a R_a^{-1} B_a^T P_a + Q_a = 0 \\ & (A_a^T - P_a B_a R_a^{-1} B_a^T + (\Delta K)^T B_a^T) E + E (A_a - B_a R_a^{-1} B_a^T P_a + B_a (\Delta K)) \\ & + A_a^T P_a + P_a A_a - P_a B_a R_a^{-1} B_a^T P_a + Q_a + (\Delta K)^T R_a (\Delta K) = 0 \end{aligned} \quad (5.31)$$

Subtraction of equations in (5.31) gives the single Lyapunov equation

$$\begin{aligned} & (A_a^T - P_a B_a R_a^{-1} B_a^T + (\Delta K)^T B_a^T) E + \\ & E (A_a - B_a R_a^{-1} B_a^T P_a + B_a (\Delta K)) + (\Delta K)^T R_a (\Delta K) = 0 \end{aligned} \quad (5.32)$$

which has E as a solution. Equation (5.32) can be rewritten by using more compact notation as:

$$\tilde{A}_{cl}^T E + E \tilde{A}_{cl} + (\Delta K)^T R_a (\Delta K) = 0 \quad (5.33)$$

where $\tilde{A}_{cl} = A_a - B_a R_a^{-1} B_a^T P_a + B_a (\Delta K)$. Theorem 5.1.1 implies that \tilde{A}_{cl} is Hurwitz which in turn implies that E is uniquely defined and $E = E^T \geq 0$. Using standard theory of Lyapunov equations E is positive definite if and only if the pair $(\tilde{A}_{cl}, \Delta K)$ is observable, which is equivalent to the observability of the pair $(A_a - B_a R_a^{-1} B_a^T P_a, \Delta K)$. The result is established in Theorem 5.2.2. \square

Theorem 5.2.2. *Consider the fully-connected multi-agent network consisting of at least four agents. Then, if a single link is removed between any two agents, E will be singular.*

Proof. The assumption $N_d \geq 4$ ensures that the assumptions of Theorem 5.1.1 are satisfied. Thus \tilde{A}_{cl} is Hurwitz and $E = E^T \geq 0$. To show that E is singular it suffices to show that the pair $(A_a - B_a R_a^{-1} B_a^T P_a, \Delta K)$ is unobservable. For notational simplicity assume temporarily that $N_d = 4$ and that link (1, 2) has

been removed. The unobservability condition which needs to be established is equivalent to the existence of $\lambda \in \mathbb{C}$ such that the matrix:

$$\left(\begin{array}{c} A_{cl_a} - \lambda I \\ \hline \Delta K \end{array} \right) \quad (5.34)$$

is rank deficient (see Definition 3.1.6) where $A_{cl_a} = A_a - B_a R_a^{-1} B_a^T P_a$. This can be written out in full as:

$$\left(\begin{array}{cccc} A - XP_{a_{11}} - \lambda I & -XP_{a_{12}} & -XP_{a_{12}} & -XP_{a_{12}} \\ -XP_{a_{12}} & A - XP_{a_{11}} - \lambda I & -XP_{a_{12}} & -XP_{a_{12}} \\ -XP_{a_{12}} & -XP_{a_{12}} & A - XP_{a_{11}} - \lambda I & -XP_{a_{12}} \\ -XP_{a_{12}} & -XP_{a_{12}} & -XP_{a_{12}} & A - XP_{a_{11}} - \lambda I \\ \hline 0 & -R^{-1}B^T P_{a_{12}} & 0 & 0 \\ -R^{-1}B^T P_{a_{12}} & 0 & 0 & 0 \\ 0 & 0 & 0 & 0 \\ 0 & 0 & 0 & 0 \end{array} \right)$$

where $X = BR^{-1}B^T$. Next we introduce the state-space transformation:

$$\left(\begin{array}{c} A_{cl_a} - \lambda I \\ \hline \Delta K \end{array} \right) \xrightarrow{T_1} \left(\begin{array}{c} T_1(A_{cl_a} - \lambda I)T_1^{-1} \\ \hline \Delta K T_1^{-1} \end{array} \right).$$

in which T_1 is chosen as:

$$T_1 = \begin{pmatrix} I & I & I & I \\ 0 & I & 0 & 0 \\ 0 & -I & I & 0 \\ 0 & I & I & I \end{pmatrix}, \quad (5.35)$$

which gives

$$\left(\begin{array}{cccc} (A - XP) - \lambda I & 0 & 0 & 0 \\ -XP_{a_{12}} & (A - XP_{diff}) - \lambda I & 0 & 0 \\ 0 & 0 & (A - XP_{diff}) - \lambda I & 0 \\ -3XP_{a_{12}} & 0 & 0 & (A - XP_{diff}) - \lambda I \\ \hline 0 & -R^{-1}B^T P_{a_{12}} & 0 & 0 \\ -R^{-1}B^T P_{a_{12}} & 0 & 0 & R^{-1}B^T P_{a_{12}} \\ 0 & 0 & 0 & 0 \\ 0 & 0 & 0 & 0 \end{array} \right) \quad (5.36)$$

where $P_{diff} = P_{a_{11}} - P_{a_{12}}$. The matrix in (5.36) loses rank along the third column if λ is chosen as an eigenvalue of the matrix $A - X(P_{a_{11}} - P_{a_{12}})$ (using Theorem 4.2.2). Since the rank of a matrix remains invariant under similarity transformations the system $(\tilde{A}_{cl}, \Delta K)$ is unobservable in this case and hence E is singular. The proof can be generalised for $N_d \geq 4$ agents by extending the transformation matrix T_1 to the large-scale transformation matrix T_{1link} :

$$T_{1link} = \begin{pmatrix} T_1 & X \\ O & I \end{pmatrix} \quad (5.37)$$

where $O \in \mathbb{R}^{(N_d-4) \times (N_d-4)}$ and $I \in \mathbb{R}^{(N_d-4) \times (N_d-4)}$ denote the zero and the unit matrix, respectively, and $X = \begin{pmatrix} I & \dots & I \\ 0 & \dots & 0 \\ 0 & \dots & 0 \\ I & \dots & I \end{pmatrix} \in \mathbb{R}^{4 \times (N_d-4)}$.

The result can also be generalised if an arbitrary (rather than link (1,2)) is removed (see subsequent discussion). \square

Remark 5.2.1. *Theorem 5.2.2 is proved under assumption that link between agents 1 and 2 is removed from the complete graph of any size. Removing a different link will change the structure of ΔK , but eigenvalue distribution in \tilde{P} and \tilde{A}_{cl} will be unchanged using Definition 3.1.3 (i.e. all similar matrices have the same spectrum). This can also be seen by considering the automorphism group of a graph \mathcal{G} that arises in the enumeration of nodes (known as labeling) which is reviewed below.*

Definition 5.2.1. [Cam01] *An automorphism of a graph \mathcal{G} is a permutation in which the graph is mapped onto itself while preserving the edge-node connectivity. Therefore, g is a permutation of the node set \mathcal{V} , such that, for any two nodes i and j we have $ig \sim jg$ (i.e. the image of the node i under the permutation g is adjacent to the image of the node j under the same permutation) if and only if $i \sim j$.*

Property 5.2.1. *The automorphism group arises in the enumeration of graphs (known as labeling). Therefore, the permuted graph can be obtained from the original graph by relabeling its nodes. For example, Figure 5.3 shows the graph \mathcal{G}_1 and its permuted graph \mathcal{G}_{1p} . Graph \mathcal{G}_{1p} is obtained from \mathcal{G}_1 by permuting labels of node 2 and node 3. Then, the eigenvalues of the adjacency matrix of graph \mathcal{G}_1 defined in Property 5.2.1, will be preserved in the adjacency matrix of its permutation $\mathbf{A}(\mathcal{G}_{1p})$.*

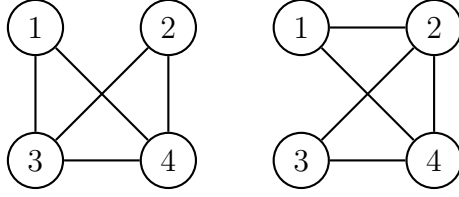


Figure 5.3: Graph \mathcal{G}_1 and its permuted graph $\mathcal{G}_{1,p}$

Therefore, E is singular for any of $\frac{N_d(N_d-1)}{2}$ configurations corresponding to complete graph of N_d agents with a single link removed. The analysis can be extended to the case when more than one link is removed from a complete network. Then, by using appropriate transformation matrices we can always choose the direction where E is singular. For example, if two links are removed from multi-agent network of N_d agents and maximum degree is $d_{max} = N_d - 1$, the corresponding transformation matrix is:

$$T_{2links} = \begin{pmatrix} T_2 & X \\ O & I \end{pmatrix} \quad (5.38)$$

where $O \in \mathbb{R}^{(N_d-4) \times (N_d-4)}$ and $I \in \mathbb{R}^{(N_d-4) \times (N_d-4)}$ denote the zero and the unit matrix, respectively, and

$$T_2 = \begin{pmatrix} I & I & I & I \\ 0 & I & 0 & 0 \\ 0 & I & I & 0 \\ 0 & I & I & I \end{pmatrix}, \quad X = \begin{pmatrix} I & \dots & I \\ 0 & \dots & 0 \\ 0 & \dots & 0 \\ I & \dots & I \end{pmatrix} \in \mathbb{R}^{4 \times (N_d-4)}. \quad (5.39)$$

However, the complexity of the analysis will increase with the number of agents and number of links to be removed. An numerical example is given in Section 5.2.3.

Next, some properties of the solution of the (large-scale) distributed problem described by Lyapunov equation (5.15) are presented.

Remark 5.2.2. *The solution to the Lyapunov equation associated with distributed or perturbed LQR problem, \tilde{P} , has a special structure due to the existing symmetry in the solution and degree of the individual nodes (number of agents connected to the each node). For example, in the case of a complete graph with four agents that is perturbed by (1,2) edge elimination (see*

Figure 5.4), \tilde{P} is given by

$$\tilde{P} = \left(\begin{array}{cc|cc} X & \alpha & \gamma & \gamma \\ \alpha & X & \gamma & \gamma \\ \hline \gamma & \gamma & Y & \beta \\ \gamma & \gamma & \beta & Y \end{array} \right). \quad (5.40)$$

The diagonal blocks of \tilde{P} will be equal for all nodes of the same degree (i.e. nodes 1 and 2 have degree 2, while nodes 3 and 4 have degree 3; therefore $\tilde{P}_{11} = \tilde{P}_{22} = X$ and $\tilde{P}_{33} = \tilde{P}_{44} = Y$). The off-diagonal blocks are characterized by the degree of nodes connected by (i, j) th edge. As we are dealing with undirected graph (i, j) th edge elimination is equivalent to (j, i) th edge elimination. The corresponding blocks will be different if the edge connects two nodes of degrees 2 and 3, respectively (i.e. nodes 2 and 3, nodes 2 and 4, nodes 1 and 3, nodes 1 and 4), and if it connects two nodes of the same degree (i.e. nodes 1 and 2 have degree 2, while nodes 3 and 4 have the same degree that is 3). Therefore, $\tilde{P}_{12} = \alpha$, $\tilde{P}_{34} = \beta$ and $\tilde{P}_{13} = \tilde{P}_{14} = \tilde{P}_{23} = \tilde{P}_{24} = \gamma$.

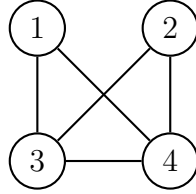


Figure 5.4: Complete graph with $N_d = 4$ agents perturbed by $(1, 2)$ edge elimination

5.2.2 Measures of Performance Loss for Distributed Configurations

First, the Weyl's inequalities are reviewed, as these are used in later work.

Theorem 5.2.3. (Weyl's inequalities) [Wey12] *Let $A, B \in \mathbb{C}^{n \times n}$ be both Hermitian and let $\{\lambda_j(A)\}_{j=1}^n$, $\{\lambda_j(B)\}_{j=1}^n$ and $\{\lambda_j(A+B)\}_{j=1}^n$ denote the set of eigenvalues of A , B and $A+B$, respectively. The eigenvalues are arranged in decreasing order, such as $\lambda_1 \geq \lambda_2 \geq \dots \geq \lambda_n$. Then, for any $1 \leq k \leq n$ we have*

$$\lambda_k(A) + \lambda_n(B) \leq \lambda_k(A+B) \leq \lambda_k(A) + \lambda_1(B). \quad (5.41)$$

Due to the symmetry, the following is also true:

$$\lambda_k(B) + \lambda_n(A) \leq \lambda_k(A+B) \leq \lambda_k(B) + \lambda_1(A). \quad (5.42)$$

In the last part of this section we compare the cost of the distributed controller obtained by the method outlined in Theorem 5.1.1 with the (optimal) cost of the LQR centralized controller. Not surprisingly we have the following result:

Proposition 5.2.1. *The cost imposed by the distributed LQR problem will be always equal or higher than actual LQR cost imposed by the centralized design.*

Proof. Although the result is obvious (the cost of the centralized optimal controller cannot exceed the cost of the distributed controller) we give a direct proof. The result is immediate if the distributed controller is not stabilising, so assume that the distributed cost is finite. From Theorem 5.2.1 it is known that $\tilde{P} = P_a + E$ with all matrices being symmetric positive semi-definite. Applying Weyl's inequality to $\tilde{P} = P_a + E$ gives:

$$\lambda_k(P_a) + \lambda_n(E) \leq \lambda_k(\tilde{P}) \text{ for any } 1 \leq k \leq n$$

where the eigenvalues are indexed in decreasing order. The required result follows from Theorem 5.2.1 since $\lambda_n(E) \geq 0$. \square

According to Proposition 5.2.1 the cost of the distributed LQR problem is always greater than or equal to the cost of the optimal centralized controller. A natural question arising is under what conditions the two costs are equal. The following result gives necessary and sufficient conditions for equality of the two costs:

Theorem 5.2.4. *The cost of a stabilising distributed controller defined in Theorem 5.1.1 is equal to the cost of the centralized optimal LQR controller if and only if the pair $(A_a - B_a R_a^{-1} B_a^T P_a, \Delta K)$ is unobservable and $\tilde{\mathbf{x}}_0 \in \text{Ker}(E)$ where $E = \tilde{P} - P_a$.*

Proof. The cost of a stabilising distributed controller is:

$$J(\tilde{\mathbf{u}}, \tilde{\mathbf{x}}_0) = \tilde{\mathbf{x}}_0^T \tilde{P} \tilde{\mathbf{x}}_0 = \tilde{\mathbf{x}}_0^T P_a \tilde{\mathbf{x}}_0 + \tilde{\mathbf{x}}_0^T E \tilde{\mathbf{x}}_0 \quad (5.43)$$

in which the first term on the right-hand-side of the last equality represents the optimal LQR cost of the centralized controller. Since $E = E^T \geq 0$, the term $\tilde{\mathbf{x}}_0^T E \tilde{\mathbf{x}}_0$ is zero if and only if E is singular and $\tilde{\mathbf{x}}_0 \in \text{Ker}(E)$, the first condition being equivalent to the unobservability of the pair $(A_a - B_a R_a^{-1} B_a^T P_a, \Delta K)$ as shown in Theorem 5.2.2. \square

Remark 5.2.3. *Theorem 5.2.2 and Theorem 5.2.4 can be extended along various directions. Consider first the case of near-optimal distributed configurations for which the cost increase along specific directions $\boldsymbol{\xi}$ is small relative to the optimal LQR cost. For these directions the pair $(A_a - B_a R_a^{-1} B_a^T P_a, \Delta K)$ is close to unobservability, in the sense that for certain $\lambda_0 \in \mathbb{C}$ and $\|\boldsymbol{\xi}\| = 1$ the norm of the vector*

$$\begin{pmatrix} \lambda_0 I - A_a + B_a R_a^{-1} B_a^T P_a \\ R_a^{1/2} K_a \end{pmatrix} \boldsymbol{\xi} \quad (5.44)$$

is small. Specifically, let $E = E^T > 0$ be a solution of (5.26) with $\lambda_{\min}(E) = \epsilon > 0$. Then, the cost of the corresponding distributed controller (guaranteed to be stabilising under the previous assumptions) is:

$$J(\tilde{\mathbf{u}}, \tilde{\mathbf{x}}_0) = \tilde{\mathbf{x}}_0^T \tilde{P} \tilde{\mathbf{x}}_0 = \tilde{\mathbf{x}}_0^T P_a \tilde{\mathbf{x}}_0 + \tilde{\mathbf{x}}_0^T E \tilde{\mathbf{x}}_0 \quad (5.45)$$

where the term $\tilde{\mathbf{x}}_0^T E \tilde{\mathbf{x}}_0 \geq \epsilon \|\tilde{\mathbf{x}}_0\|^2$. In particular, if $\tilde{\mathbf{x}}_0$ is chosen to lie in the eigenspace of E corresponding to its minimum eigenvalue, $\tilde{\mathbf{x}}_0^T E \tilde{\mathbf{x}}_0 = \epsilon \|\tilde{\mathbf{x}}_0\|^2$. Therefore, for small values of ϵ and along these directions the cost increase from the optimal level will be minimal. Next consider the case that $E = E^T \geq 0$ and singular. Let $\lambda_1 \geq \dots \geq \lambda_m > \lambda_{m+1} = \dots = \lambda_{m+r} > \lambda_{m+r+1} = \dots = \lambda_n = 0$. In this case there is no cost increase along all directions in the null-space of E . If $\tilde{\mathbf{x}}_0$ lies in the r -dimensional eigenspace corresponding to $\lambda_{m+1}(E)$, then the cost increase is exactly $\lambda_{m+1}(E) \|\tilde{\mathbf{x}}_0\|^2$. Thus the sequence of eigenvalues

of E indicate the progressive deviation from optimality if the initial state lies in the corresponding eigenspace. A final measure of deviation from optimality for each decentralized control scheme is average cost. Assuming that $\tilde{\mathbf{x}}_0$ is uniformly distributed on the surface of an n -dimensional hyper-sphere we define the average cost as the expected value:

$$\mu(E) := \frac{\int_{\|\xi\|=1} \xi^T E \xi \, dS}{\int_{\|\xi\|=1} dS} = \frac{\text{trace}(E)}{nN_d} \quad (5.46)$$

which may be considered as a measure of average cost increase due to decentralization over all initial state directions.

5.2.3 Numerical Example: Performance Loss Analysis for Different Distributed Configurations

Consider a network of $N = 6$ identical, dynamically decoupled agents represented by a complete graph. Their collective dynamics is given by

$$\dot{\tilde{\mathbf{x}}}(t) = \tilde{A}\tilde{\mathbf{x}} + \tilde{B}\tilde{\mathbf{u}}, \quad \tilde{\mathbf{x}}(0) = \tilde{\mathbf{x}}_0 \quad (5.47)$$

where $\tilde{A} = I_6 \otimes A$ and $\tilde{B} = I_6 \otimes B$ with A and B defined as

$$A = \begin{pmatrix} -1 & 0 & -2 \\ -2 & -3 & -4 \\ 1 & 0 & -1 \end{pmatrix}, \quad B = \begin{pmatrix} 1 & 1 \\ 0 & 2 \\ -1 & 3 \end{pmatrix}. \quad (5.48)$$

The interconnection structure is depicted in Figure 5.5. The cost function

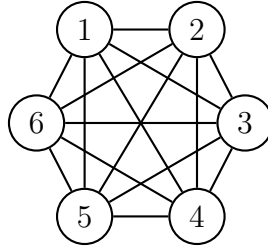


Figure 5.5: Fully connected (complete) multi-agent network of $N = 6$ agents

defined in (4.6) uses the following weights for the state information: $Q_{a_{ii}} = Q_1 = I_3$ and $Q_{a_{ij}} = Q_2 = I_3$, while the weight on the control effort is $R_a = I_6 \otimes R$ with $R = I_2$. By using the distributed control method proposed in

Section 5.1 each agent is stabilised and for the configuration given in Figure 5.5 the cost is optimal due to the equivalence with centralized LQR problem. For a given initial state vector $\tilde{\mathbf{x}}_0$, such that $\|\tilde{\mathbf{x}}_0\| = 1$, we get the stabilising centralized LQR solution, P_a and therefore the optimal (minimal) cost. For this case the cost measures are given in Table 5.1.

Table 5.1: Cost measures for optimal (centralized) LQR design

Minimum Cost	Average Cost	Maximum Cost
0.103	1.343	2.601

Next, we consider a number of different distributed configurations obtained by removing one, two or three links from a complete graph in Figure 5.5. Using results from Section 5.2.1 the number of different distributed configurations reduces to 6 and these are depicted in Figure 5.6. Please note that number of links removed could be larger than three. Then, the asymptotic stability will be still achieved and same conclusions would apply.

The performance loss is measured by using alternative methods presented in Remark 5.2.3 and results are given in Table 5.2. As an additional information, the maximum and minimum degree are given for each configuration.

Table 5.2: Cost measures for suboptimal distributed LQR configurations

Cost Measure	Single cut (d_{max}, d_{min})	Double cut (d_{max}, d_{min})	Triple cut (d_{max}, d_{min})
Minimum Cost	0.103 (5,4)	0.104 (5,4)	0.103 (4,4)
		0.104 (5,3)	0.104 (5,3)
			0.105 (5,2)
Average Cost	1.345 (5,4)	1.347 (5,4)	1.354 (4,4)
		1.347 (5,3)	1.350 (5,3)
			1.350 (5,2)
Maximum Cost	2.609 (5,4)	2.609 (5,4)	2.630 (4,4)
		2.618 (5,3)	2.618 (5,3)
			2.627 (5,2)

It can be seen that all costs are highly dependent on how well network is connected (i.e. they all increase as the minimum degree, d_{min} , drops for a fixed d_{max}). Additionally, for each configuration there is at least one direction for

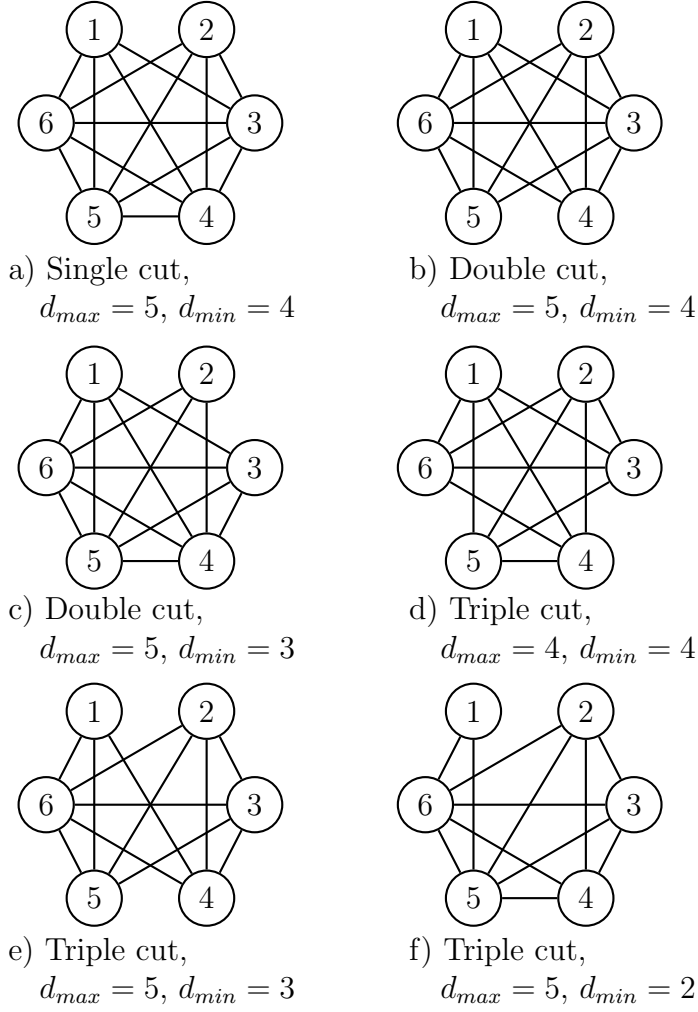


Figure 5.6: Different distributed configurations for the multi-agent network consisting of $N = 6$ agents

which optimality is preserved compared to the centralized design. For example in the case of triple cut with $d_{min} = 2$ E is singular ($rank(E) = 9$) which implies the equality in costs for specific directions as claimed in Theorem 5.2.2 and Theorem 5.2.4. This does not necessarily imply that this direction coincides with the direction of the eigenvector corresponding to $\lambda_{min}(P_a)$. Note that when three links are removed in the case under consideration, equality with $\lambda_{min}(P_a)$ occurs only for a configuration corresponding to a minimum and maximum degree equal 4. Therefore, the minimum value among all minimal costs occurs when all agents share the same degree and we have a so-called *regular network*.

Additionally, we give the probability distribution of distributed cost deviation from optimality in the case of a single link cut. The number of different initial

state vectors, $\tilde{\mathbf{x}}_0$, that has been consider equals 10000 and for each of them $\|\tilde{\mathbf{x}}_0\| = 1$. Results are depicted in Figure 5.7. It is shown that there will exist a number of initial state vectors that will result in E being singular matrix and optimality will be preserved.

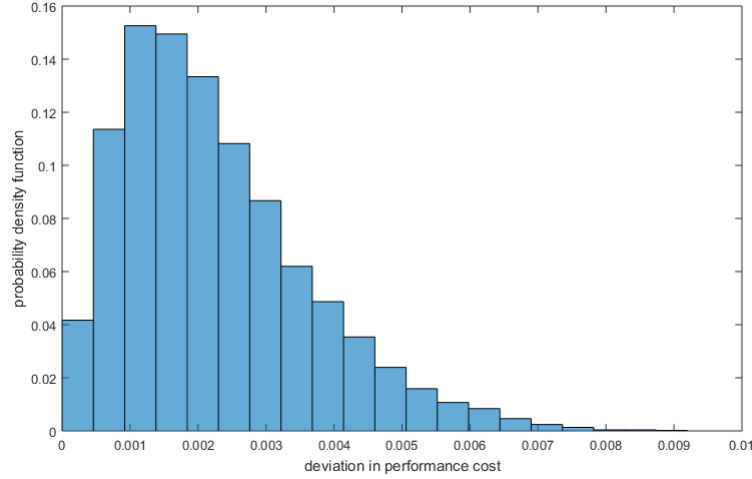


Figure 5.7: Probability distribution of the performance cost deviation from optimality

5.3 Summary

This chapter provided a method for designing distributed controller for dynamically decoupled multi-agent systems. The proposed controller was compared with respect to the performance cost with the centralized solution. It was shown that for specific distributed control configurations the optimality can be preserved.

The main theoretical methods presented here will be applied to a high order dynamical system in subsequent chapters. In the next chapter a nonlinear dynamical model of an experimental aircraft will be presented. Also, the need for an adequate control system to provide the asymptotic stability of the aircraft will be illustrated.

Chapter 6

Application Example: LQR Control of X-RAE1 UAV

In this chapter we present a six degrees-of-freedom (6-DOF) dynamical model of an experimental RPV (Remotely Piloted Vehicle), namely X-RAE1. First, we give a brief overview of the motions of an aircraft which is followed by the description of three different coordinate systems used to develop the X-RAE1's equations of motion.

Next the 6-DOF nonlinear equations of an aircraft are developed. This model is then linearised and decomposed into two motions for specific flight conditions. Linearisation is performed by assuming small perturbations around the operating point of the aircraft for the straight flight case at forward velocity of 30m/s.

Finally, in the last section we propose an LQR control design for altitude control and disturbance rejection for the linearised X-RAE1 model. Also, it is shown that the LQR-based controller can be used to successfully stabilise the nonlinear X-RAE1 model. The design is further extended to the multi-agent distributed control case which is given in the subsequent chapter.

6.1 Motions of an Aircraft

The motion of an aircraft can be described by three translational motions and three rotational motions which are coupled together. The translational motions are:

1. *Forward and backward translation* across the longitudinal axis (x -axis),
2. *Left and right translation* across the lateral axis (y -axis), and
3. *Up and down translation* across the vertical axis (z -axis).

The rotational motions are:

1. *Pitch* - a rotational motion in which aircraft turns around the lateral axis (y -axis) by raising or lowering the nose of the aircraft,
2. *Roll* - a rotational motion in which aircraft turns around the longitudinal axis (x -axis) by raising one wing higher while the other wing dips lower, and
3. *Yaw* - a rotational motion in which aircraft turns around the vertical axis (z -axis) by moving the nose of the aircraft to the pilot's left or right side.

These movements are depicted in Figure 6.1 where the direction of arrows indicates positive motion in each axis.

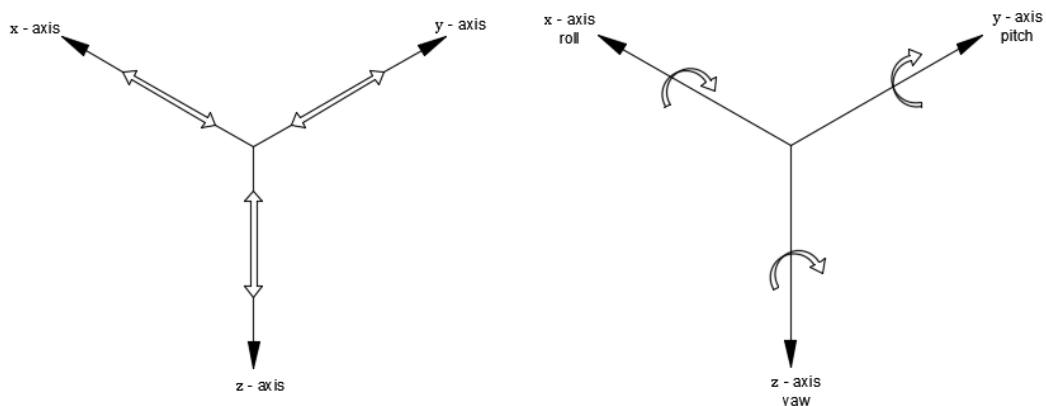


Figure 6.1: The three translational movements and the three rotational movements [Elg13]

6.2 Coordinate Systems and Axes Transformations

In order to develop the X-RAE1's equations of motion the fundamental principles of Newtonian mechanics are used. Before applying Newton's laws to a rigid body (aircraft) the suitable systems of axes are defined as well as the process of converting from one system to another. These are: the Earth-fixed coordinate system (an inertial axis system fixed to the Earth), the body-fixed coordinate system (a system fixed to the aircraft) and the stability axis system (a body fixed system defined with respect to the relative wind) [Elg13].

To describe the position and orientation of an aircraft relative to the Earth the *Earth-fixed coordinate system* (x_f, y_f, z_f) is used. It is considered to be fixed in space where x_f - y_f plane is normal to the local gravitational vector with the x_f -axis pointing north and the y_f -axis pointing east. The z_f -axis points downward, completing the right-handed Cartesian system. The Earth-fixed coordinate system is depicted in Figure 6.2 a) [Phi10].

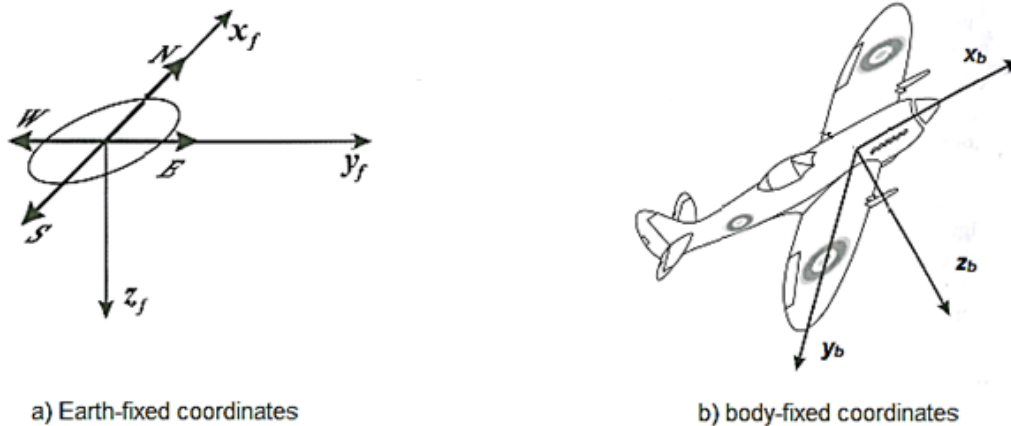


Figure 6.2: Coordinate systems: a) Earth-fixed coordinate system b) Body-fixed coordinate system [Phi10]

The aerodynamic forces and moments acting on the aircraft are most conveniently described in terms of the *body-fixed coordinate system* (x_b, y_b, z_b). The body-fixed coordinate system is the right-handed Cartesian system which has its origin O_b located at the aircraft center of gravity. The $x_b O_b z_b$ plane coincides with the aircraft's plane of symmetry. The x_b -axis points forward toward the nose of the aircraft. The y_b -axis points in the direction of the right wing, while

the z_b -axis points downward. The body-fixed coordinate system is depicted in Figure 6.2 b) [Phi10].

The *stability axis system* (x, y, z) coincides with the body-fixed coordinate system that is rotated by the angle of attack α with its origin located at the aircraft center of gravity. The x -axis points in the direction of the relative wind onto the x - z plain of the aircraft, while the y -axis points in the direction of the right wing. The z -axis points downward, completing the right-handed Cartesian system.

In order to transform the data between different reference axes the *Euler angle formulation* is used. The orientation of the body-fixed coordinate system (x_b, y_b, z_b) relative to the Earth-fixed coordinate system (x_f, y_f, z_f) is described in terms of three consecutive rotations through three *Euler angles*. The three Euler angles are: the bank angle Φ , the elevation angle Θ , and the azimuth angle or heading Ψ . As these angles can be related to roll, pitch, and yaw, we will be referring to them as the roll angle, the pitch angle, and the yaw angle, respectively. A positive roll angle Φ is when the aircraft rolls to the right (i.e. the right wing points downward). A positive pitch angle Θ is when the aircraft nose pitches up. A positive yaw angle Ψ is when the nose of the aircraft points to the right.

With reference to Figure 6.3, (x_f, y_f, z_f) coordinate system is first rotated about the z_f -axis through an angle Ψ to the coordinate system (x_1, y_1, z_1) . Then, (x_1, y_1, z_1) coordinate system is rotated about y_1 -axis through an angle Θ to the coordinate system (x_2, y_2, z_2) . Finally, (x_2, y_2, z_2) coordinate system is rotated about x_2 -axis through an angle Φ to the coordinate system (x_b, y_b, z_b) [Phi10]. The three rotations depicted in Figure 6.3 can be combined into one transformation matrix. Then, the rotation matrix used to transform the components of any vector from body-fixed coordinates to Earth-fixed coordinates, R_B^F , is given by

$$R_B^F = \begin{pmatrix} c_\theta c_\psi & s_\phi s_\theta c_\psi - c_\phi s_\psi & c_\phi s_\theta c_\psi + s_\phi s_\psi \\ c_\theta s_\psi & s_\phi s_\theta s_\psi + c_\phi c_\psi & c_\phi s_\theta s_\psi - s_\phi c_\psi \\ -s_\theta & s_\phi c_\theta & c_\phi c_\theta \end{pmatrix} \quad (6.1)$$

where $s_\phi = \sin(\Phi)$, $c_\phi = \cos(\Phi)$, $s_\theta = \sin(\Theta)$, $c_\theta = \cos(\Theta)$, $s_\psi = \sin(\Psi)$, and $c_\psi = \cos(\Psi)$.

Further, by inverting the rotation matrix R_B^F we get the new rotational matrix

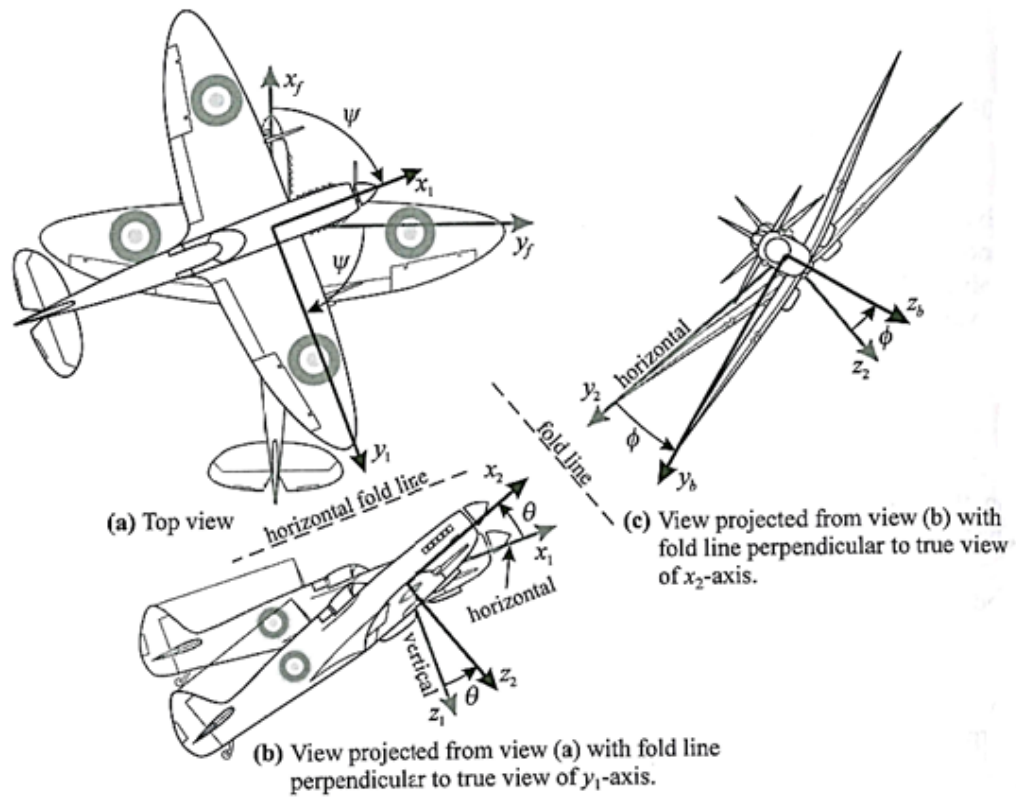


Figure 6.3: True views of the three Euler angles shown following the standard conventions of engineering graphics and descriptive geometry [Phi10]

R_F^B that can be used to transform the components of any vector from Earth-fixed coordinates to body-fixed coordinates. Due to orthogonality the inverse of the rotational matrix in (6.1) is its transpose. Therefore, $R_F^B = (R_B^F)^T$.

6.3 Aircraft Equations of Motion

Before deriving the equations of motion of an aircraft, we give the overview of the assumptions made. These assumptions are used throughout the chapter.

The aircraft is assumed to be a rigid body that has a symmetry about x - z plane. The mass of the aircraft is assumed to be constant at all times. Further, the rotation, as well as the curvature of the Earth are neglected, and the atmosphere is assumed still with respect to the Earth.

The derivation of the equations of motion for a rigid symmetric aircraft is usually attributed to Bryan [Bry11]. His model has been a basis for the further development of the equations that are given in standard text books, such as [Coo97], [ER95], [Bla91], etc.

Next, we will present the derivation of force and moment equations, i.e translational and rotational dynamics together with external forces and moments considered. These will be summarised in the end with the full set of the equations of motion and notations used.

6.3.1 The Force Equations - Translational Dynamics

First, the inertial acceleration components that are the result of externally acting forces to the aircraft are defined by using Newton's second law. This law defines a force to be equal to the change in momentum per unit time. Taking into account that the mass of the aircraft, m , is assumed to be constant at all times the law reduces to:

$$\mathbf{F} = m \left(\frac{d\mathbf{V}_T}{dt} \right)_F \quad (6.2)$$

where \mathbf{V}_T is the velocity vector defined with respect to the Earth.

It is well-known that Newton's second law is only valid with respect to the Earth-fixed coordinate system. Therefore, for derivation in body-fixed axes, the aircraft's rotation with respect to the Earth-fixed coordinate system has to be taken into account. The rate of change of the velocity vector in the Earth-fixed frame is given by

$$\dot{\mathbf{V}}_{T_F} = \dot{\mathbf{V}}_{T_B} + \boldsymbol{\Omega}_B \times \mathbf{V}_{T_B} \quad (6.3)$$

where \mathbf{V}_{T_B} , $\dot{\mathbf{V}}_{T_B}$, $\boldsymbol{\Omega}_B$ are the velocity vector, the rate of change of the velocity vector, and the angular velocity vector, respectively. Please note that all three vectors are defined with respect to the body-fixed coordinate system.

The components of velocity vector in the body-fixed coordinate system, \mathbf{V}_{T_B} , along the body axes (x_b, y_b, z_b) are denoted (U, V, W) where U, V, W are forward, side and downward velocity along the x_b -axis, y_b -axis and z_b -axis, respectively. Similarly, the components of angular velocity in the body-fixed coordinate system, $\boldsymbol{\Omega}_B$, along (x_b, y_b, z_b) are denoted (P, Q, R) where P, Q, R are roll, pitch and yaw angular velocity along the x_b -axis, y_b -axis and z_b -axis, respectively.

Then, (6.3) can be rewritten as:

$$\begin{pmatrix} \dot{U} \\ \dot{V} \\ \dot{W} \end{pmatrix}_F = \begin{pmatrix} \dot{U} \\ \dot{V} \\ \dot{W} \end{pmatrix}_B + \begin{pmatrix} QW - RV \\ RU - PW \\ PV - QU \end{pmatrix}_B. \quad (6.4)$$

Each of the velocity components comprise a linear term and two additional terms due to rotational motion. By substituting (6.4) into (6.2), three force equations can be derived as:

$$\begin{aligned} X &= m(\dot{U} + QW - RV) \\ Y &= m(\dot{V} + RU - PW) \\ Z &= m(\dot{W} + PV - QU) \end{aligned} \quad (6.5)$$

where $X, Y,$ and Z are the resultant components of total force, \mathbf{F} , acting on the rigid body along the axes $x_b, y_b,$ and z_b , respectively.

6.3.2 The Moment Equations - Rotational Dynamics

Next, we consider the moments produced by the forces acting on the rigid body of mass m . The moment equations are determined by applying Newton's second law which states that the time change of angular momentum of the aircraft is equal to the applied moments acting on the aircraft:

$$\mathbf{M}_s = \frac{d\mathbf{H}}{dt} \quad (6.6)$$

where \mathbf{M}_s is the vector of all externally applied moments. Then, $\mathbf{M}_s = (L, M, N)^T$, where L , M and N are rolling moment, pitching moment and yawing moment, respectively.

The components of angular momentum vector, \mathbf{H} , along the axes x_b , y_b and z_b are denoted (H_x, H_y, H_z) , respectively. For a rigid body \mathbf{H} in the body-fixed coordinate system is defined as the product of the inertia matrix J and the angular velocity vector $\boldsymbol{\Omega}_B$, such as

$$\mathbf{H}_B = J\boldsymbol{\Omega}_B = \begin{pmatrix} I_x & -I_{xy} & -I_{xz} \\ -I_{xy} & I_y & -I_{yz} \\ -I_{xz} & -I_{yz} & I_z \end{pmatrix} \begin{pmatrix} P \\ Q \\ R \end{pmatrix} \quad (6.7)$$

where I_x , I_y , I_z are the moments of inertia about x_b , y_b and z_b , respectively, while I_{xy} , I_{yz} , I_{xz} are the products of inertia about x_b and y_b axes, y_b and z_b axes, and x_b and z_b axes, respectively. As the aircraft is assumed to be a rigid body that has a symmetry about x_b - z_b plane $I_{xy} = I_{yz} = 0$.

By taking into account the aircraft's rotation with respect to the Earth-fixed coordinate system, the rate of change of the angular momentum vector, $\dot{\mathbf{H}}$, in the Earth-fixed frame is given by

$$\dot{\mathbf{H}}_F = \dot{\mathbf{H}}_B + \boldsymbol{\Omega}_B \times \mathbf{H}_B. \quad (6.8)$$

Therefore, the three moment equations of motion with respect to the body-fixed coordinate system are given by

$$\begin{aligned} L &= I_x \dot{P} - (I_y - I_z)QR - I_{xz}(PQ + \dot{R}) \\ M &= I_y \dot{Q} + (I_x - I_z)PR + I_{xz}(P^2 - R^2) \\ N &= I_z \dot{R} - (I_x - I_y)PQ + I_{xz}(QR - \dot{P}). \end{aligned} \quad (6.9)$$

The set of equations in (6.9) describe rolling motion, pitching motion and yawing motion, respectively [Coo97].

6.3.3 External Forces and Moments

Together, two set of equations in (6.5) and (6.9) define 6-DOF equations of motion for a rigid body with the uniform mass distribution. In order to develop the equations of motion further the terms on the left-hand side of each equation are described with respect to the acting forces and moments. In general, these can be classified into three categories:

1. Gravitational terms ($\mathbf{F}_G, \mathbf{M}_G$),
2. Aerodynamic terms ($\mathbf{F}_A, \mathbf{M}_A$), and
3. Power (thrust) terms ($\mathbf{F}_T, \mathbf{M}_T$).

Each of the categories is briefly explained in the following sections (for more details see [Coo97]).

Gravity Forces and Moments

In Earth-fixed coordinate system, the representation of the gravitational force vector \mathbf{F}_G is:

$$\mathbf{F}_{G_F} = \begin{pmatrix} 0 \\ 0 \\ mg \end{pmatrix}, \quad (6.10)$$

as the gravitational force is proportional to the mass m acting in z -direction. In the equation above g refers to the magnitude of the acceleration of gravity. By using the transpose of the rotational matrix defined in (6.1), the gravitational force vector in body-fixed coordinate system becomes

$$\mathbf{F}_{G_B} = \begin{pmatrix} F_{G_x} \\ F_{G_y} \\ F_{G_z} \end{pmatrix}_B = mg \begin{pmatrix} -\sin \Theta \\ \sin \Phi \cos \Theta \\ \cos \Phi \cos \Theta \end{pmatrix} \quad (6.11)$$

where Φ and Θ are the roll angle and the pitch angle, respectively.

The time derivatives of the Euler angles ($\dot{\Phi}, \dot{\Theta}, \dot{\Psi}$) can be related to the body-fixed components of the angular velocity vector (P, Q, R) which will be given later.

Since the origin of the aircraft in the body-fixed coordinate system coincides with the centre of gravity there is no weight moment about any of the axes. Therefore, $\mathbf{M}_G = (L_{M_G}, M_{M_G}, N_{M_G})^T = \mathbf{0}^T$.

Aerodynamic Forces and Moments

The usual procedure for finding the aerodynamic force and moment terms is to assume that these are dependent on the disturbed motion variables and their derivatives. This is expressed as a function comprising the sum of a number of Taylor series, where each Taylor series involves one motion variable ($U, V, W, P, Q,$ or R) or its derivative. For more details see [Hop70].

For simulation purposes, the aerodynamic force and moment terms were derived by using the velocity of the aircraft with respect to the Earth \mathbf{V}_T , the angle of attack α and the sideslip angle β , which are depicted in Figure 6.4 [Elg13].

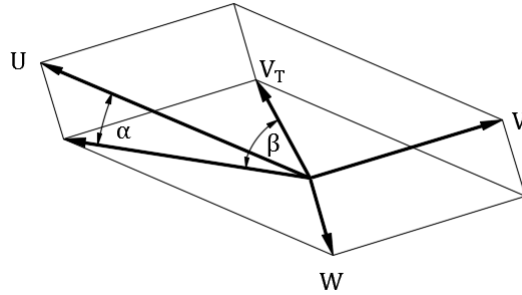


Figure 6.4: Graphical representation of the velocity vector \mathbf{V}_T , the angle of attack α and the sideslip angle β [Elg13]

As the atmosphere is assumed to be still, the relative wind velocity is $-\mathbf{V}_T$. The orientation of air velocity vector with respect to the body coordinate system is given through the angle of the attack and the angle of sideslip which

can be defined as

$$\begin{aligned}\alpha &= \tan^{-1} \frac{W}{U} \\ \beta &= \sin^{-1} \frac{V}{V_T}.\end{aligned}\tag{6.12}$$

Further, the aerodynamic force vector can be expressed as

$$\mathbf{F}_A = \begin{pmatrix} L \\ D \\ Y \end{pmatrix} = \frac{1}{2} \rho V_T^2 S \begin{pmatrix} C_L \\ C_D \\ C_y \end{pmatrix}\tag{6.13}$$

where

- L, D, Y are the aerodynamic force vector components named lift, drag and side force, respectively;
- ρ is the air density;
- S is the reference area of the aircraft;
- C_L, C_D, C_y are lift, drag and side force coefficients, respectively.

The lift force is normal to the component of the velocity vector on the longitudinal x_b - z_b plane, the drag force is parallel to the component of the velocity vector on the longitudinal x_b - z_b plane, while the side force acts along the y_b -axis. Their projections onto x_b, y_b and z_b are denoted as $F_{A_x}, F_{A_y}, F_{A_z}$, respectively, and these will be evaluated later.

Similarly the aerodynamic moment terms can be derived as

$$\mathbf{M}_A = \begin{pmatrix} L_A \\ M_A \\ N_A \end{pmatrix} = \frac{1}{2} \rho V_T^2 S \begin{pmatrix} bC_l \\ cC_m \\ bC_n \end{pmatrix}\tag{6.14}$$

where C_l, C_m, C_n are rolling, pitching and yawing moment coefficients, respectively, and b and c are the wing span and the mean aerodynamic chord of the wing, respectively. For more details see [McC11].

Thrust Forces and Moments

The thrust, \mathbf{T} , is assumed to act on the x_b - z_b plane along a thrust line with eccentricity e_T from the centre of gravity and angular displacement ε_T from x -axis in body-fixed coordinate system which is depicted in Figure 6.5 [Elg13].

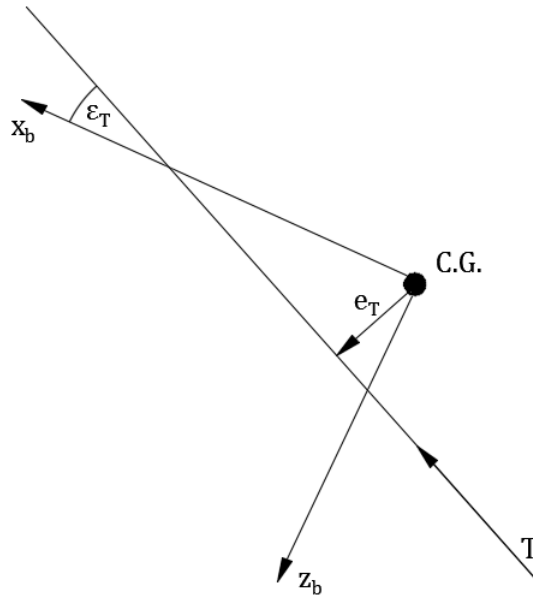


Figure 6.5: Graphical representation of the thrust \mathbf{T} [Elg13]

The thrust produces the forward force along the x_b -axis, F_{T_x} , the downward force along the z_b -axis, F_{T_z} , and the pitching moment across the y_b -axis due to the eccentricity of the thrust line, M_T . Please note that all gyroscopic effects are neglected, as well as the rolling moment caused by the torque moment of the engine. Then, the thrust force and moment terms are given by

$$\begin{aligned} F_{T_x} &= T \cos \varepsilon_T \\ F_{T_z} &= -T \sin \varepsilon_T \\ M_T &= T e_T. \end{aligned} \tag{6.15}$$

6.3.4 Complete Set of the Equations of Motion of X-RAE1

By combining the gravitational forces (6.11) into the inertial terms of (6.5) and (6.9), equations (6.5) and (6.9) can be rewritten as:

$$\begin{aligned}
 m(\dot{U} + QW - RV + g \sin \Theta) &= F_{A_x} + F_{T_x} = X \\
 m(\dot{V} + RU - PW - g \cos \Theta \sin \Phi) &= F_{A_y} = Y \\
 m(\dot{W} + PV - QU - g \cos \Theta \cos \Phi) &= F_{A_z} + F_{T_z} = Z
 \end{aligned} \tag{6.16}$$

and

$$\begin{aligned}
 I_x \dot{P} - (I_y - I_z)QR - I_{xz}(PQ + \dot{R}) &= L_A = L \\
 I_y \dot{Q} + (I_x - I_z)PR + I_{xz}(P^2 - R^2) &= M_A + M_T = M \\
 I_z \dot{R} - (I_x - I_y)PQ + I_{xz}(QR - \dot{P}) &= N_A = N.
 \end{aligned} \tag{6.17}$$

Additionally, we have to take into account that aerodynamic forces and moments L , D and M_A are estimated with reference to the point $A.C.$ at distance h_0 from the centre of gravity (see Figure 6.6). Then, the following equations

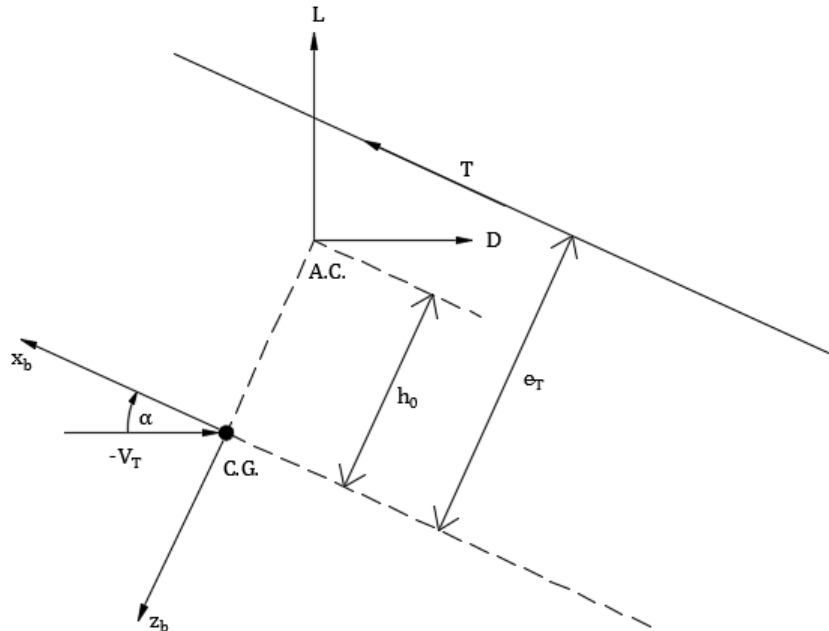


Figure 6.6: Longitudinal aerodynamic forces and moments and thrust representation for X-RAE1

can be derived:

$$\begin{aligned}
F_{A_x} &= \frac{1}{2}\rho V_T^2 S(C_L \sin \alpha - C_D \cos \alpha) \\
F_{A_y} &= \frac{1}{2}\rho V_T^2 S C_y \\
F_{A_z} &= \frac{1}{2}\rho V_T^2 S(-C_L \cos \alpha - C_D \sin \alpha).
\end{aligned} \tag{6.18}$$

The complete set of the equations of motion of X-RAE1 with respect to the body-fixed axes can be presented now:

1) Translational equations of motion:

$$\begin{aligned}
\dot{U} &= RV - QW - g \sin \Theta + [\bar{q}S(C_L \sin \alpha - C_D \cos \alpha) + T]/m \\
\dot{V} &= PW - RU + g \cos \Theta \sin \Phi + (\bar{q}S C_y)/m \\
\dot{W} &= QU - PV + g \cos \Theta \cos \Phi + [\bar{q}S(-C_L \cos \alpha - C_D \sin \alpha)]/m
\end{aligned} \tag{6.19}$$

2) Rotational equations of motion:

$$\begin{aligned}
\dot{P}I_x - \dot{R}I_{xz} &= QR(I_y - I_z) + PQI_{xz} + \bar{q}SbC_l \\
\dot{Q}I_y &= PR(I_z - I_x) - (P^2 - R^2)I_{xz} + \bar{q}ScC_m + \\
&\quad \bar{q}S(C_L \sin \alpha - C_D \cos \alpha)h_0 + Te_T \\
\dot{R}I_z - \dot{P}I_{xz} &= PQ(I_x - I_y) + QRI_{xz} + \bar{q}SbC_n.
\end{aligned} \tag{6.20}$$

As the Euler angles Φ , Θ and Ψ are not the integrals of P , Q and R we have to introduce new motion quantities:

3) Euler angle dynamics:

$$\begin{aligned}
\dot{\Phi} &= P + Q \tan \Theta \sin \Phi + R \tan \Theta \cos \Phi \\
\dot{\Theta} &= Q \cos \Phi - R \sin \Phi \\
\dot{\Psi} &= (R \cos \Phi + Q \sin \Phi)/\cos \Theta.
\end{aligned} \tag{6.21}$$

Differential equations (6.21) will complete the equations of motion, as these will yield the aircraft's orientation as a function of time in terms of Φ , Θ and Ψ [Phi10]. Equations (6.19)-(6.21) together with the angle of attack $\alpha = \tan^{-1} \frac{W}{U}$ form the full 6-DOF nonlinear dynamic model of X-RAE1 where:

- U , V , W are forward, side and downward velocities along the x_b -axis, y_b -axis and z_b -axis, respectively;

- P, Q, R are roll, pitch and yaw angular velocities around the x_b -axis, y_b -axis and z_b -axis, respectively;
- Φ, Θ, Ψ are roll, pitch and yaw angles;
- T is the thrust;
- C_L, C_D, C_y are lift, drag and side force coefficients;
- C_l, C_m, C_n are rolling, pitching and yawing moment coefficients;
- I_x, I_y and I_z are moments of inertia about the corresponding body axes;
- I_{xz} is the product of inertia;
- $\bar{q} = \frac{1}{2}\rho V_T^2 = \frac{1}{2}\rho(U^2 + V^2 + W^2)$ is the dynamic pressure;
- $m, g, S, e_T, h_0, \rho, b$ and c are known parameters.

X-RAE1's layout and its control surfaces are depicted in Figure 6.7. Next,

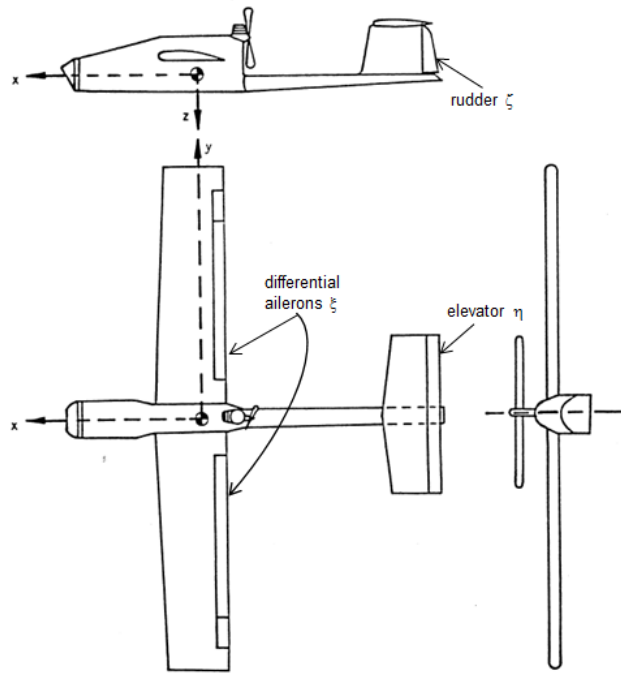


Figure 6.7: X-RAE1 layout [Mil87]

the nonlinear model presented above is linearised and the LQR-based control scheme proposed in Chapter 5 is used to stabilise the system. In addition, it is shown that the proposed controller can be used to control effectively the nonlinear X-RAE1 system for a standard set of initial conditions. The proposed design will be extended to the case of multi-agent network control in Chapter 7.

6.4 Linear Model of X-RAE1

In order to design a linear controller, the nonlinear model described by the nine equations of motion in (6.19)-(6.21) is linearised and decomposed into two motions, longitudinal and lateral, respectively.

6.4.1 Longitudinal and Lateral Equations of Motion

The longitudinal motion is the motion where the aircraft only moves in the x - z plane which is equivalent to translation along the x -axis, translation along the z -axis, and rotation about the y -axis. Therefore, the equations describing the longitudinal motion are:

$$\begin{aligned}
 F_{A_x} + F_{T_x} &= m(\dot{U} + QW - RV + g \sin \Theta) \\
 F_{A_z} + F_{T_z} &= m(\dot{W} + PV - QU - g \cos \Theta \cos \Phi) \\
 M_A + M_T &= I_y \dot{Q} + (I_x - I_z)PR + I_{xz}(P^2 - R^2) \\
 \dot{\Theta} &= Q \cos \Phi - R \sin \Phi.
 \end{aligned} \tag{6.22}$$

On the other side the lateral motion is the motion out of the x - z plane which is equivalent to the translation along the y -axis, the rotation about the x -axis, and the rotation about the z -axis. The lateral motion is described by the set of equations which are:

$$\begin{aligned}
 F_{A_y} &= m(\dot{V} + RU - PW - g \cos \Theta \sin \Phi) \\
 L_A &= I_x \dot{P} - (I_y - I_z)QR - I_{xz}(PQ + \dot{R}) \\
 N_A &= I_z \dot{R} - (I_x - I_y)PQ + I_{xz}(QR - \dot{P}) \\
 \dot{\Theta} &= Q \cos \Phi - R \sin \Phi \\
 \dot{\Psi} &= (R \cos \Phi + Q \sin \Phi) / \cos \Theta.
 \end{aligned} \tag{6.23}$$

The two sets of equations in (6.22)-(6.23) are not decoupled as such. However, decoupling is possible for the linearised model under specific flight conditions which is presented in the following sections.

6.4.2 Perturbed Equations of Motion

Linearisation is performed by assuming small perturbations around the operating point of the aircraft and by considering specific aerodynamic properties [Elg13]. If the lower case notation denotes the deviation of each motion quantity from the trim value, i.e. $dU = u$, and the zero subscripts denote trimmed conditions about which the small perturbations are performed, the equations of motion (6.16), (6.17) and (6.21) can be written as:

$$\begin{aligned} dX &= m [\dot{u} + W_0 q + Q_0 w - R_0 v - V_0 r + (g \cos \Theta_0) \theta] \\ dY &= m [\dot{v} + U_0 r + R_0 u - W_0 p - P_0 w - (g \cos \Theta_0 \cos \Phi_0) \phi + (g \sin \Theta_0 \sin \Phi_0) \theta] \\ dZ &= m [\dot{w} + V_0 p + P_0 v - U_0 q - Q_0 u + (g \cos \Theta_0 \sin \Phi_0) \phi + (g \sin \Theta_0 \cos \Phi_0) \theta] \\ \\ dL &= I_x \dot{p} - (I_y - I_z)(R_0 q + Q_0 r) - I_{xz}(Q_0 p + P_0 q + \dot{r}) \\ dM &= I_y \dot{q} + (I_x - I_z)(R_0 p + P_0 r) + I_{xz}(2P_0 p - 2R_0 r) \\ dN &= I_z \dot{r} - (I_x - I_y)(Q_0 p + P_0 q) + I_{xz}(R_0 q + Q_0 r - \dot{p}) \end{aligned}$$

$$\begin{aligned} \dot{\phi} &= p + q \tan \Theta_0 \sin \Phi_0 + r \tan \Theta_0 \cos \Phi_0 + [(Q_0 \cos \Phi_0 - R_0 \sin \Phi_0) \tan \Theta_0] \phi \\ &\quad + [Q_0 \sin \Theta_0 + R_0 \cos \Phi_0 (1 + \tan^2 \Theta_0)] \theta \\ \dot{\theta} &= q \cos \Phi_0 - r \sin \Phi_0 - (Q_0 \sin \Phi_0 + R_0 \cos \Theta_0) \phi \\ \dot{\psi} &= r \cos \Phi_0 / \cos \Theta_0 + q \sin \Phi_0 / \cos \Theta_0 + [(Q_0 \cos \Phi_0 - R_0 \sin \Phi_0) / \cos \Theta_0] \phi \\ &\quad + [(Q_0 \sin \Phi_0 + R_0 \cos \Phi_0) \tan \Theta_0 / \cos \Theta_0] \theta \end{aligned} \tag{6.24}$$

where dX , dY , dZ , dL , dM and dN are the total differentials of the aerodynamic and thrust forces and moments.

As an example we give the differential dX of the aerodynamic and thrust forces along the x -axis assuming that $X = X(U, W, Q, \eta, \dot{\eta}, \delta_T)$:

$$dX = \frac{\partial X}{\partial U} u + \frac{\partial X}{\partial \dot{U}} \dot{u} + \frac{\partial X}{\partial W} w + \frac{\partial X}{\partial \dot{W}} \dot{w} + \frac{\partial X}{\partial Q} q + \frac{\partial X}{\partial \dot{Q}} \dot{q} + \frac{\partial X}{\partial \eta} \eta + \frac{\partial X}{\partial \dot{\eta}} \dot{\eta} + \frac{\partial X}{\partial \delta_T} \delta_T.$$

The partial derivatives of the aerodynamic forces and moments with respect to the motion quantities (U , V , W , P , Q , R) are called *stability derivatives*, while the partial derivatives of the aerodynamic forces and moments with respect to the control deflections and settings (η elevator deflection, δ_T throttle setting, ζ rudder deflection and ξ aileron deflection) are called *control deriva-*

tives. The evaluation of aerodynamic and thrust derivatives as well as moments and products of inertia is omitted here as this is the result of previous research in [Mil87], [Als04] and [Elg13].

As we are interested only in longitudinal motion, in particular the straight flight conditions at constant velocity of 30m/s, the simplified perturbed equations for this type of motion are presented next.

6.4.3 Linearised Model for the Straight Flight

For a straight, steady, symmetric and horizontal flight at a constant velocity $V_{T_0} = 30\text{m/s}$, the following trimmed values are considered:

$$\begin{aligned}
U_0 &= V_{T_0} \cos \alpha_0, \\
W_0 &= V_{T_0} \sin \alpha_0, \\
V_0 &= P_0 = Q_0 = R_0 = 0, \\
\Theta_0 &= \alpha_0, \text{ and} \\
\Phi_0 &= \Psi_0 = 0.
\end{aligned} \tag{6.25}$$

Then, the set of longitudinal perturbed equations reduces to:

$$\begin{aligned}
m [\dot{u} + W_0 q + (g \cos \Theta_0) \theta] &= \frac{\partial X}{\partial U} u + \frac{\partial X}{\partial W} w + \frac{\partial X}{\partial \dot{W}} \dot{w} + \frac{\partial X}{\partial Q} q + \frac{\partial X}{\partial \eta} \eta + \frac{\partial X}{\partial \delta_T} \delta_T \\
m [\dot{w} - U_0 q + (g \sin \Theta_0) \theta] &= \frac{\partial Z}{\partial U} u + \frac{\partial Z}{\partial W} w + \frac{\partial Z}{\partial \dot{W}} \dot{w} + \frac{\partial Z}{\partial Q} q + \frac{\partial Z}{\partial \eta} \eta + \frac{\partial Z}{\partial \delta_T} \delta_T \\
I_y \dot{q} &= \frac{\partial M}{\partial U} u + \frac{\partial M}{\partial W} w + \frac{\partial M}{\partial \dot{W}} \dot{w} + \frac{\partial M}{\partial Q} q + \frac{\partial M}{\partial \eta} \eta + \frac{\partial M}{\partial \delta_T} \delta_T \\
\dot{\theta} &= q.
\end{aligned} \tag{6.26}$$

The trim values α_0 , η_0 and δ_{T_0} as well as the values of the aerodynamic and thrust derivatives have to be evaluated. The complete analysis for straight horizontal flight at $V_{T_0} = 30\text{m/s}$ is given in [Elg13] and [Mil87] and the trim values are shown in Table 6.1. The linear state-space longitudinal model derived from this analysis is following:

$$\dot{\mathbf{x}} = A\mathbf{x} + B\mathbf{u}, \quad \mathbf{x}(0) = \mathbf{x}_0 \tag{6.27}$$

Table 6.1: Trim conditions for a nominal velocity of 30m/s

Angle of attack	$\alpha_0 = -0.0867$ rad
Elevator	$\eta_0 = -0.0054$ rad
Throttle	$\delta_{T_0} = 0.6854$ or 68.54%

where $\mathbf{x} = \begin{pmatrix} u & w & q & \theta \end{pmatrix}^T$, $\mathbf{u} = \begin{pmatrix} \eta & \delta_T \end{pmatrix}^T$ are the state and input vectors of the i th system at time t , respectively, and

$$A = \begin{pmatrix} -0.142 & -0.227 & 2.493 & -9.771 \\ -1.033 & -4.476 & 28.639 & 0.837 \\ -0.042 & -2.744 & -15.351 & -0.134 \\ 0 & 0 & 1 & 0 \end{pmatrix}, \quad B = \begin{pmatrix} -1.136 & 1.444 \\ -13.060 & 0 \\ -137.157 & -2.036 \\ 0 & 0 \end{pmatrix}.$$

Next, the system in (6.27) is augmented with height dynamics for altitude control. The height equation in Earth-fixed coordinates is given by

$$\dot{H} = U \sin \Theta - W \cos \Theta. \quad (6.28)$$

Then, the perturbed height dynamics become

$$\dot{h} = \sin \Theta_0 u - \cos \Theta_0 w + V_{T_0} \theta \quad (6.29)$$

which reduces to

$$\dot{h} = -0.087u - 0.996w + 30\theta. \quad (6.30)$$

for a straight horizontal flight at $V_{T_0} = 30\text{m/s}$.

Accordingly, we will show in Section 6.5 that LQR control design proposed here provides the asymptotic tracking of step references.

In addition, the system in (6.27) is augmented by the dynamical model for the elevator actuator. The actuator dynamics are represented by the linear second order system whose transfer function is given by

$$H_a = \frac{\omega_n^2}{s^2 + 2\zeta\omega_n s + \omega_n^2} \quad (6.31)$$

where ω_n is the natural frequency and ζ is the dumping ratio. Then, in the

state-space form we have:

$$\begin{pmatrix} \ddot{\eta} \\ \dot{\eta} \end{pmatrix} = \begin{pmatrix} -2\zeta\omega_n & \omega_n^2 \\ 1 & 0 \end{pmatrix} \begin{pmatrix} \dot{\eta} \\ \eta \end{pmatrix} + \begin{pmatrix} \omega_n^2 \\ 0 \end{pmatrix} \eta_d \quad (6.32)$$

where η_d is the elevator demand. For the X-RAE1 system presented here values for ω_n and ζ are chosen to be 25 and 0.6, respectively.

Then, the final state-space representation of the linear X-RAE1 model that will be used for simulation purposes is given as:

$$\begin{pmatrix} \dot{u} \\ \dot{w} \\ \dot{q} \\ \dot{\theta} \\ \dot{h} \\ \ddot{\eta} \\ \dot{\eta} \end{pmatrix} = \begin{pmatrix} -0.142 & -0.227 & 2.493 & -9.771 & 0 & 0 & -1.136 \\ -1.033 & -4.476 & 28.639 & 0.837 & 0 & 0 & -13.060 \\ -0.042 & -2.744 & -15.351 & -0.134 & 0 & 0 & -137.157 \\ 0 & 0 & 1 & 0 & 0 & 0 & 0 \\ -0.087 & -0.996 & 0 & 30 & 0 & 0 & 0 \\ 0 & 0 & 0 & 0 & 0 & -30 & -625 \\ 0 & 0 & 0 & 0 & 0 & 1 & 0 \end{pmatrix} \begin{pmatrix} u \\ w \\ q \\ \theta \\ h \\ \dot{\eta} \\ \eta \end{pmatrix} + \begin{pmatrix} 0 & 1.444 \\ 0 & 0 \\ 0 & -2.036 \\ 0 & 0 \\ 0 & 0 \\ 625 & 0 \\ 0 & 0 \end{pmatrix} \begin{pmatrix} \eta_d \\ \delta_T \end{pmatrix}. \quad (6.33)$$

The eigenvalues of the open-loop system (6.33) are $\{0, -0.032 \pm i0.419, -9.953 \pm i7.044, -15 \pm i20\}$. The system is not asymptotically stable, but stable in the sense of Lyapunov with:

- Two stable aerodynamic modes:
 1. *Phugoid*, a low-frequency lightly-damped mode ($-0.032 \pm i0.419$);
 2. *Short period*, a high-frequency heavily-damped mode ($-9.953 \pm i7.044$);
- A zero-eigenvalue mode introduced by the height dynamics.

System dynamics are simulated in Matlab[®] and Simulink[®] environment [MR15]. We give the state responses (apart from η and $\dot{\eta}$) in Figures 6.8-6.10. The upper half of each figure represents the state response of the system to a one-second-duration pulse to the elevator actuator input η_d and the lower

half of each figure represents the state response of the system to an impulse disturbance to the downward velocity w .

It is apparent, from the nature of the modes and the responses, that we need to control the phugoid mode to avoid the low frequency oscillations and also the short period in order to suppress rapidly the transient effects mainly on the pitching rate q . The zero eigenvalue also causes in general a shift to the operating point (see height response) in the presence of an impulse disturbance to the states (i.e. a non zero initial state vector), hence the need for altitude control. The design of an adequate control system based on LQR is presented in the next section.

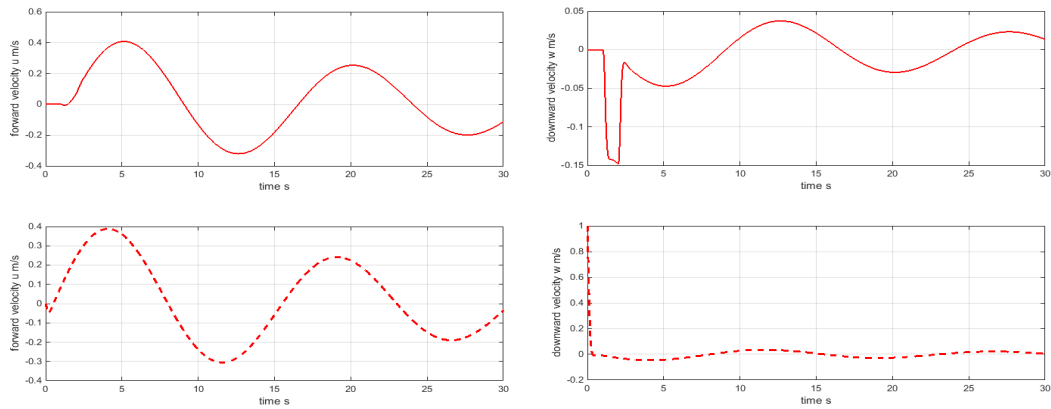


Figure 6.8: Forward and downward velocity responses of the open-loop linear X-RAE1 system when a pulse is applied to elevator (solid line) and in the presence of an impulse disturbance in w (dashed line)

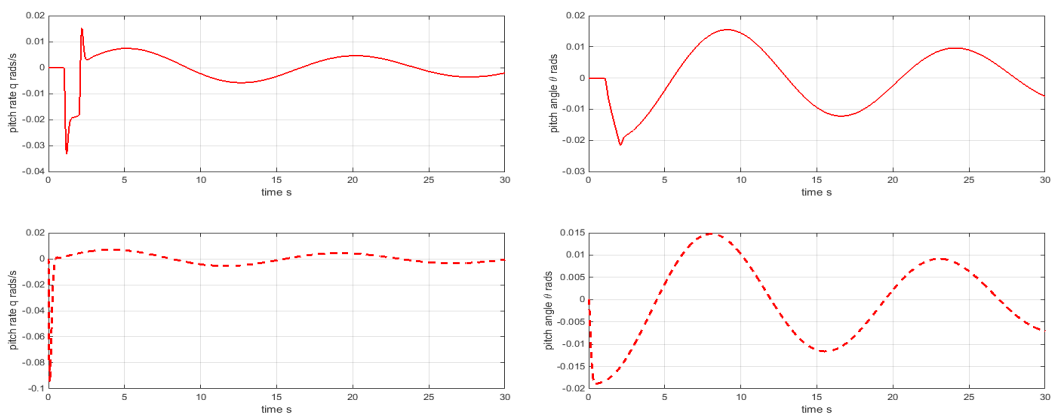


Figure 6.9: Pitch rate and pitch angle responses of the open-loop linear X-RAE1 system when a pulse is applied to elevator (solid line) and in the presence of an impulse disturbance in w (dashed line)

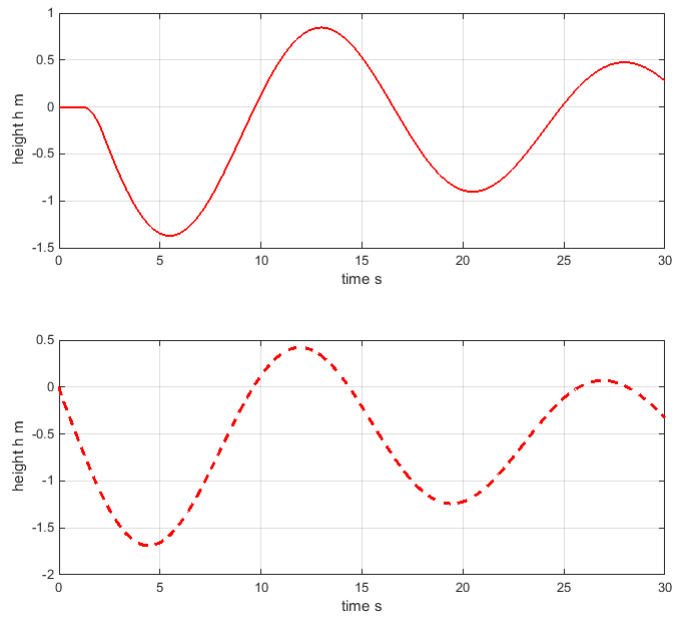


Figure 6.10: Height response of the open-loop linear X-RAE1 system when a pulse is applied to elevator (solid line) and in the presence of an impulse disturbance in w (dashed line)

6.5 LQR Control Design

In this section we propose LQR control design for the linear X-RAE1 model in (6.33). The LQR control aim is to minimise a quadratic control function given by

$$J(\mathbf{u}_i(t), \mathbf{x}_{i0}) = \int_0^{\infty} (\mathbf{x}_i(t)^T Q \mathbf{x}_i(t) + \mathbf{u}_i(t)^T R \mathbf{u}_i(t)) dt. \quad (6.34)$$

The weighting matrices, Q and R , are chosen as:

$$Q = \begin{pmatrix} 0.7 & 0 & 0 & 0 & 0 & 0 & 0 \\ 0 & 1 & 0 & 0 & 0 & 0 & 0 \\ 0 & 0 & 0.05 & 0 & 0 & 0 & 0 \\ 0 & 0 & 0 & 1 & 0 & 0 & 0 \\ 0 & 0 & 0 & 0 & 1 & 0 & 0 \\ 0 & 0 & 0 & 0 & 0 & 1 & 0 \\ 0 & 0 & 0 & 0 & 0 & 0 & 5 \end{pmatrix}, \quad R = \begin{pmatrix} 10 & 0 \\ 0 & 10 \end{pmatrix}. \quad (6.35)$$

In order to find the LQR gain matrix K the following ARE has to be solved that has P as its solution:

$$A^T P + P A - P B R^{-1} B^T P + Q = 0. \quad (6.36)$$

Equation (6.36) is solved by using Matlab[®] ([MR15]). As $Q \geq 0$, $R > 0$ and the standard assumptions made about stabilisability and observability of positive definiteness given in Definition 3.1.7 and Definition 3.1.8 are satisfied, it follows that P is positive definite solution of (6.36). Then, the optimal control input is given by

$$\mathbf{u} = -R^{-1} B^T P \mathbf{x} = -K \mathbf{x} \quad (6.37)$$

where

$$K = \begin{pmatrix} -0.022 & 0.067 & -0.371 & -7.703 & -0.315 & 0.296 & 4.988 \\ 0.238 & -0.026 & -0.031 & -0.465 & 0.031 & 0.001 & 0.249 \end{pmatrix}.$$

In order to simulate the model's dynamics a simulation environment is created by using Matlab[®] and Simulink[®]. Simulink[®] model for linear X-RAE1 system in (6.33) that is controlled by LQR proposed in this section is depicted in Figure 6.11. For simulation purposes the disturbance in system (6.33) is intro-

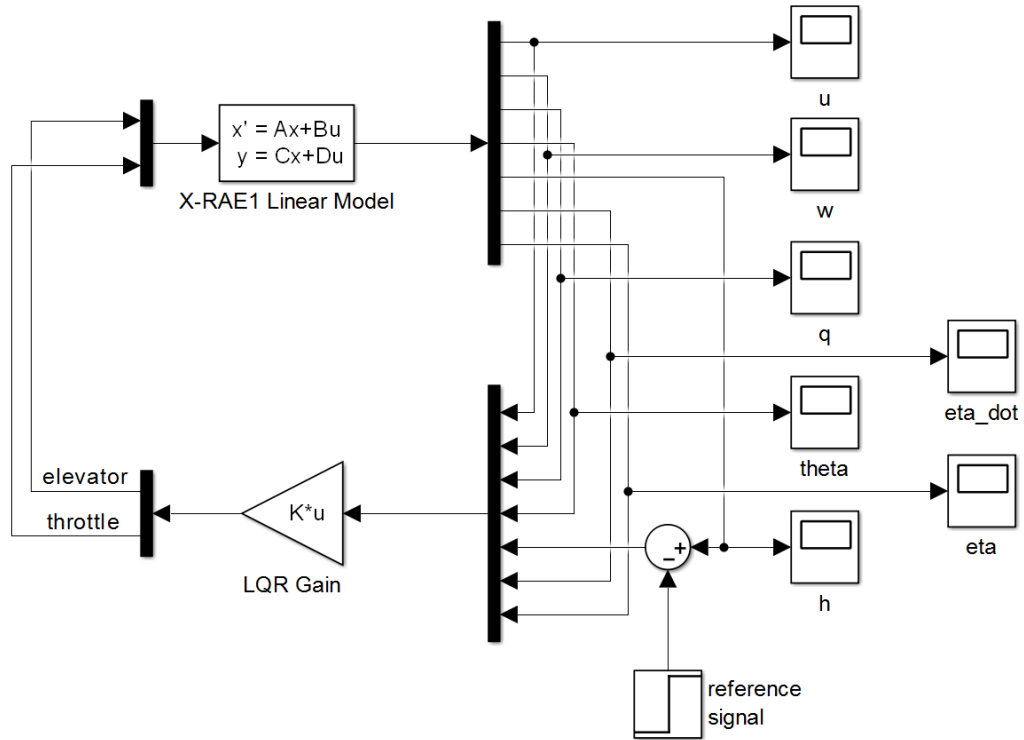


Figure 6.11: Simulink[®] model for LQR control of linear X-RAE1 model

duced as an arbitrary impulse to the downward velocity variable w , which is equivalent to the presence of environmental disturbances such as nonuniform wind.

Next, it is shown that design proposed in Figure 6.11 stabilises the system and that all states settle at 0 as time evolves. Forward and downward velocity responses of linear X-RAE1 model are depicted in the upper half of Figure 6.12; Pitch rate and pitch angle responses of linear X-RAE1 model are depicted in the upper half of Figure 6.13; Elevator rate and elevator responses of linear X-RAE1 model are depicted in the upper half of Figure 6.14.

It is shown that system is robust to environmental disturbances such as nonuniform wind. In addition, the system provides the altitude control by asymptotic reference tracking to step commands which is depicted in the upper half of Figure 6.15. Also, we give the input signals (elevator setting and throttle) in the upper half of Figure 6.16.

Next, we tested if the proposed LQR controller can also control effectively the nonlinear X-RAE1 model. Simulink[®] model for nonlinear X-RAE1 system described by six equations of motion in (6.19)-(6.20) that is controlled by using the identical LQR gain as in the linear case is depicted in Figure 6.17. Note

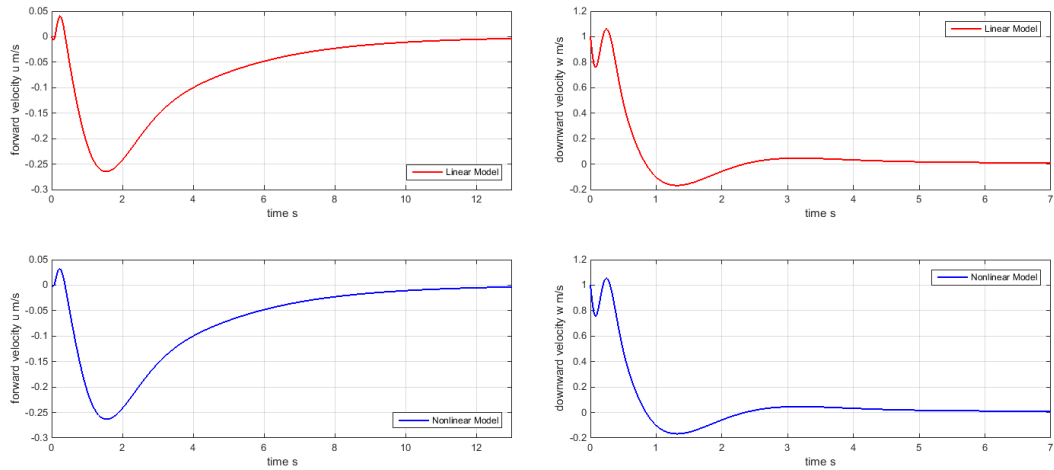


Figure 6.12: Forward and downward velocity responses of linear and nonlinear X-RAE1 model controlled by LQR in the presence of impulse disturbance and step tracking demand

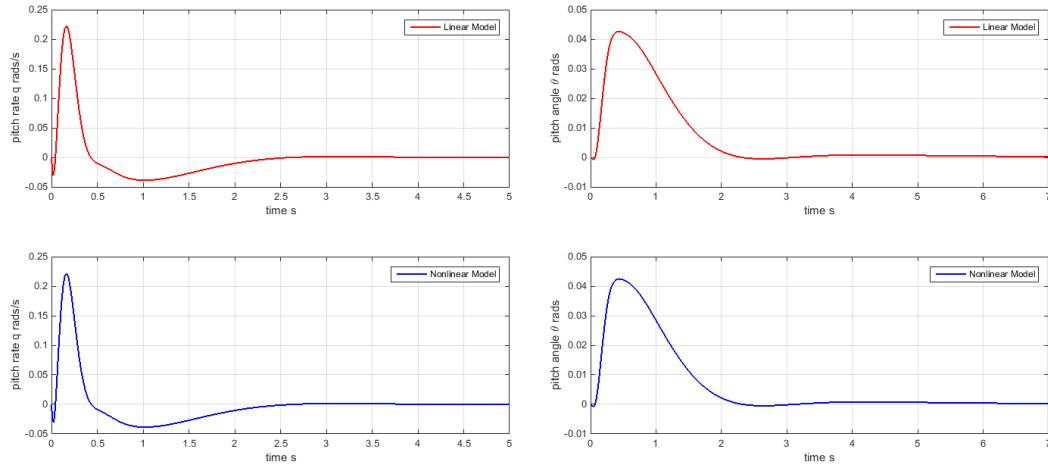


Figure 6.13: Pitch rate and pitch angle responses of linear and nonlinear X-RAE1 model controlled by LQR in the presence of impulse disturbance and step tracking demand

that nonlinear Simulink[®] model in Figure 6.17 simulates both motions, longitudinal and lateral. We are interested in straight flight conditions at constant velocity of 30m/s for which these two motions are decoupled. Therefore, only longitudinal motion is considered here and results closely match those obtained in the linear case.

The same set of results is reproduced for the nonlinear system using identical simulation parameters. Nonlinear system's state responses, with the trim values subtracted, are depicted in the lower parts of Figures 6.12- Figure 6.14. Despite substantial nonlinearity in the model, the controller was able to re-

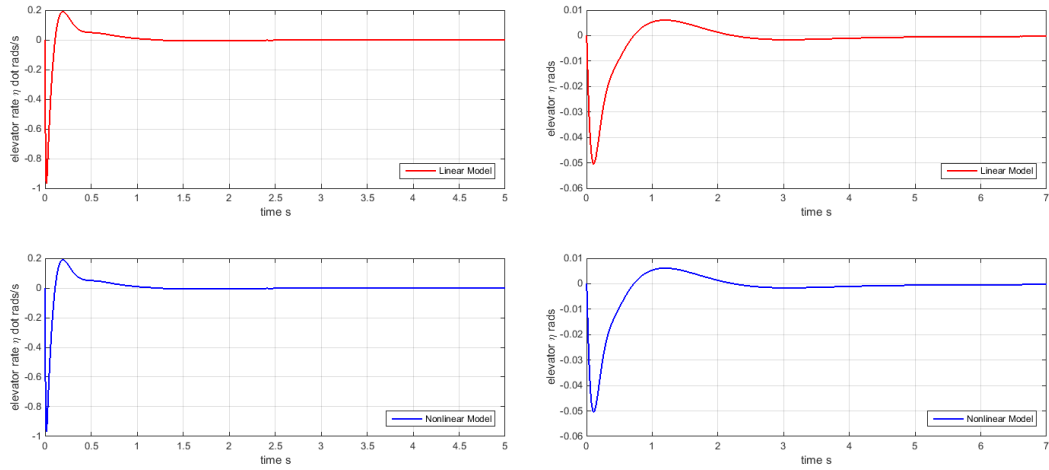


Figure 6.14: Elevator rate and elevator responses of linear and nonlinear X-RAE1 model controlled by LQR in the presence of impulse disturbance and step tracking demand

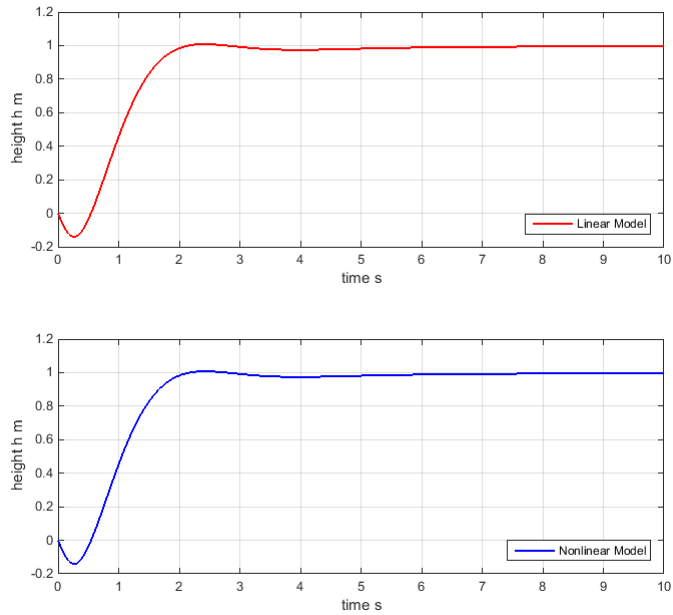


Figure 6.15: Height response of linear and nonlinear X-RAE1 model controlled by LQR in the presence of impulse disturbance and step tracking demand

produce results that are almost identical to those obtained in the linear case and also achieve disturbance rejection. Also, nonlinear system accommodates the reference tracking to step commands which is depicted in the lower part of Figure 6.15.

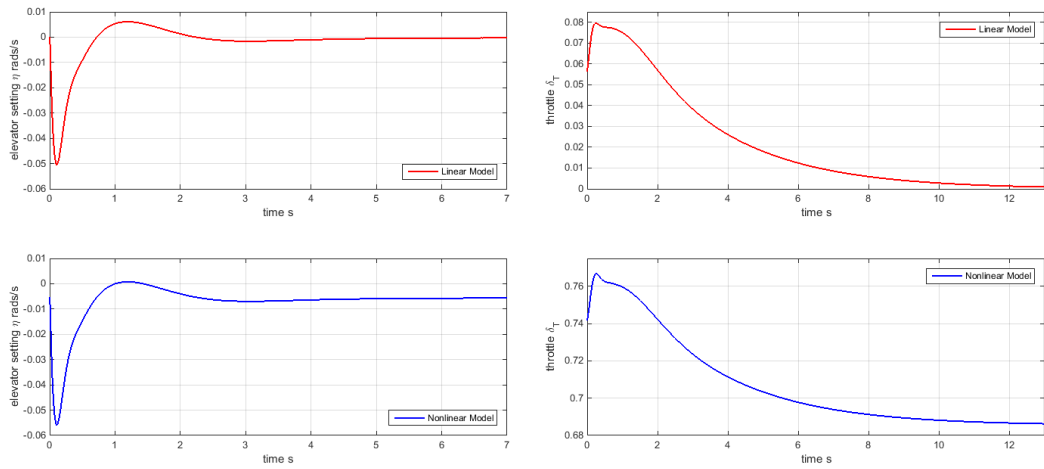


Figure 6.16: Control inputs of linear and nonlinear X-RAE1 model controlled by LQR in the presence of impulse disturbance and step tracking demand

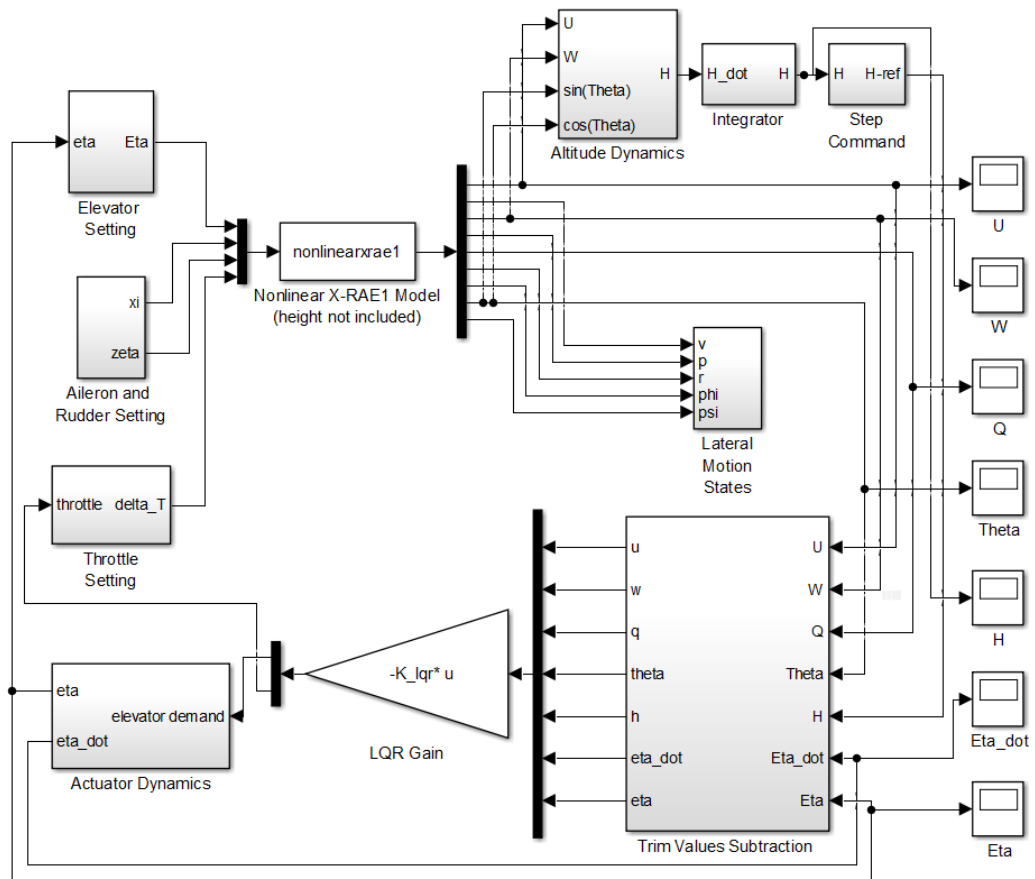


Figure 6.17: Simulink[®] model of LQR control of nonlinear X-RAE1 model

6.6 Summary

In this chapter the derivation of 6-DOF nonlinear model of an experimental RPV, X-RAE1, and its linearisation for a specific set of flight conditions were reviewed. Additionally, the LQR-based control design which provides the asymptotic stability of the system was proposed.

In the next chapter these results will be extended to distributed cooperative LQR-based scheme for controlling arbitrary formations which consist of X-RAE1s. The proposed design will be derived by using distributed LQR design methodology presented in Chapter 5.

Chapter 7

Application Example: Distributed LQR Control of Multi-Agent Network

In this chapter we present a cooperative scheme for controlling arbitrary formations of low speed experimental UAVs based on the distributed LQR design methodology presented in Chapter 5. Each UAV acts as an independent agent in the formation and its dynamics are described by a 6-DOF nonlinear model which is then linearised for control design purposes around an operating point corresponding to straight flight conditions. Both models, linear and nonlinear, have been presented in Chapter 6.

First, the distributed LQR design for formation consisting of four UAVs is presented. It is shown that the proposed controller stabilises the overall formation and can control effectively the nonlinear multi-agent system for a standard set of initial conditions. Then, it is demonstrated via numerous simulations that both systems, linear and nonlinear, provide altitude control and are robust to environmental disturbances such as nonuniform wind gusts acting on a formation. Additionally, the effect of partial loss of communication between two neighbouring UAVs on the both multi-agent systems is illustrated.

7.1 Distributed LQR Design for Formation Control

A network of four dynamically decoupled X-RAE1s (agents) moving in a plane is considered. The dynamics of the agents are fully described in equation (6.33) in Chapter 6. The interconnection structure within the network is depicted in Figure 7.1.

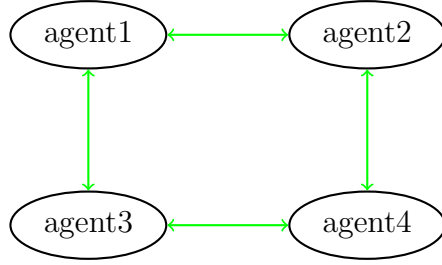


Figure 7.1: The interconnection structure within the multi-agent network

The distributed optimal control problem is defined as:

$$\begin{aligned}
 \min_{\tilde{K}} \tilde{J}(\tilde{\mathbf{u}}(t), \tilde{\mathbf{x}}_0) &= \int_0^{\infty} (\tilde{\mathbf{x}}(t)^T \tilde{Q} \tilde{\mathbf{x}}(t) + \tilde{\mathbf{u}}(t)^T \tilde{R} \tilde{\mathbf{u}}(t)) dt \\
 \text{subj. to } \dot{\tilde{\mathbf{x}}}(t) &= \tilde{A} \tilde{\mathbf{x}} + \tilde{B} \tilde{\mathbf{u}}, \quad \tilde{\mathbf{x}}(0) = \tilde{\mathbf{x}}_0 \\
 \tilde{A} &= I_4 \otimes A \quad \tilde{B} = I_4 \otimes B \\
 \tilde{K} &\in \mathcal{K}_{n,m}^{N_d}(\mathcal{G}), \\
 \tilde{Q} &\in \mathcal{K}_{n,n}^{N_d}(\mathcal{G}), \quad \tilde{R} = I_{N_d} \otimes R
 \end{aligned} \tag{7.1}$$

where A and B are as in (6.33), $\tilde{Q} = \tilde{Q}^T \geq 0$ and $\tilde{R} = \tilde{R}^T > 0$ while the class of matrices denoted as $\mathcal{K}_{n,m}^{N_d}(\mathcal{G})$ is defined in Definition 3.1.9.

Our control objective is to stabilise the formation, including each individual agent moving on a plane by using the distributed suboptimal design presented in Chapter 5 where the distributed gain matrix is given by

$$\tilde{K} = I_4 \otimes R^{-1} B^T P - M \otimes R^{-1} B^T P_{a_{12}}. \tag{7.2}$$

P is the stabilising solution of a single agent LQR problem; however it can be also expressed as $P = P_{a_{11}} + 2P_{a_{12}}$ using Theorem 4.2.1. $P_{a_{11}}$ and $P_{a_{12}}$ are diagonal and off-diagonal blocks of the stabilising solution P_{min} corresponding to the minimum size centralized LQR problem that has to be solved. M is the

symmetric and positive semi-definite matrix given by

$$M = 2I_4 - \mathbf{A}(\mathcal{G}) \quad (7.3)$$

where $\mathbf{A}(\mathcal{G})$ is the adjacency matrix representing the interconnection structure depicted in Figure 7.1:

$$\mathbf{A}(\mathcal{G}) = \begin{pmatrix} 0 & 1 & 1 & 0 \\ 1 & 0 & 0 & 1 \\ 1 & 0 & 0 & 1 \\ 0 & 1 & 1 & 0 \end{pmatrix}. \quad (7.4)$$

The minimum size centralized LQR problem that has to be solved corresponds to $N_{min} = d_{max}(\mathcal{G}) + 1$ agents, where d_{max} represents the maximum vertex degree of graph. Therefore, d_{max} of the interconnection graph in Figure 7.1 equals 2; thus the size of centralized LQR problem is $N_{min} = 3$. For more details we refer the reader to Section 5.1.

Then, the centralized LQR problem is defined as

$$\min_{K_a} J(\mathbf{u}(t), \mathbf{x}_0) \quad \text{subj. to } \dot{\mathbf{x}} = A_a \mathbf{x} + B_a \mathbf{u}, \quad \mathbf{x}(0) = \mathbf{x}_0$$

where the column vectors $\mathbf{x}(t) = [x_1(t)^T, x_2(t)^T, x_3(t)^T]^T$ and $\mathbf{u}(t) = [u_1(t)^T, u_2(t)^T, u_3(t)^T]^T$ collect the states and inputs of the 3 subsystems, while $A_a = I_3 \otimes A$ and $B_a = I_3 \otimes B$, with A and B defined as in (6.33). The cost function $J(\mathbf{u}(t), \mathbf{x}_0)$ is given by

$$J(\mathbf{u}(t), \mathbf{x}_0) = \int_0^\infty (\mathbf{x}(t)^T Q_a \mathbf{x}(t) + \mathbf{u}(t)^T R_a \mathbf{u}(t)) dt \quad (7.5)$$

with the weighting matrices Q_a and R_a given by

$$Q_a = \begin{pmatrix} 3Q & -Q & -Q \\ -Q & 3Q & -Q \\ -Q & -Q & 3Q \end{pmatrix}, \quad R_a = I_3 \otimes R \quad (7.6)$$

and Q and R defined as in (6.35).

By solving ARE corresponding to the centralized network of $N_{min} = 3$ agents:

$$A_a^T P_{min} + P_{min} A_a - P_{min} B_a R_a^{-1} B_a^T P_{min} + Q_a = 0 \quad (7.7)$$

a stabilising solution of the following form will be obtained:

$$P_{min} = \begin{pmatrix} P_{11} & P_{12} & P_{12} \\ P_{12} & P_{11} & P_{12} \\ P_{12} & P_{12} & P_{11} \end{pmatrix}. \quad (7.8)$$

Then, the distributed gain matrix \tilde{K} in (7.2) will be of the following structure:

$$\tilde{K} = \begin{pmatrix} K_{11} & K_{12} & K_{12} & 0 \\ K_{12} & K_{11} & 0 & K_{12} \\ K_{12} & 0 & K_{11} & K_{12} \\ 0 & K_{12} & K_{12} & K_{11} \end{pmatrix} \quad (7.9)$$

where

$$K_{11} = \begin{pmatrix} 0.075 & -0.110 & 0.613 & 12.683 & 0.527 & -0.507 & -8.688 \\ -0.411 & 0.042 & 0.086 & 1.531 & -0.006 & -0.002 & -0.677 \end{pmatrix}$$

and

$$K_{12} = \begin{pmatrix} -0.027 & 0.022 & -0.121 & -2.490 & -0.106 & 0.106 & 1.850 \\ 0.086 & -0.008 & -0.028 & -0.533 & -0.013 & 0.001 & 0.214 \end{pmatrix}.$$

For the given gain matrix, \tilde{K} , the closed loop system:

$$\tilde{A}_{cl} = \tilde{A} - \tilde{B}\tilde{K} = I_4 \otimes A + (I_4 \otimes B)\tilde{K} \quad (7.10)$$

is asymptotically stable.

In order to simulate the formation's dynamics a simulation environment is created for both, linear and nonlinear case, by using Matlab[®] and Simulink[®] which is given in the next section.

7.2 Simulation Results

The Simulink[®] model for LQR-based control of formation consisting of four X-RAE1s is depicted in Figure 7.2. Detailed Simulink[®] models for each individual agent (subsystem) are omitted from the figure in order to provide simplicity in design, but these are identical to the models presented in Section 6.5 (i.e. Figure 6.11 for the linear case and Figure 6.17 for the nonlinear case).

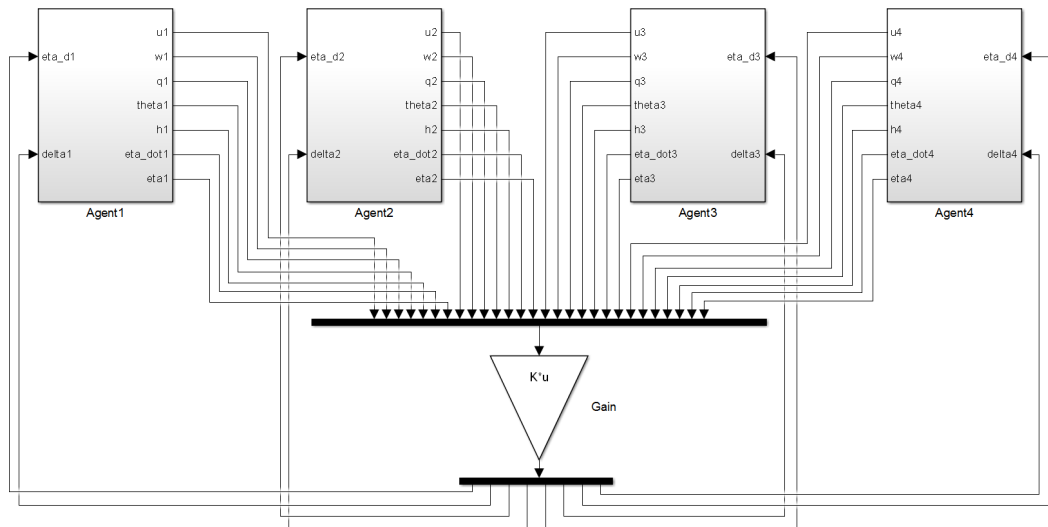


Figure 7.2: Simulink[®] model for LQR-based control of formation consisting of four X-RAE1s

In the simulations which follow, the agents' movement is illustrated by examining the deviation from nominal velocity $V_{T_0} = 30\text{m/s}$, which is the horizontal speed at which the model has been linearised. Further, the individual agents' vertical positions (i.e. heights) are depicted for each agent. The remaining state responses are plotted only for agent 1 as it is expected that all other agents will reproduce results that closely match the ones presented.

First, the altitude control problem with the disturbances rejection is considered. Then, we assume partial loss of communication between two neighbouring UAVs. Results are produced for both multi-agent systems, linear and nonlinear.

7.2.1 Altitude Control and Disturbance Rejection

For simulation purposes the disturbance in system is introduced as an arbitrary impulse to the downward velocity variable w_i of agent i , which is equivalent to the presence of environmental disturbances such as nonuniform wind for a collection of agents. Additionally, each agent is given a step command in order to investigate if the system provides altitude control.

The first simulation illustrates the height response of the each agent in the presence of environmental disturbances and step tracking demands for the case of linear dynamics. Results are depicted in Figure 7.3. Then, Figure 7.4 depicts

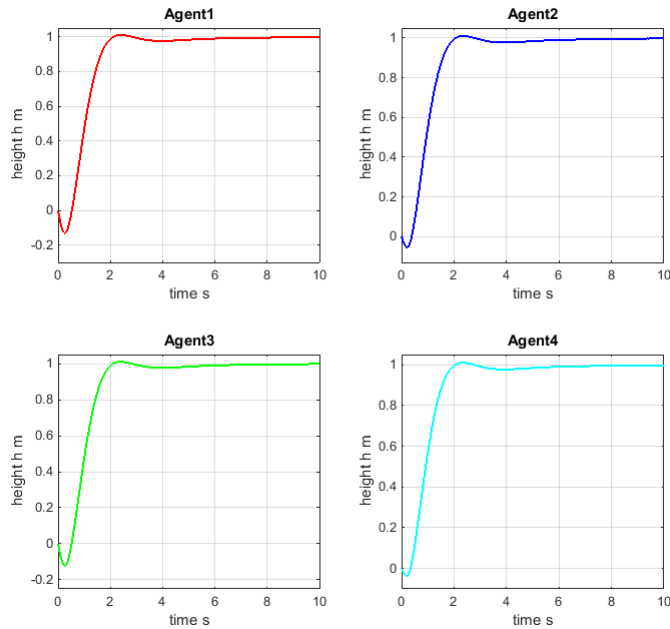


Figure 7.3: Height responses of the linear LQR multi-agent system controlled by the distributed controller in the presence of impulse disturbance and step tracking demand

the deviation of each agent's velocity from the nominal velocity of 30m/s in the presence of environmental disturbances and step tracking demands for the case of linear dynamics.

Figure 7.3 and Figure 7.4 demonstrate that in the case of linear dynamics the distributed LQR controller stabilises the formation and agents are able to recover their vertical positions. Note that the formation structure is lost with respect to the horizontal agents' positions. This can be prevented, if required, by introducing an additional state variable for horizontal regulation. Also, the

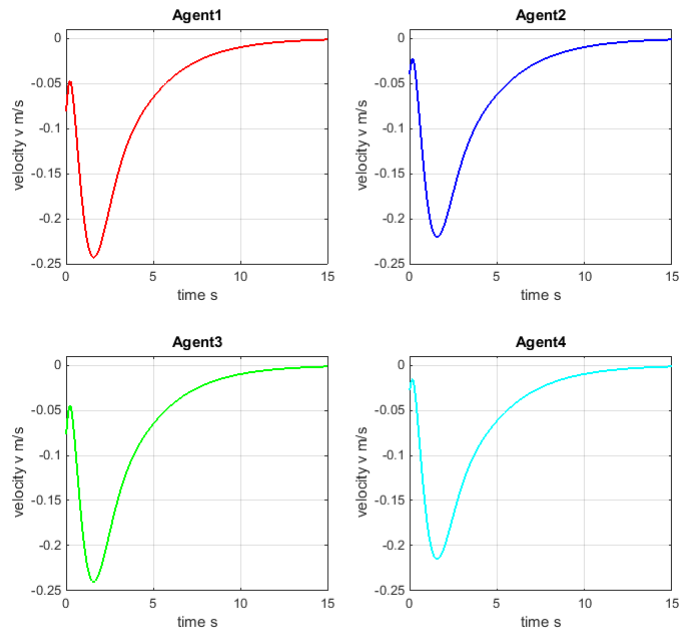


Figure 7.4: Velocity responses of the linear LQR multi-agent system controlled by the distributed controller in the presence of impulse disturbance and step tracking demand

proposed controller is able to provide asymptotic reference tracking to step commands.

Next, the same set of results is reproduced for the nonlinear system using identical simulation parameters. These are given in Figure 7.5 and Figure 7.6. Despite substantial nonlinearity in the model, the controller was able to reproduce results that closely match those obtained in the linear case.

Additionally, the remaining state responses for agent 1 in the case of linear and nonlinear dynamics are given, as it is expected that other agents' responses will closely match the results presented. These are depicted in Figures 7.7-7.9. It is shown that design proposed in Figure 7.2 stabilises the system and that all states settle at 0 in the steady-state, with an acceptable settling time.

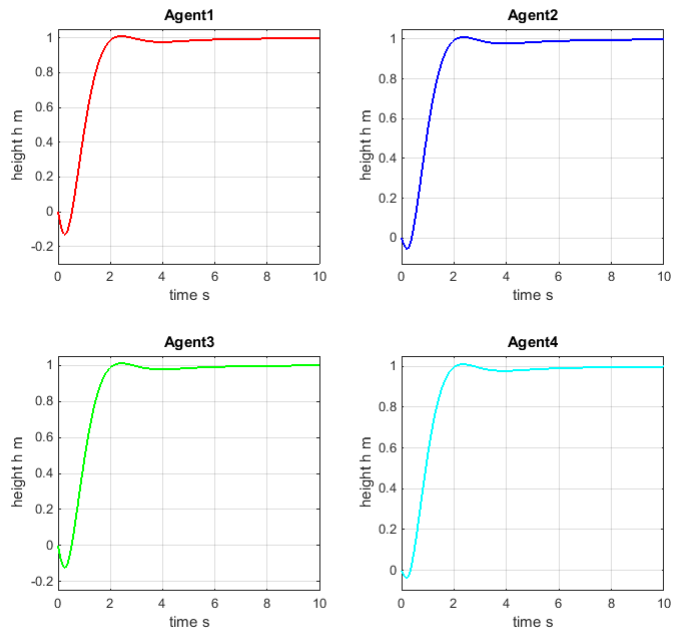


Figure 7.5: Height responses of the nonlinear LQR multi-agent system controlled by the distributed controller in the presence of impulse disturbance and step tracking demand

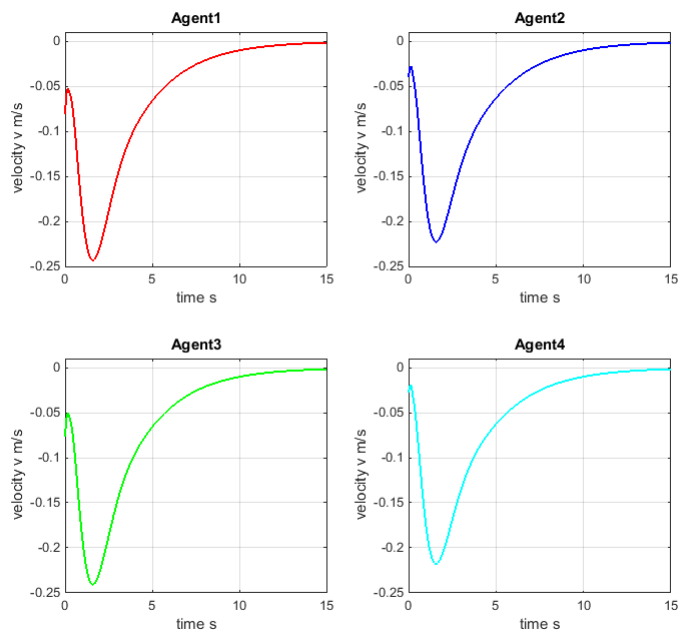


Figure 7.6: Velocity responses of the nonlinear LQR multi-agent system controlled by the distributed controller in the presence of impulse disturbance and step tracking demand

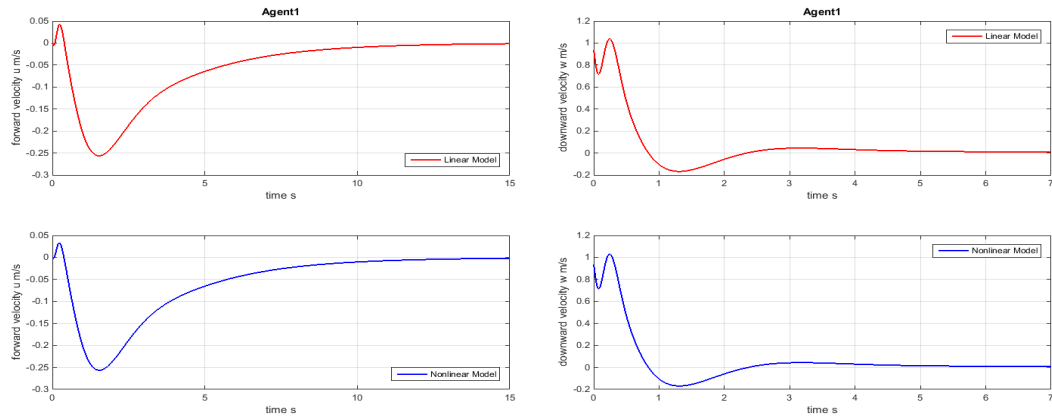


Figure 7.7: Forward and downward velocity responses of linear and nonlinear agent 1 model controlled by distributed LQR in the presence of impulse disturbance and step tracking demand to each agent in the formation

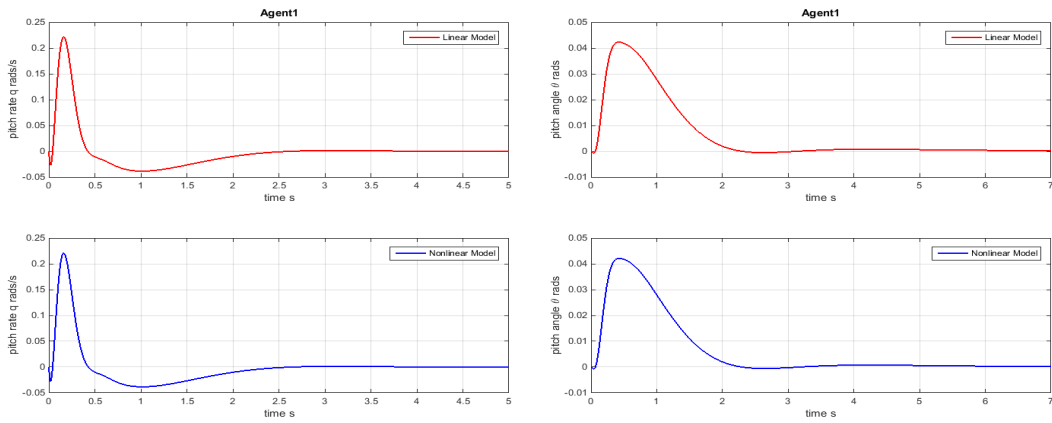


Figure 7.8: Pitch rate and pitch angle responses of linear and nonlinear agent 1 model controlled by distributed LQR in the presence of impulse disturbance and step tracking demand to each agent in the formation

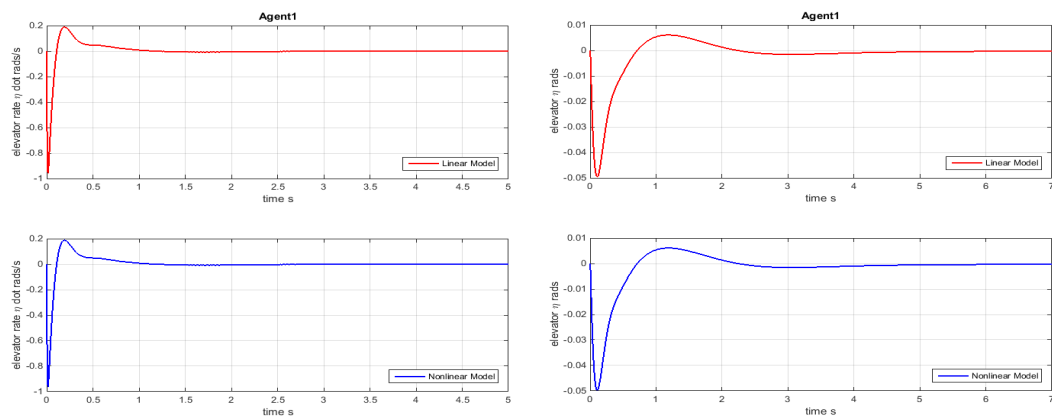


Figure 7.9: Elevator rate and elevator responses of linear and nonlinear agent 1 model controlled by distributed LQR in the presence of impulse disturbance and step tracking demand to each agent in the formation

7.2.2 Loss of Communication Between Agents

The case when the communication between two agents in the formation is partially lost, is followed by the impulse disturbance in downward velocity is considered next. The distributed LQR design described in Section 7.1 is used to control the system.

First, the linear system is initially disturbed by an impulse in the downward velocity of each agent. This is then followed by the failure of link communication between agent 1 and agent 2 (in both directions) at $t = 5.9\text{s}$ and by the impulse disturbance to agent 1 at $t = 6\text{s}$. The height and velocity responses of the linear model are depicted in Figure 7.10 and Figure 7.11.

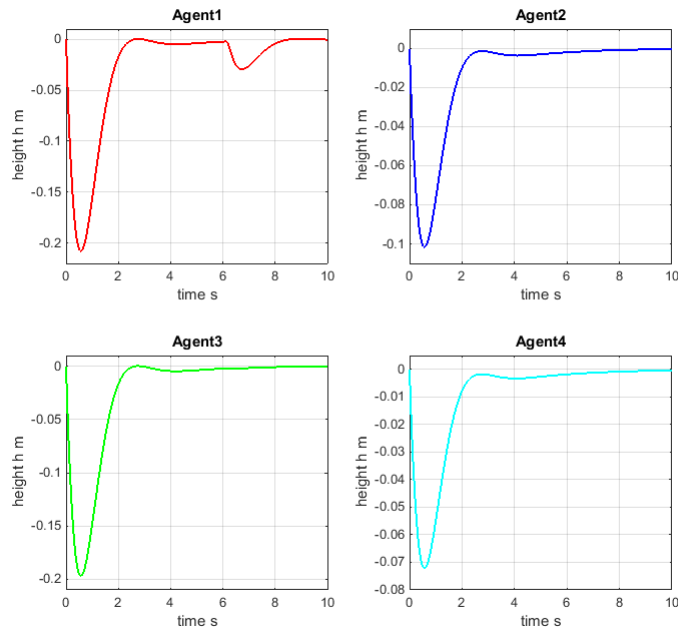


Figure 7.10: Height responses of the linear LQR system controlled by the distributed controller in the presence of link failure between agent 1 and agent 2 followed by an impulse disturbance to agent 1

Results are reproduced for the nonlinear dynamics case for identical simulation parameters. The height and velocity responses of the nonlinear model are depicted in Figure 7.12 and Figure 7.13.

Additionally, the remaining state responses for agent 1 in the case of linear and nonlinear dynamics are given next. These are depicted in Figures 7.14-7.16.

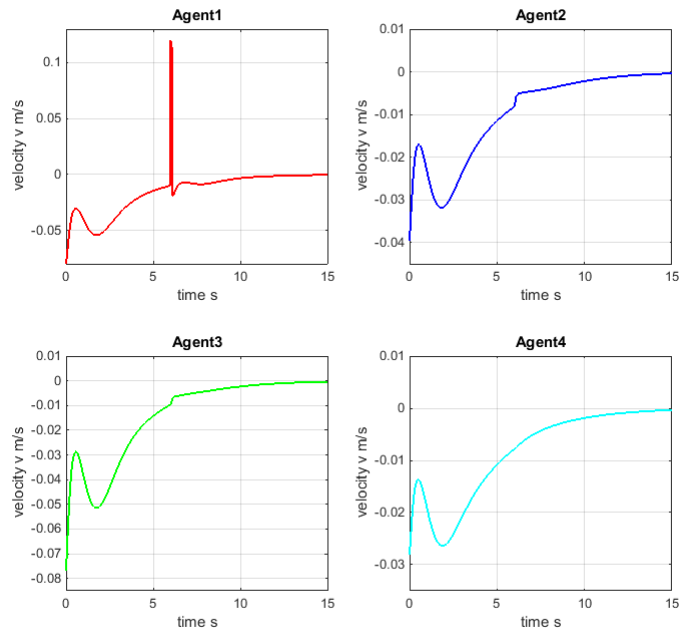


Figure 7.11: Velocity responses of the linear LQR system controlled by the distributed controller in the presence of link failure between agent 1 and agent 2 followed by an impulsive disturbance to agent 1

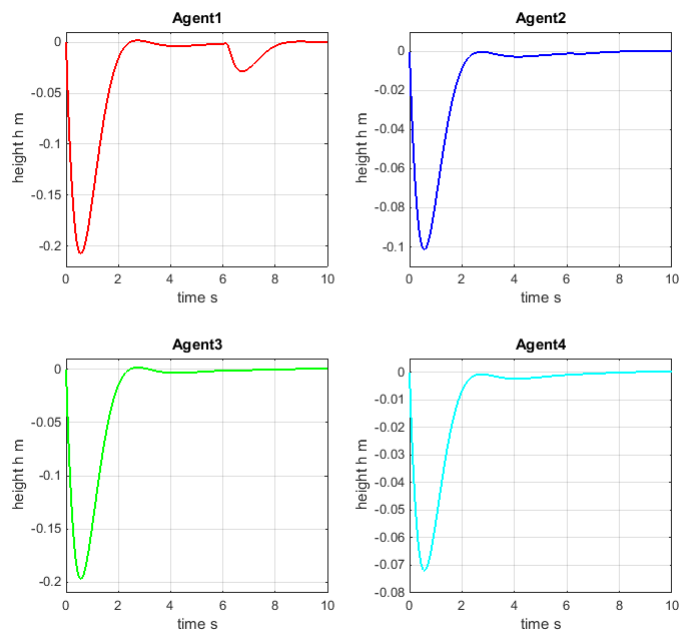


Figure 7.12: Height responses of the nonlinear LQR system controlled by the distributed controller in the presence of link failure between agent 1 and agent 2 followed by an impulsive disturbance to agent 1

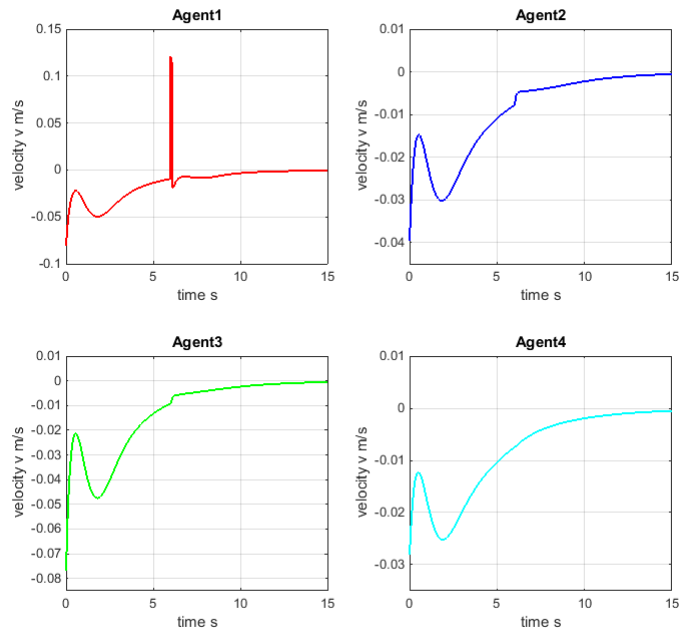


Figure 7.13: Velocity responses of the nonlinear LQR system controlled by the distributed controller in the presence of link failure between agent 1 and agent 2 followed by an impulsive disturbance to agent 1

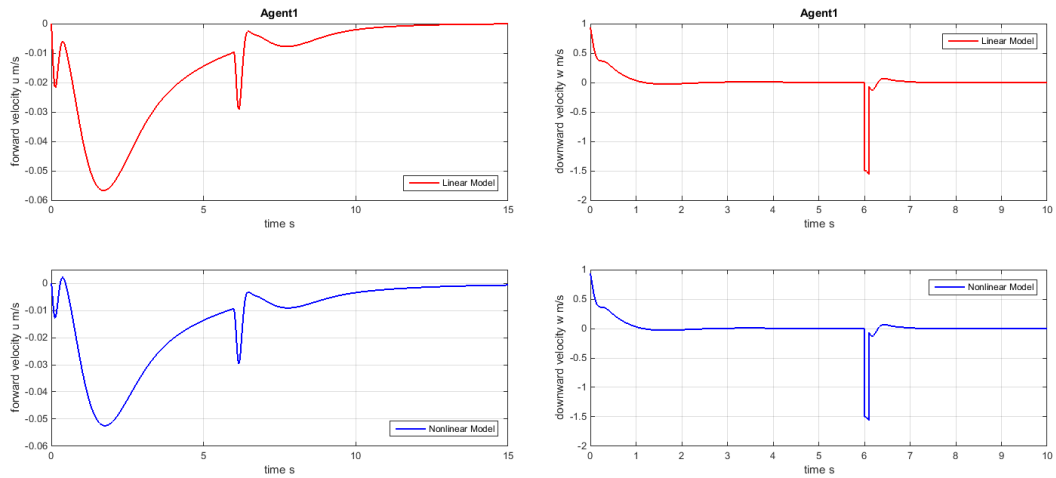


Figure 7.14: Forward and downward velocity responses of linear and nonlinear agent 1 model controlled by distributed LQR in the presence of link failure between agent 1 and agent 2 followed by an impulse disturbance to agent 1

It is shown that design proposed in Figure 7.2 stabilises the system and that all states settle at 0 as time evolves. Therefore, the proposed distributed LQR controller is robust to the loss of communication as long as the connectivity of network is preserved.

To summarise the results presented in this chapter, it was shown that the

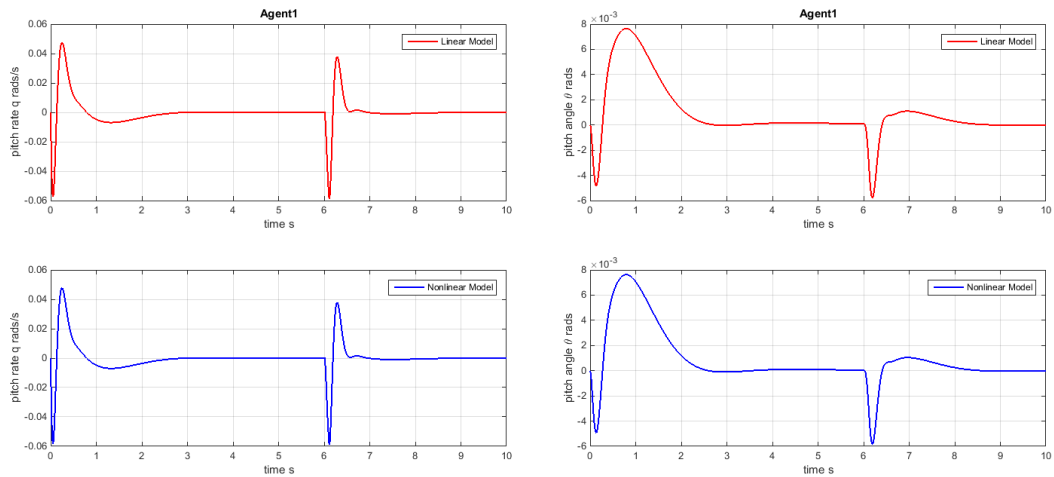


Figure 7.15: Pitch rate and pitch angle responses of linear and nonlinear agent 1 model controlled by distributed LQR in the presence of link failure between agent 1 and agent 2 followed by an impulse disturbance to agent 1

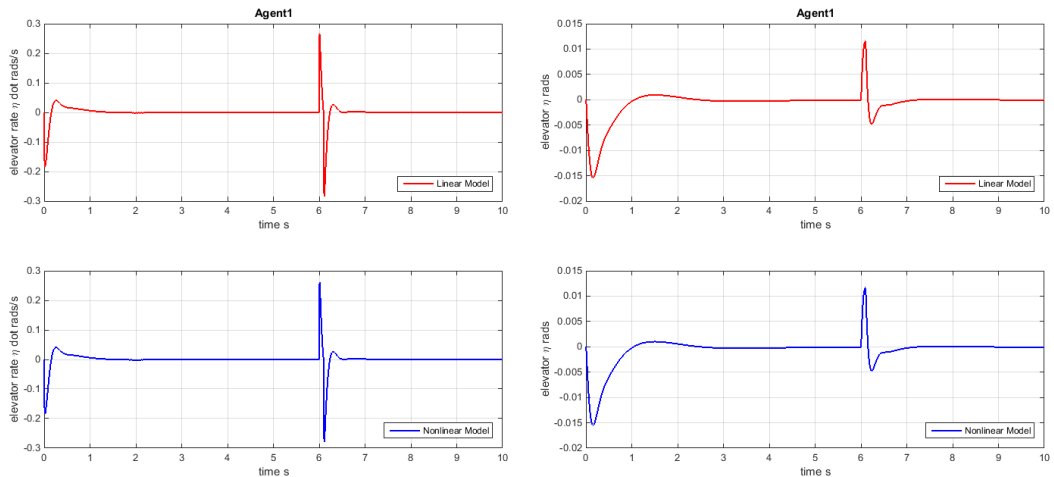


Figure 7.16: Elevator rate and elevator responses of linear and nonlinear agent 1 model controlled by distributed LQR in the presence of link failure between agent 1 and agent 2 followed by an impulse disturbance to agent 1

proposed controller is able to provide asymptotic reference tracking to step commands and is robust to environmental disturbances and to the communication loss between a pair of agents for both, linear and nonlinear, models. The nonlinear model gives the results that closely match those obtained in the linear case, which is due to the fact that the disturbances used enable operation close to the assumed linearised model. Therefore, it was illustrated that the linearisation is robust and that proposed controller guarantees the robustness properties.

7.3 Summary

In this chapter a real-life application of multi-agent network where distributed LQR controller is used to stabilise the formation and provide altitude control was given. Additionally, robustness properties of the design were illustrated for different simulation conditions.

Next, we will give the concluding remarks of the thesis and we will provide a number of future research directions.

Chapter 8

Conclusion

In this chapter, the results presented in the thesis are summarised and connections to other related areas are highlighted. Additionally, the main contributions of the work are provided, as well as future extensions and possible research directions arising from this work.

8.1 Summary of the Thesis

In this thesis, optimal control methods for designing distributed cooperative control schemes in multi-agent networks are explored. The tools from LQR control theory are employed to analyse the family of distributed suboptimal LQR controllers and their application to formation control of low speed experimental UAVs.

In Chapter 1 the motivation for the work carried out in this thesis was presented to set the stage for the results derived in subsequent chapters. Additionally, the thesis objectives were given, as well as the thesis outline and the statement of contributions. The chapter was concluded by the list of publications. In Chapter 2 up-to-date research in the areas of cooperative and distributed control, and their application to large-scale UAV networks were discussed. The main approaches in formation tracking were introduced, as well as the application of distributed control techniques to the area of optimal control.

In Chapter 3 and Chapter 4 we examined the LQR theoretical framework on

which this thesis has been developed and we described how this framework can be used for centralized multi-agent network control. By investigating the structural properties of the centralized solutions we obtained a special case where the size of the problem (i.e. the size of ARE) that has to be solved reduces to a single agent problem. Also, we briefly investigated the gain and phase margin properties of the proposed design.

In Chapter 5 the distributed LQR framework was presented. The effectiveness of the approach was illustrated via an example of a multi-agent network consisting of agents described by double integrator dynamics. Then, the proposed distributed controller was compared with respect to the performance cost to the centralized control design and the cost difference was quantified by using different cost measures. Necessary and sufficient conditions were derived for which a distributed control configuration pattern arising from the optimal centralized solution does not entail loss of performance if the initial state vector lies in a certain subspace of state-space which is identified.

Chapters 6 and 7 applied the main theoretical methods presented in previous chapters to a high order dynamical system. The proposed distributed LQR design was used to stabilise an experimental RPV, X-RAE1, described by 6-DOF nonlinear model that was linearised for a specific set of flight conditions. The problem was extended to the effective altitude control of arbitrary formations of X-RAE1s. It was shown that the proposed schemes are robust to environmental disturbances such as nonuniform wind gusts acting on a formation and to the loss of communication between a pair of agents. The results were reproduced for the nonlinear model and it was shown that these closely match the results obtained in the linear case.

The formation control example considered in this thesis has received considerable attention in the literature as stated in the literature overview presented in Chapter 1. Formation control has been increasingly used in modern military systems and it can be easily extended to cooperative surveillance problems, rendezvous problems, etc. However, designs proposed in this thesis are not limited to this application area. These can be successfully used in mobile sensor networks, transportation systems such as intelligent highways, air traffic control, etc.

This thesis provided a number of contributions which are summarised in the following paragraphs:

1. The structure and spectral properties of the solution of the (large-scale) centralized LQR system were reviewed. A special case of centralized LQR control was proposed where by imposing a specific structure on the weighting matrices, the solution can be constructed by solving a single agent ARE (Algebraic Riccati Equation).
2. The structure and spectral properties of the solution of the (large-scale) distributed LQR system were reviewed. It was shown that the proposed distributed controller preserves the gain and phase margin properties which are guaranteed in classical LQR control. The effectiveness of distributed LQR approach was illustrated through an example of a multi-agent network consisting of agents described by double integrator dynamics.
3. The method for comparing with respect to the performance cost the family of distributed LQR-suboptimal controllers with the optimal centralized controller was developed. The cost increase due to decentralization was quantified by looking into worst-case, best-case and average deviation from optimality. Additionally, necessary and sufficient conditions have been derived for which a distributed control configuration pattern arising from the optimal centralized solution does not entail loss of performance if the initial state vector lies in a certain subspace of state-space which is identified. The procedure was extended for analysing the performance loss of an arbitrary distributed configuration which is illustrated via an example.

Additionally, it was verified that the proposed distributed LQR framework can be used to efficiently control a multi-agent network comprising high order nonlinear dynamics for a specific set of initial conditions.

8.2 Directions for Future Work

In closing, a number of future research directions are suggested:

- We presented a method for computing the performance loss of various distributed configurations relative to the performance of optimal centralized controller. Cost increase was quantified with respect to the different measures which are worst-case, best-case and average case deviations from optimality. Therefore, it would be of great interest to investigate how connectivity measures of the network obtained by removing a set of links correlates with the LQR cost measures presented. Also, it would be interesting to establish the precise relation between the maximum and minimum degree of the network, on one, and the cost resulting by a particular configuration on the other side.
- Another important question, both from a theoretical and practical point of view, involves the information structure of the control problem. If there is no access to the global information within the network setting, i.e. if the full state vector is not available for feedback, the LQR control design framework is no longer adequate (as not all states are measurable) and dynamic estimation-based control schemes are needed. This issue can be addressed by using a stochastic optimal state estimator (Kalman filter). Due to the fact that there is duality between the Kalman filtering problem and the LQR control problem, dual results of the filtering problem to those of the LQR problem are expected, leading to the decomposition of the global Kalman filter into a number of local Kalman filters.
- This thesis investigates only LQR designs based on state feedback. Other open questions in the problem setting encountered here concern designs based on output feedback where the stability margins are no longer guaranteed. It is well known that by using loop transfer recovery (LTR) methods the stability margins can be recovered partially. Therefore, it is worth investigating if it is possible to construct stabilising distributed controllers that use output feedback in the framework similar to the one presented in this thesis.
- One of the assumptions made in the development of the distributed LQR controller used in this work was that all agents within network are described by identical dynamics. It would be of great interest to inves-

tigate how the system will respond to the presence of perturbations in the model. Additionally, one could ask how big these perturbations can grow before the stability of whole multi-agent network breaks down. An answer to this question is likely to be obtained by applying recent results from robust control theory.

- In this work we considered one optimality criterion, i.e. quadratic norm, that has proved to be inadequate in the presence of random disturbances whose spectral characteristics are not known precisely. It could be beneficial to consider alternative optimisation criteria, such as H_∞ norm-based which have proved effective in such cases and also in problems characterised by significant model uncertainty. Therefore, an important research question would be to investigate if these methods are still valid for network problems of the type considered here.

Bibliography

- [AB09] D. Angeli and P. A. Bliman. Convergence speed of unsteady distributed consensus: Decay estimate along the settling spanning-trees. *SIAM Journal on Control and Optimization*, 48(1):1–32, 2009.
- [AC03] A. Alessandri and P. Coletta. Design of observers for switched discrete-time linear systems. In *Proceedings of the American Control Conference*, volume 4, pages 2785–2790, 2003.
- [Als04] S. I. Alswailem. *Application of robust control in unmanned vehicle flight control system design*. PhD thesis, College of Aeronautics, Cranfield University, 2004.
- [AM85] W. N. Anderson and T. D. Morley. Eigenvalues of the Laplacian of a graph. *Linear and Multilinear Algebra*, 18(2):141–145, 1985.
- [AM89] B. D. O. Anderson and J. B. Moore. *Optimal control: linear quadratic methods*. Prentice-Hall, Inc., Englewood Cliffs, NJ, USA, 1989.
- [AMS07] G. Arslan, J. R. Marden, and J. S. Shamma. Autonomous vehicle-target assignment: A game-theoretical formulation. *Journal of Dynamic Systems, Measurement, and Control*, 129(5):584–596, 2007.
- [BA98] T. Balch and R. C. Arkin. Behavior-based formation control for multirobot teams. *IEEE Transactions on Robotics and Automation*, 14(6):926–939, 1998.
- [BHOT05] V. D. Blondel, J. M. Hendrickx, A. Olshevsky, and J. N. Tsitsiklis. Convergence in multiagent coordination, consensus, and flocking. In *Proceedings of the 44th IEEE Conference on Decision and Control*, pages 2996–3000, 2005.

- [BK08] F. Borrelli and T. Keviczky. Distributed LQR design for identical dynamically decoupled systems. *IEEE Transactions on Automatic Control*, 53(8):1901–1912, 2008.
- [Bla91] J. H. Blakelock. *Automatic control of aircraft and missiles*. John Wiley & Sons, New York, NY, USA, 1991.
- [BLH00] R. W. Beard, J. Lawton, and F. Y. Hadaegh. A feedback architecture for formation control. In *Proceedings of the American Control Conference*, volume 6, pages 4087–4091, 2000.
- [BLH01] R. W. Beard, J. Lawton, and F. Y. Hadaegh. A coordination architecture for spacecraft formation control. *IEEE Transactions on Control Systems Technology*, 9(6):777–790, 2001.
- [BM99] A. Bemporad and M. Morari. *Robust model predictive control: A survey*, pages 207–226. Springer, London, 1999.
- [BPD02] B. Bamieh, F. Paganini, and M. A. Dahleh. Distributed control of spatially invariant systems. *IEEE Transactions on Automatic Control*, 47(7):1091–1107, 2002.
- [Bry11] G. H. Bryan. *Stability in aviation: An introduction to dynamical stability as applied to the motions of aeroplanes*. Macmillan and Company, limited, London, UK, 1911.
- [Cam01] P. J. Cameron. Automorphisms of graphs, 2001.
- [CGW91] P. E. Caines, R. Greiner, and S. Wang. Classical and logic-based dynamic observers for finite automata. *IMA Journal of Mathematical Control and Information*, 8(1):45–80, 1991.
- [Che14] C. Chen. *On the robustness of the linear quadratic regulator via perturbation analysis of the Riccati equation*. PhD thesis, Dublin City University, 2014.
- [CJKT02] E. Camponogara, D. Jia, B. H. Krogh, and S. Talukdar. Distributed model predictive control. *IEEE Control Systems*, 22(1):44–52, 2002.
- [CMB06] J. Cortes, S. Martinez, and F. Bullo. Robust rendezvous for mobile autonomous agents via proximity graphs in arbitrary dimensions. *IEEE Transactions on Automatic Control*, 51(8):1289–1298, 2006.

- [CMKB04] J. Cortes, S. Martinez, T. Karatas, and F. Bullo. Coverage control for mobile sensing networks. *IEEE Transactions on Robotics and Automation*, 20(2):243–255, 2004.
- [Coo97] M. V. Cook. *Flight dynamics principles*. Arnold, London, UK, 1997.
- [CR10] Y. Cao and W. Ren. Optimal linear consensus algorithms: An LQR perspective. *IEEE Transactions on Systems, Man, and Cybernetics, Part B (Cybernetics)*, 40(3):819–830, 2010.
- [CRL09] Y. Cao, W. Ren, and Y. Li. Distributed discrete-time coordinated tracking with a time-varying reference state and limited communication. *Automatica*, 45(5):1299–1305, 2009.
- [CT04] T. C. Collier and C. Taylor. Self-organization in sensor networks. *Journal of Parallel and Distributed Computing*, 64(7):866–873, 2004.
- [CW05] Y. C. Chen and Z. Wang. Formation control: a review and a new consideration. *IEEE/RSJ International Conference on Intelligent Robots and Systems*, pages 3181–3186, 2005.
- [DB00] R. C. Dorf and R. H. Bishop. *Modern control systems*. Prentice-Hall, Inc., Upper Saddle River, NJ, USA, 2000.
- [DeG74] M. H. DeGroot. Reaching a consensus. *Journal of the American Statistical Association*, 69(345):118–121, 1974.
- [DF08] W. Dong and J. A. Farrell. Cooperative control of multiple non-holonomic mobile agents. *IEEE Transactions on Automatic Control*, 53(6):1434–1448, 2008.
- [DJ09] T. Dierks and S. Jagannathan. Neural network control of mobile robot formations using rise feedback. *IEEE Transactions on Systems, Man, and Cybernetics, Part B (Cybernetics)*, 39(2):332–347, 2009.
- [DK07] D. V. Dimarogonas and K. J. Kyriakopoulos. On the rendezvous problem for multiple nonholonomic agents. *IEEE Transactions on Automatic Control*, 52(5):916–922, 2007.

- [DMEP11] P. Deshpande, P. P. Menon, C. Edwards, and I. Postlethwaite. A distributed control law with guaranteed LQR cost for identical dynamically coupled linear systems. In *Proceedings of the 2011 American Control Conference*, pages 5342–5347, 2011.
- [Do08] K. D. Do. Formation tracking control of unicycle-type mobile robots with limited sensing ranges. *IEEE Transactions on Control Systems Technology*, 16(3):527–538, 2008.
- [DVM04] D. Del Vecchio and R. M. Murray. Existence of discrete state estimators for hybrid systems on a lattice. In *Proceedings of 43rd IEEE Conference on Decision and Control*, volume 1, pages 1–6, 2004.
- [ED02] M. G. Earl and R. D’Andrea. A study in cooperative control: the roboflag drill. In *Proceedings of the American Control Conference*, volume 3, pages 1811–1812, 2002.
- [Elg13] I. Elgayar. *Mathematical modelling, flight control system design and air flow control investigation for low speed UAVs*. PhD thesis, School of Engineering and Mathematical Sciences, City University London, 2013.
- [ER95] B. Etkin and L. D. Reid. *Dynamics of flight: Stability and control*. John Wiley & Sons, New York, NY, USA, 1995.
- [Fax02] J. A. Fax. *Optimal and cooperative control of vehicle formations*. PhD thesis, Control and Dynamical Systems, California Institute of Technology, Pasadena, CA, 2002.
- [FM04] J. A. Fax and R. M. Murray. Information flow and cooperative control of vehicle formations. *IEEE Transactions on Automatic Control*, 49(9):1465–1476, 2004.
- [FPEN01] G. F. Franklin, D. J. Powell, and A. Emami-Naeini. *Feedback control of dynamic systems*. Prentice-Hall, Inc., Upper Saddle River, NJ, USA, 4th edition, 2001.
- [FTBG06] G. Ferrari-Trecate, A. Buffa, and M. Gati. Analysis of coordination in multi-agent systems through partial difference equations. *IEEE Transactions on Automatic Control*, 51(6):1058–1063, 2006.

- [FZLW14] T. Feng, H. Zhang, Y. Luo, and Y. Wang. Distributed LQR design for multi-agent systems on directed graph topologies. *International Joint Conference on Neural Networks*, pages 2732–2737, 2014.
- [GAP⁺09] R. Ghabcheloo, A. P. Aguiar, A. Pascoal, C. Silvestre, I. Kaminer, and J. Hespanha. Coordinated path-following in the presence of communication losses and time delays. *SIAM Journal on Control and Optimization*, 48(1):234–265, 2009.
- [GJ86] M. J. Grimble and M. A. Johnson. *Optimal control and stochastic estimation: Theory and applications*. John Wiley & Sons, Inc., New York, NY, USA, 1986.
- [GKL03] D. Garcia, A. Karimi, and R. Longchamp. Infinity norm measurement of sensitivity function based on limit cycles in a closed-loop experiment. In *European Control Conference*, pages 2073–2078, 2003.
- [GS14] R. Ghadami and B. Shafai. Distributed observer-based LQR design for multi-agent systems. In *Proceedings of World Automation Congress*, pages 520–525, 2014.
- [Hes05] J. P. Hespanha. *Lecture notes on LQR/LQG controller design*. University of California, 2005.
- [Hop70] H. R. Hopkin. *A scheme of notation and nomenclature for aircraft dynamics and associated aerodynamics*. Aeronautical Research Council Reports and Memoranda. Her Majesty’s Stationery Office, London, UK, 1970.
- [Jin07] Z. Jin. *Coordinated control for networked multi-agent systems*. PhD thesis, California Institute of Technology, 2007.
- [JLM02] A. Jadbabaie, J. Lin, and A. Stephen Morse. Coordination of groups of mobile autonomous agents using nearest neighbor rules. In *Proceedings of the 41st IEEE Conference on Decision and Control*, pages 2953–2958, 2002.
- [JMB04] A. Jadbabaie, N. Motee, and M. Barahona. On the stability of the Kuramoto model of coupled nonlinear oscillators. In *Proceedings*

- of the *American Control Conference*, volume 5, pages 4296–4301, 2004.
- [JME06] M. Ji, A. Muhammad, and M. Egerstedt. Leader-based multi-agent coordination: controllability and optimal control. In *Proceedings of the American Control Conference*, pages 1358–1363, 2006.
- [KBB05] T. Keviczky, F. Borrelli, and G. J. Balas. Stability analysis of decentralized RHC for decoupled systems. In *Proceedings of the 44th IEEE Conference on Decision and Control, and the European Control Conference*, pages 1689–1694, 2005.
- [KBB06] T. Keviczky, F. Borrelli, and G. J. Balas. Decentralized receding horizon control for large scale dynamically decoupled systems. *Automatica*, 42(12):2105–2115, 2006.
- [KD05] M. E. Khatir and E. J. Davison. Cooperative control of large systems. in *V. Kumar, N. Leonard, and A. S. Morse (Eds), Cooperative Control, A Post-Workshop Volume of 2003 Block Island Workshop on Cooperative Control*, 309:119–136, 2005.
- [Kel67] A. K. Kelmans. Properties of the characteristic polynomial of a graph. *Kibernetiky - na sluzbu kommunizma*, 4:27–41, 1967.
- [Kev05] T. Keviczky. *Decentralized receding horizon control of large scale dynamically decoupled systems*. PhD thesis, Control Science and Dynamical Systems Center, University of Minnesota, Minneapolis, 2005.
- [Kno11] F. Knorn. *Topics in cooperative control*. PhD thesis, Hamilton Institute, National University of Ireland, 2011.
- [KS72] H. Kwakernaak and R. Sivan. *Linear optimal control systems*. John Wiley & Sons, Inc., New York, NY, USA, 1972.
- [LBY03] J. R. T. Lawton, R. W. Beard, and B. J. Young. A decentralized approach to formation maneuvers. *IEEE Transactions on Robotics and Automation*, 19(6):933–941, 2003.
- [LCD04] C. Langbort, R. S. Chandra, and R. D’Andrea. Distributed control design for systems interconnected over an arbitrary graph. *IEEE Transactions on Automatic Control*, 49(9):1502–1519, 2004.

- [LCT⁺04] Y. Lee, T. Collier, C. Taylor, J. Riggle, and E. Stabler. Adaptive communication among collaborative agents: preliminary results with symbol grounding. *Artificial Life and Robotics*, 8(2):127–132, 2004.
- [LDC11] Z. Li, Z. Duan, and G. Chen. On H_∞ and H_2 performance regions of multi-agent systems. *Automatica*, 47(4):797–803, 2011.
- [LDCH10] Z. Li, Z. Duan, G. Chen, and L. Huang. Consensus of multi-agent systems and synchronization of complex networks: A unified viewpoint. *IEEE Transactions on Circuits and Systems I: Regular Papers*, 57(1):213–224, 2010.
- [Lew86] F. L. Lewis. *Optimal control*. John Wiley & Sons, Inc., New York, NY, USA, 1986.
- [LFJ11] F. Lin, M. Fardad, and M. R. Jovanovic. Augmented lagrangian approach to design of structured optimal state feedback gains. *IEEE Transactions on Automatic Control*, 56(12):2923–2929, 2011.
- [LFJ12] F. Lin, M. Fardad, and M. R. Jovanovic. Optimal control of vehicular formations with nearest neighbor interactions. *IEEE Transactions on Automatic Control*, 57(9):2203–2218, 2012.
- [LFM07] Z. Lin, B. Francis, and M. Maggiore. State agreement for continuous-time coupled nonlinear systems. *SIAM Journal on Control and Optimization*, 46(1):288–307, 2007.
- [LG09] C. Langbort and V. Gupta. Minimal interconnection topology in distributed control design. *SIAM Journal on Control and Optimization*, 48(1):397–413, 2009.
- [LK89] R. C. Luo and M. G. Kay. Multisensor integration and fusion in intelligent systems. *IEEE Transactions on Systems, Man, and Cybernetics*, 19(5):901–931, 1989.
- [LSA81] N. Lehtomaki, N. Sandell, and M. Athans. Robustness results in linear-quadratic Gaussian based multivariable control designs. *IEEE Transactions on Automatic Control*, 26(1):75–93, 1981.
- [McC11] N. H. McClamroch. *Steady aircraft flight and performance*. Princeton University Press, NJ, USA, 2011.

- [MD07] N. C. Martins and M. A. Dahleh. *Modal estimation of jump linear systems: An information theoretic viewpoint*. John Wiley & Sons, Ltd, New York, NY, USA, 2007.
- [Mil87] E. Milonidis. *The development of the mathematical model of an RPV and and investigation on the use of an EKV for the identification of its aerodynamical derivatives*, MPhil Thesis, College of Aeronautics, Cranfield University. 1987.
- [Moh91] B. Mohar. The Laplacian spectrum of graphs. *Graph Theory, Combinatorics, and Applications*, 2:871–898, 1991.
- [MR15] Matlab and Simulink Release. *Version R2015a*. The MathWorks Inc., Natick, Massachusetts, 2015.
- [MSA07] S. Mannor, J. S. Shamma, and G. Arslan. Online calibrated forecasts: Memory efficiency versus universality for learning in games. *Machine Learning*, 67(1):77–115, 2007.
- [Mur00] R. A. Murphey. *Target-based weapon target assignment problems*. Springer, Boston, MA, 2000.
- [Mur07] R. M. Murray. Recent research in cooperative control of multi-vehicle systems. *Journal of Dynamic Systems, Measurement, and Control*, 129(5):571, 2007.
- [MV08] P. Massioni and M. Verhaegen. New approaches to distributed control of satellite formation flying. In *Proceedings of 3rd International Symposium on Formation Flying, Missions and Technologies*, 2008.
- [MV09] P. Massioni and M. Verhaegen. Distributed control for identical dynamically coupled systems: A decomposition approach. *IEEE Transactions on Automatic Control*, 54(1):124–135, 2009.
- [NL08] S. Nair and N. E. Leonard. Stable synchronization of mechanical system networks. *SIAM Journal on Control and Optimization*, 47:661–683, 2008.
- [OS05] R. Olfati-Saber. Distributed Kalman filter with embedded consensus filters. In *Proceedings of the 44th IEEE Conference on Decision and Control*, pages 8179–8184, 2005.

- [OS06] R. Olfati-Saber. Flocking for multi-agent dynamic systems: Algorithms and theory. *IEEE Transactions on Automatic Control*, 51(3):401–420, 2006.
- [OSFM07] R. Olfati-Saber, J. A. Fax, and R. M. Murray. Consensus and cooperation in networked multi-agent systems. In *Proceedings of the IEEE*, volume 95, pages 215–233, 2007.
- [OSM02] R. Olfati-Saber and R. M. Murray. Distributed cooperative control of multiple vehicle formations using structural potential functions. *IFAC Proceedings Volumes*, 35(1):495–500, 2002.
- [OSM03] R. Olfati-Saber and R. M. Murray. Consensus protocols for networks of dynamic agents. In *Proceedings of the American Control Conference*, volume 2, pages 951–956, 2003.
- [OSM04] R. Olfati-Saber and R. M. Murray. Consensus problems in networks of agents with switching topology and time-delays. *IEEE Transactions on Automatic Control*, 49(9):1520–1533, 2004.
- [OSS05] R. Olfati-Saber and J. S. Shamma. Consensus filters for sensor networks and distributed sensor fusion. In *Proceedings of the 44th IEEE Conference on Decision and Control*, pages 6698–6703, 2005.
- [OT09] A. Olshevsky and J. N. Tsitsiklis. Convergence speed in distributed consensus and averaging. *SIAM Journal on Control and Optimization*, 48(1):33–55, 2009.
- [PDL01] F. Paganini, J. Doyle, and S. Low. Scalable laws for stable network congestion control. In *Proceedings of the 40th IEEE Conference on Decision and Control*, volume 1, pages 185–190, 2001.
- [Phi10] W. A. Phillips. *Mechanics of flight*. John Wiley & Sons, Inc., Hoboken, NJ, USA, 2010.
- [PJ05] A. Papachristodoulou and A. Jadbabaie. Synchronization in oscillator networks: Switching topologies and non-homogeneous delays. In *Proceedings of the 44th IEEE Conference on Decision and Control*, pages 5692–5697, 2005.
- [PLS08] D. A. Paley, N. E. Leonard, and R. Sepulchre. Stabilization of symmetric formations to motion around convex loops. *Systems & Control Letters*, 57(3):209–215, 2008.

- [Pre02] A. Preumont. *Vibration control of active structures: An introduction*. Solid mechanics and its applications. Springer Netherland, 2002.
- [PW09] A. P. Popov and H. Werner. A robust control approach to formation control. In *Proceedings of the European Control Conference*, pages 4428–4433, 2009.
- [QWH08] Z. Qu, J. Wang, and R. A. Hull. Cooperative control of dynamical systems with application to autonomous vehicles. *IEEE Transactions on Automatic Control*, 53(4):894–911, 2008.
- [RA08] J. A. Rogge and D. Aeyels. Vehicle platoons through ring coupling. *IEEE Transactions on Automatic Control*, 53(6):1370–1377, 2008.
- [RBA05] W. Ren, R. W. Beard, and E. M. Atkins. A survey of consensus problems in multi-agent coordination. In *Proceedings of the American Control Conference*, pages 1859–1864, 2005.
- [RC11] W. Ren and Y. Cao. *Distributed coordination of multi-agent networks*. Springer-Verlag London, 2011.
- [Ren07] W. Ren. Distributed attitude alignment in spacecraft formation flying. *International Journal of Adaptive Control and Signal Processing*, 21(2-3):95–113, 2007.
- [Rey87] C. W. Reynolds. Flocks, herds and schools: A distributed behavioral model. In *Proceedings of the 14th Annual Conference on Computer Graphics and Interactive Techniques*, pages 25–34, 1987.
- [SA76] M. G. Safonov and M. Athans. Gain and phase margin for multi-loop LQG regulators. *IEEE Conference on Decision and Control including the 15th Symposium on Adaptive Processes*, 15(2):173–179, 1976.
- [SB00] D. J. Stilwell and B. E. Bishop. Platoons of underwater vehicles. *IEEE Control Systems*, 20(6):45–52, 2000.
- [Sha07] J. S. Shamma. *Cooperative control of distributed multi-agent systems*. John Wiley & Sons, Inc., New York, NY, USA, 2007.

- [SME13] A. Seuret, P. P. Menon, and C. Edwards. LQR performance for multi-agent systems: Benefits of introducing delayed inter-agent measurements. In *IEEE Conference on Decision and Control*, 2013.
- [SOSM05] D. P. Spanos, R. Olfati-Saber, and R. M. Murray. Dynamic consensus for mobile networks. *16th IFAC World Congress*, 2005.
- [SPL05] R. Sepulchre, D. Paley, and N. Leonard. *Collective motion and oscillator synchronization*. Springer, Berlin, Heidelberg, 2005.
- [SWL09] H. Su, X. Wang, and Z. Lin. Flocking of multi-agents with a virtual leader. *IEEE Transactions on Automatic Control*, 54(2):293–307, 2009.
- [TBA86] J. N. Tsitsiklis, D. Bertsekas, and M. Athans. Distributed asynchronous deterministic and stochastic gradient optimization algorithms. *IEEE Transactions on Automatic Control*, 31(9):803–812, 1986.
- [TJP03a] H. G. Tanner, A. Jadbabaie, and G. J. Pappas. Stable flocking of mobile agents, part I: Fixed topology. In *Proceedings of 42nd IEEE Conference on Decision and Control*, volume 2, pages 2010–2015, 2003.
- [TJP03b] H. G. Tanner, A. Jadbabaie, and G. J. Pappas. Stable flocking of mobile agents part II: Dynamic topology. In *Proceedings of 42nd IEEE Conference on Decision and Control*, volume 2, pages 2016–2021, 2003.
- [TJP07] H. G. Tanner, A. Jadbabaie, and G. J. Pappas. Flocking in fixed and switching networks. *IEEE Transactions on Automatic Control*, 52(5):863–868, 2007.
- [TL96] K. Tan and M. A. Lewis. Virtual structures for high-precision cooperative mobile robotic control. In *Proceedings of the 1996 IEEE/RSJ International Conference on Intelligent Robots and Systems*, volume 1, pages 132–139, 1996.
- [TPS98] C. Tomlin, G. J. Pappas, and S. Sastry. Conflict resolution for air traffic management: a study in multi-agent hybrid systems. *IEEE Transactions on Automatic Control*, 43(4):509–521, 1998.

- [Tsi84] J. N. Tsitsiklis. *Problems in decentralized decision making and computation*. PhD thesis, Department of Electrical Engineering and Computer Science, Massachusetts Institute of Technology, 1984.
- [Tun08] S. E. Tuna. Synchronizing linear systems via partial-state coupling. *Automatica*, 44(8):2179–2184, 2008.
- [VCBJ+95] T. Vicsek, A. Czirók, E. Ben-Jacob, I. Cohen, and O. Shochet. Novel type of phase transition in a system of self-driven particles. *Physical Review Letters*, 75:1226–1229, 1995.
- [VSH99] M. Veloso, P. Stone, and K. Han. The CMUnited-97 robotic soccer team: Perception and multi-agent control. *Robotics and Autonomous Systems*, 29(23):133–143, 1999.
- [Wan91] P. K. C. Wang. Navigation strategies for multiple autonomous mobile robots moving in formation. *Journal of Robotic Systems*, 8(2):177–195, 1991.
- [WD73] S. H. Wang and E. Davison. On the stabilization of decentralized control systems. *IEEE Transactions on Automatic Control*, 18(5):473–478, 1973.
- [Wey12] H. Weyl. Das asymptotische verteilungsgesetz der eigenwerte linearer partieller differentialgleichungen (mit einer anwendung auf die theorie der hohlraumstrahlung). *Mathematische Annalen*, 71:441–479, 1912.
- [WM97] S. C. Weller and N. C. Mann. Assessing rater performance without a 'gold standard' using consensus theory. *Medical Decision Making*, 17(1):71–79, 1997.
- [WYGL13] Q. Wang, C. Yu, H. Gao, and F. Liu. A distributed control law with guaranteed convergence rate for identically coupled linear systems. In *Proceedings of the European Control Conference*, pages 2286–2291, 2013.
- [XBL05] L. Xiao, S. Boyd, and S. Lall. A scheme for robust distributed sensor fusion based on average consensus. In *4th International Symposium on Information Processing in Sensor Networks*, pages 63–70, 2005.

- [XWL09] J. Xiang, W. Wei, and Y. Li. Synchronized output regulation of linear networked systems. *IEEE Transactions on Automatic Control*, 54(6):1336–1341, 2009.
- [ZDG96] K. Zhou, J. C. Doyle, and K. Glover. *Robust and optimal control*. Prentice-Hall, Inc., Upper Saddle River, NJ, USA, 1996.
- [ZLL06] J. Zhou, J. Lu, and J. Lu. Adaptive synchronization of an uncertain complex dynamical network. *IEEE Transactions on Automatic Control*, 51(4):652–656, 2006.